INVESTIGATION ON MODIFIED GROUND SOURCE HEAT PUMP USED FOR SPACE HEATING AND COOLING APPLICATION

A Thesis

Submitted in partial fulfilment of the requirements for the

award of the degree of

DOCTOR OF PHILOSOPHY

in

Mechanical Engineering

By

Aashish Sharma

(41600317)

Supervised by

Dr Ravindra D. Jilte

LOVELY PROFESSIONAL UNIVERSITY
PUNJAB
2021

CERTIFICATE

I hereby certify that the work which is being presented in the thesis entitled "**Investigation on modified ground source heat pump used for space heating and cooling application**" in partial fulfillment of the requirement for the award of the degree of **Doctor of Philosophy** and submitted to the Department of Mechanical Engineering of Lovely Professional University, Phagwara (Punjab) is an authentic record of my work carried out during the period from January 2017 to March 2021 under the supervision of **Dr. Ravindra Jilte**, Professor, School of Mechanical Engineering, Lovely Professional University.

29/4/21

(**Aashish Sharma**)

This is to certify that the above statement is correct to the best of our knowledge.

Date: 29/04/2021

(**Dr. Ravindra D. Jilte**)

Supervisor

The PhD. Viva-Voce Examination of **Aashish Sharma** has been held on _____

Signature of Supervisor   Signature of External Examiner

ABSTRACT

Energy consumption and Global warming are two interlinked terms. Globally, the amount of pollution rising is alarming, and the primary reason for this is fossil fuel consumption for generating energy. It is essential for the economy and social harmony of a nation. Industries consume this energy to produce goods which also creates pollution. After the transportation sector, buildings are the second-highest contributor to GHG emissions. And within the building sector alone, 50% of total energy consumed is for heating and cooling purpose. In another term, significant energy consumption is for maintaining thermal comfort. Thermal comfort is defined as the space maintained at a temperature of 25^0C with an airspeed of 5 km/hr.

There are many active and passive techniques used for heating and cooling buildings. These passive technologies include solar energy, which is also extensively used for generating electricity to curb the high energy demand. For the past couple of decades, Earth Air Heat Exchanger (EAHE) or Ground Source Heat Pump (GSHP) have been developed for this very purpose. Lots of work has been done to bring this technology to the public. The principle of GHE is based on an elementary phenomenon that we all have experienced. We feel the water from a well be warm in winters and cold in summers. It is not the water temperature in the well that changes; instead, it is the reference temperature (ambient temperature) that is changing. As we go under the earth's surface, the underground temperature tends to be at a constant temperature. The external climate has a prolonged and minimum impact on the temperature of the earth. Taking this phenomenon to our advantage, we bury a pipe system under the ground, and then the working fluid can pass through it. In summers, as the ambient temperature is at a higher temperature so when the heated fluid passes through this pipe, it will reject the heat into the ground. Similarly, this will become the opposite in winters, meaning cold working fluid will absorb heat from the surrounding area and get heated.

The performance of the Ground Heat Exchanger (GHE) is crucial for the GSHP system. The current system requires a long pipe length to be buried underground. This is done to increase the overall heat transfer surface area, which results in a higher rate of heat

transfer. The current study focuses on reducing the overall length of the pipe or increasing the performance of a GHE so that less underground space is required to install a horizontal GSHP system. A novel pipe geometry has been designed to achieve high heat transfer for a given pipe length. This spirally corrugated pipe help in rotating the fluid as it moves in the pipe. This fluid rotation reduces the formation of the laminar sublayer near the pipe surface, thus enhancing the overall heat transfer coefficient. As the overall heat transfer coefficient increasing so does increase the heat transfer.

If we change the working fluid from standard fluid, i.e., water, with a better heat transfer fluid, the heat transfer can be further enhanced. Here in this thesis, apart from water, Al_2O_3 – water nanofluid and Microencapsulated Phase Change Material (MPCM) slurry is also evaluated numerically. Even at low concentration, Nanofluids' enhanced thermal properties make them an ideal working fluid for heat transfer applications. As the concentration of nanoparticles in the base fluid increases, the heat-carrying capacity also increases, but simultaneously the viscosity also increases. Al_2O_3 – water nanofluid is the commonly used nanofluid due to its cost-effectiveness and no adverse impact on the environment. When tiny or small particles of phase change material are encapsulated in homogeneous or heterogeneous capsules is known as Microencapsulation. This technique helps in handling flowing materials efficiently. These particles are manufactured or fabricated by two processes: a) Chemical Process and b) Physical process. In the application where the particle size must be less than 100 µm, a chemical process is used; otherwise, the physical process is used. Then this microencapsulated PCM is added to water or any other base fluid. From previous studies, it has been found that MPCM has enormous potential to be used as a working fluid in various heat transfer applications.

For the analysis, a numerical model is created in ANSYS Fluent. The investigation is done for both seasons, i.e., summer and winter. Three different Reynolds number at three different inlet temperatures for each case were analysed.

Based on the result of the numerical simulations, it can be established that the pipe geometries can have a significant impact on the performance of the GHE system. As

we know, in heat exchangers, corrugations and surface modifications are commonly used because they are very effective in heat transfer enhancement. It also promotes secondary recirculation flow by inducing non-axial velocity components. Spiral corrugation increases heat transfer enhancement due to secondary flow swirls and surface curvatures pass by fluid layers, which also causes pressure losses. The simulations carried out in the research are mainly focused on seeing the effect of novel pipe geometry on GHE. It would be of great help in designing the novel systems with spirally corrugated pipe layout as it will increase the rate of heat transfer for the same area. It will help in reducing the overall space requirement for long pipe length. Also, it is found that the pumping power required for MPCM slurry is higher than water, but simultaneously we can see that it provides the highest heat transfer. If we design pipe so that central flow is not much disturbed and fluid near the surface swirls, we can significantly decrease pressure drop. Thus, the designers can choose between these two factors for a trade-out to achieve maximum effectiveness at a low cost.

Further analysis can be done considering the whole GSHP system, and its complete cost analysis can be done. The fact that soil properties also affect thermal performance, a study with various backfill materials can be done to understand its effect along with our novel pipe design. PCM can also be integrated into this system to provide constant energy.

ACKNOWLEDGMENT

First, I feel great pleasure in acknowledging my deepest gratitude to my revered guide and mentor, **Dr Ravindra D. Jilte**, Professor, Mechanical Engineering Department, Lovely Professional University, Punjab, India, whose guidance, motivation, and vigilant supervision I succeeded in completing my work. He infused the enthusiasm to continue this work into me.

I am also ever grateful to Jeet, a PhD candidate, for his generous help. My sincere thanks are due to all the faculty members and non-teaching staff of the School of Mechanical Engineering, Lovely Professional University, Punjab, for availing me all the necessary facilities and co-operation for this work.

Words are inadequate to express my heartfelt gratitude to my affectionate **parents** and my **wife,** who have so much confidence in me and by whose efforts and blessings I have reached here. Not to forget my lovely daughter **Anaya,** who has been my constant driving force for completing this work.

I find it hard to express my gratitude to the **Almighty** in words for bestowing upon me his most profound blessings and providing me with the most beautiful opportunity in the form of life of a human being and for the warmth and kindness he has shown upon me by giving me life's best.

Finally, I wish to express my heartiest thanks to my friends ans colleagues for their support, love, and inspiration.

(AASHISH SHARMA)

Table of Contents

List of Tables

List of Figures

Abbrevations		*Units*	
EAHE	Earth Air Heat Exchanger	m	meter
GHE	Ground Heat Exchanger	°C	Celsius
GSHP	Ground Source Heat Pump	m/s	velocity
HETS/HEAHE	Horizontal Earth Air Heat Exchanger System	*Subscripts*	
ATEHE	Air-to-Earth Heat Exchanger	l	length
RES	Renewable Energy Sources	d	diameter
MOE	Ministry of Environment	r	radius
CFC	Chlorofluorocarbon	i	inlet
HVAC	Heating, Ventilation and Air conditioning	o	outlet
SAHD	Solar Air Heating Duct	S	Summer
PV	Photovoltaic	W	Winter
PID	Proportional Integral Derivative		
CFD	Computational Fluid Dynamics		
FVM	Finite Volume Method		
COP	Coefficient of Performance		
FFT	Fast Fourier Transform		
EPBT	Energy Payback time		
EER	Energy Efficiency Ratio		
PVC	Polyvinyl Chloride		
HDPE	High-Density Polyethylene		
MS	Mild Steel		
MPCMs	Microencapsulated Phase Change Material Slurry		

1 INTRODUCTION

Climate change due to the rapid increase in greenhouse gases (GHG) has a significant role in the world's social, economic, and environmental changes. This rise in global pollution is caused by various factors, i.e., industries, transport, residential and commercial buildings. After industry and transport, the building sector is one of the significant sources of GHG emissions. Most of the time, a human spends his time building, whether home, school, college, or office. Using various technologies to maintain the thermal comfort in a building increases the energy consumption in a building, thus indirectly contributing to the GHG emissions (emissions associated with energy production). Adopting low-carbon technologies for maintaining thermal comfort can contribute to the solution to the problem of global warming.

Fossil fuels are the primary energy sources, which power all the economic and building sectors. Although initially available in large quantities, they are neither infinite nor renewable. Furthermore, this energy conversion into valuable work by combustion and thermal engines (subject to the fundamental laws of thermodynamics) is highly inefficient. It has undesirable side effects (greenhouse gases, urban smog, thermal pollution, acidification of lakes and rivers, etc.). Therefore, it is imperative to seek and adopt alternate renewable energy sources and methods that improve conversion efficiency and diminish fossil-fueled engines' negative impacts. In this respect, waste heat, solar energy, geothermal, and biomass have recently emerged as alternative energy sources. Within these, the renewable thermal sources (such as geothermal and solar energy) and industrial or mobile engine waste heat are treated as low-grade heat sources, as the available temperature is significantly lower compared to that of fossil fuel.

Energy resources can be primarily categorized into two forms: Renewable and Non-renewable energy. In the last couple of decades, renewable energy has caught the various government and private agencies' attention. It has a significant potential to fill the gap between the supply and demand of fossil fuels. We can see that alternate sources like Solar energy or Wind energy have already become popular among the stakeholders.

1

The primary energy source in India is Coal. The energy gap is filled by exporting electricity from our neighbouring countries. As energy is most important for a nation's growth, some serious efforts must enhance its generation. India is geographically diverse with varied topographical features, from the Himalayan range to coastal plains, from the hot desert of Thar to the cold desert in Ladakh. India is situated between the latitudes 804' and 3706' N and longitudes 6807' and 97025' E, and it has a total covered area of 3.167 million square kilometres. India, the second most populated country after China, has a considerable scope of efficient thermally comfortable dwellings.

1.1 Renewable energy sources

1.1.1 Solar Energy:

Sun is considered as the life provider to the earth. The energy that comes in the form of heat and light is a continuous and unlimited energy source. If not utilized, it will be wasted. We have seen lots of developments in solar energy harnessing and have created a new industry sector. It can directly be used in solar water heaters or Solar ducts and can be used passively to generate electricity by using Photovoltaic cells.

1.1.2 Wind Energy:

Due to the Sun's heating, the temperature difference is created across the globe. Due to this, a pressure difference is made, and Winds occur. We can harness this energy with the help of Wind Turbines (WT). Generation capacities are high and can range from 500 kW to 5 MW [1]. In 2015, An inland wind turbine produced 7.5 MW of the highest power.

1.1.3 Hydropower:

Currently, hydropower is the highest energy producer among all renewable energy sources across the globe. Due to the availability of various sources of water, there is enormous potential for power generation. It can be harnessed by creating huge Dams like Three Georges Dam, China, or Small, Mini, or Micro hydropower stations. India has a substantial unutilized potential of generating power using hydro energy [1].

1.1.4   Geothermal Energy:

In this context, ground source heat extraction (or rejection) techniques, providing substantial energy savings, can find wide potential applications in Indian conditions, including space heating, air conditioning, refrigeration, cooking, distillation, drying, spa, fishing, water sports. According to a recent report of MNRE (Ministry of New and Renewable Energy, India), the total energy produced by the renewable energy sector in India constituting nearly 12% of the total energy produced, and it has now increased up to 29.989 GW of power. Wind energy alone contributes almost 67.18% of total renewable energy under the renewable energy sector, while small hydro and solar PV contribute nearly 12.55% and 7.26% of total renewable energy in India, respectively. The remaining 13.1% of renewable energy is harvested from small biomass, bagasse co-generation, and biowaste. But surprisingly, the proportion of geothermal energy in India is negligible as of now in its gross renewable energy production. Among various renewable energy resources, geothermal energy has been regarded as the most efficient heating and cooling method.

Energy production is one of the main contributors to a country's economic growth, but saving energy is a great challenge today. We want to reduce the use of high-quality electricity and encourage the use of renewables. Renewable energy sources (RES) are supplying up to 14 per cent of the world's overall energy demand [2], [3]. Included are biomass, geothermal energy, water [1]. The energy sector in developing countries is seen as a critical sector, with higher demand than its production. In the residential, industrial, and agricultural industries, India consumes more energy than China, Japan, Russia [4]

In the last decade, energy use in buildings has risen dramatically. It was proposed that energy audits in buildings during construction be used to boost energy efficiency in buildings. Developing governments have introduced campaigns and amended stringent regulations against energy use. EU countries have agreed to cut their annual primary energy consumption by 20 per cent by 2020 [5]. The Japanese MOE has launched a campaign to persuade people to wear lighter clothes and to put air conditioning at 28°C.

[6]. In India in 1977, the government set up a Petroleum Conservation Association to promote petroleum products and reduce its reliance on petroleum products [7]. RES can be a solid alternative to non-renewable sources, research undertaken by the US Energy Department says. Over the years, it will be possible to schedule solar power, wind energy, geothermal energy, and ocean power. These sources will replace the existing sources tremendously if they are correctly used.

The energy consumption depends on the temperature and moisture because their changes influence space heating or cooling. An Air conditioning system is usually used in summer in commercial buildings. The heat sink increases the performance and cools the machine compared to normal air. Earth-Air Heat Exchange heating/cooling is a passive way to minimize heat losses in buildings by ventilation and thermal comfort. This device uses geothermal energy by burying in open spaces or under construction in a certain depth a network of pipes of various combinations [8].

1.2   Earth Air Heat Exchanger (EAHE) or Ground Heat Pump (GHP)

Depending on the current scenario, energy saving has become an essential element for economic growth countries like the US, Russia, India have been taking initiatives to save energy. EAHE is a new passive technology efficient to save energy used by many countries to achieve thermal comfort in buildings. EAHE is a non-conventional technique that has found applications in residential buildings with air conditioning systems, greenhouses, commercial buildings which utilize the earth's underground soil temperature.

In ancient times, the Iranian architects used wind towers and underground air tunnels for cooling and heating buildings in 3000 B.C [9]. During the industrial revolution, these natural techniques faded with time. As the world's energy reservoir is depleting fast, governments of different countries are taking initiatives to promote green energy techniques, and EAHE is one such technique.

EAHE system depends on any location's ambient temperature, which can be used for both cooling and heating during summers and winter seasons. During winters, the temperature underground is higher than the ambient temperature and vice versa during summers [10]. Researchers found that the underground soil temperature, also known as the earth's undisturbed temperature remains constant at a depth of 2.5 –3m [9]. EAHE uses a network of pipes buried in the ground. The burial depth of pipes is done between 1.5– 3 m. Earth is used as a heat sink or source. The temperature is either increased or decreased by conduction with underground soil. Then the air is delivered to the outlet maintaining a temperature difference with the ambient temperature.

In summers, the ambient temperature is around approximately 39- 45°C [11], depending on the location. The hot air flows through the buried pipes; the soil's stable temperature cools down the air temperature and delivers it to the outlet. The air flowing in the building is cool, thus maintaining a lower temperature inside the building than the outside temperature, as shown in figure 1.

In winters, the ambient temperature is approximately 4- 9°C [11]. Depending on the location, the same process helps in heating the air, thus maintaining the high temperature inside the building, keeping the inside environment warmer than the outside. The heat dissipated/generated by the soil is transferred to the pipes by conduction which causes the temperature to increases/decrease inside the buried pipes [8]. For the continuous flow of air through the inlet, specific mechanical devices such as fans, blowers, or passive systems are installed to create adequate pressure difference.
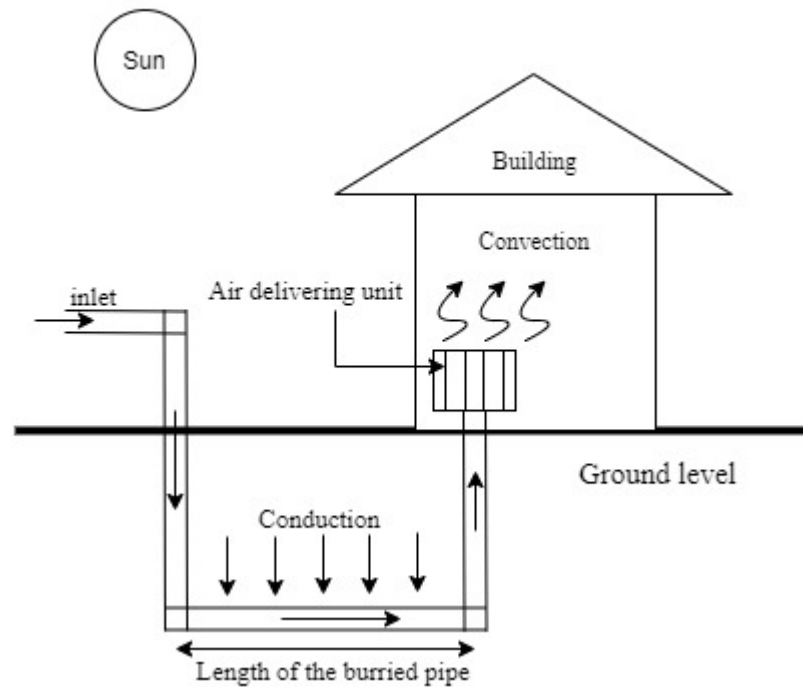
Figure 1: Working Principle of EAHE

The performance of EAHE depends on the pipe material, diameter of the pipe, length of pipe, soil characteristics, moisture content, the temperature difference between earth and ambient air, etc. [8], [9], [12]. The pipe material should have high thermal conductivity like mild steel, PVC pipes, cemented pipes, depending on the soil characteristics [13]. The underground soil temperature is mainly affected by a particular location's climatic condition and soil characteristics [14].

Earth's undisturbed temperature must be known if the soil characteristics have to be determined of any location. The effectiveness of EAHE depends on the depth of the pipe installed, thermal diffusivity of the soil, length and diameter of the pipe, Ambient Temperature of a particular location, the thermal conductivity of the pipe and airflow velocity[13], [9], [16], [17], [18]. It is generally seen that these systems' effectiveness is quite high compared to conventional HVAC systems [19]. Nowadays, researchers have been using EAHE of configurations to study the performance and to save energy. Results showed that EAHE is an energy-efficient system used instead of our prevailing

conventional approach used for thermal comfort. Some research that proved the compatibility of this system with conventional system is discussed here.

Sodha et al. [20] determined the annual cooling potential of an underground air pipe system considering the effect of length, radius, and mass flow rate. The analysis was done for the hot, dry composite climate of Jodhpur and Delhi. Mihalakakou et al. [21] predicted the soil and air temperature below the surface considering the soil's heat and moisture gradient. Results proposed the difference between the inlet and outlet temperature as the energy potential of the EAHE system. Ascion et al. [22] showed that in wet and humid soil having a pipe length of 50 m buried to a depth of 3 m, the best performance of an EAHE system can be achieved. Lee et al. [23] used Energyplus software and created a mathematical model from EAHE. A detailed algorithm was used to calculate the variation in each pipe's soil temperature variation for every simulation time step. Thiers et al. [24] laid several pipes in parallel at the same depth. In this study, a finite volume method with a limited number of meshes was used. Two concentric cylindrical meshes were used for each pipe to study the interaction between several parallel pipes laid at the same depth. One year later, Tittelein et al. [25] developed a new numerical method for EAHE. It showed that heat flux entering the pipe is a function of the air temperature flowing through the pipe. The problem faced using the model mentioned above was that it took a long time to accurately calculate the heat exchanger's behaviour due to the type of mesh required. Bisoniya et al. [19] examined the EAHE system in different seasons and found a high-temperature drop irrespective of the seasons at lower air velocities. The same was validated using a simulation model developed on Computational fluid dynamics (CFD). Ralegaonkar et al. [26] in Nagpur, India, compared the EAHE system with a conventional system and concluded that the EAHE system saves energy up to 90% compared to traditional methods. Chaudhary et al. [27] used PVC pipes or mild steel pipes; he used bamboo and soil-cement mixture plaster. It was seen that it reduced humidity by 30-40 % and reduced outlet temperature by 30-35%. Thus, all design parameters (pipe material, the pipe diameter, length of pipe, soil characteristics, moisture content, temperature difference between earth and ambient air) contribute to the performance and save energy.

1.3 Classification of EAHE or GHP

The EAHE systems are designed based on three configurations: open-loop and closed-loop, and hybrid systems [28], [29].

1.3.1 Open-loop System:

The ambient air is passed through the buried pipes for pre-heating or pre-cooling of air, as shown in figure 2. Then the air passes through a conventional system to cool down or get warm-up before entering the space. The atmosphere is then passed away through ventilation. Woodson et al. [30] used an open-loop EAHE design with PVC pipes having a length of 25m, diameter 125mm buried at a depth of 1.5m. The pipes were laid in a serpentine pattern. It was seen the air drawn from outside reduces temperature by more than 7.5°C. The outdoor temperature varied from 25°C to 43°C, and the soil temperature of 30.4°C remained the same at a depth of 1.5m.
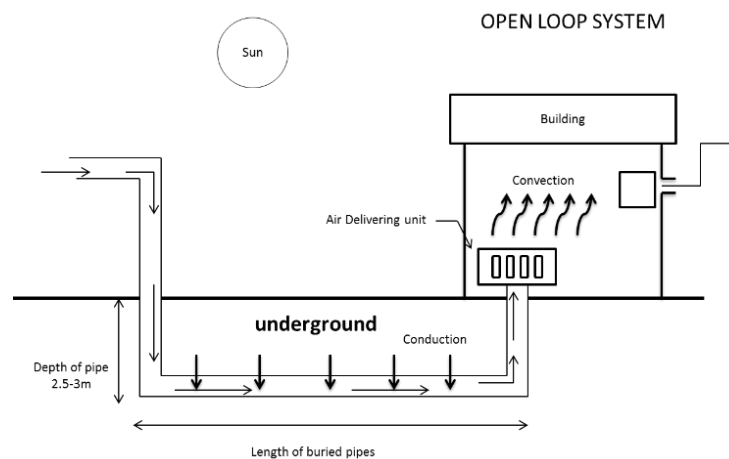
Figure 2: Open Loop System

1.3.2 Closed-loop system:

Closed-loop systems are also known as earth coupled systems, as shown in figure 3. Air sucked from the inlet travels through a loop of pipes buried underground and extracts the heat from the ground [29]. The ground loops are arranged either vertically

or horizontally. The vertical loops are more expensive than a horizontal loop, and also, closed-loop is efficient than the open-loop system. A closed-loop system reduces the problem of humidity.
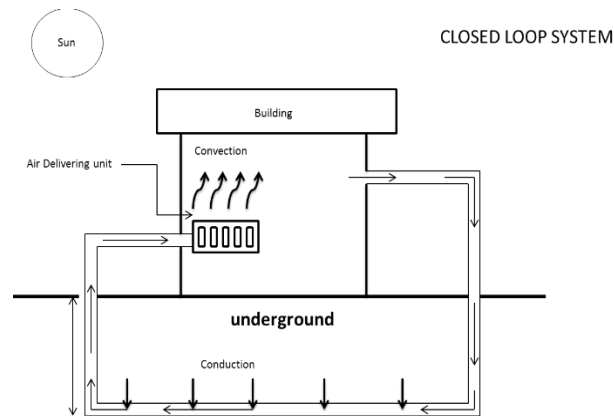
Figure 3: Closed Loop System

1.3.3   Hybrid Systems:

The EAHE is coupled with other heating/cooling devices such as air conditioners, heaters, solar chimneys, solar air heaters. These devices improve the comfort and efficiency of the EAHE systems. Researchers like Jakhar et al. [31] coupled the Earth to air heat exchanger with a solar air heating duct. The aim was to evaluate the heating potential of EAHE with or without a solar air heating duct. TRNSYS 17 was used as the simulation tool. Results were validated with an experimental setup in Ajmer, India. The evaluation was done for inlet flow at different inlet temperatures, and it was concluded that at a depth of 3.7m and length of 34m, optimum outlet temperature could be achieved. Sikarwar et al. [32] used the EAHE system with an air conditioner to reduce energy consumption and improve the COP. Results showed that the ground-coupled condenser is seen as feasible under extreme summer and winter seasons with an air conditioner. Chlela et al. [33] used EAHE with a heat recovery balanced ventilation system to investigate energy consumption and thermal comfort. It was found that the EAHE system reduces energy consumption and control the CO_2 emissions and

to ensure good thermal comfort. Nowadays, hybrid EAHE has become one of the prominent technologies to increase the efficiency of the system.

The EAHE is also classified based on pipe layout in the ground and according to the mode of arrangement [34].

Based on pipe layout, the EAHE classified as:

- Horizontal / straight Loop
- Vertical Looped
- Slinky/spiral Looped
- Pond / Helical Looped
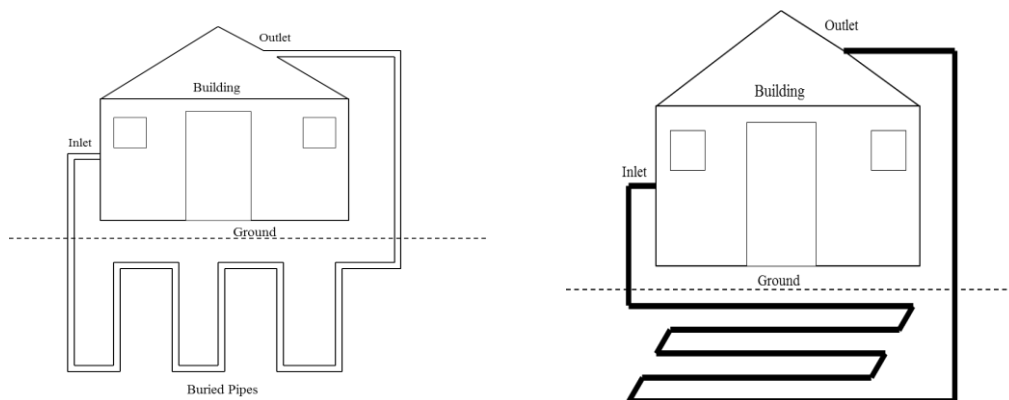
Figure 4: Horizontal Loop and Vertical Loop System

Based on mode of arrangement, EAHE is classified as:

- One tube system
- Parallel tube system

One tube system is not appropriate to meet the requirements of an air conditioning system in a building. This is because the tube is too large for use in generation. Parallel tube systems are used to reduce the pressure drop and increase the system's thermal performance.
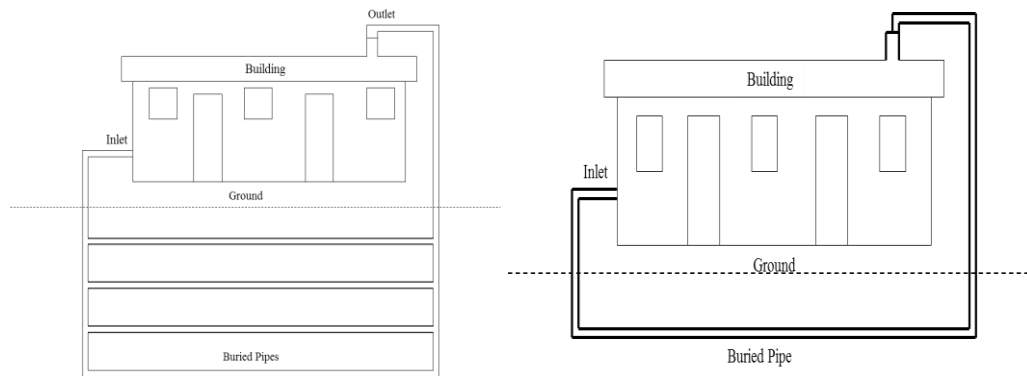
Figure 5: Parallel Tube and One Tube System

1.4   Advantages and Disadvantages of EAHE

The EAHE systems have several advantages over the conventional system [9]:

1. Air is used as a working fluid.
2. It consumes less energy as compared to prevailing conventional systems.
3. Design is simple hence requires less maintenance and low cost.
4. Pollution is minimized as no refrigerant or compressors are used in this system.

The disadvantages are:

1. The cost of installation is high.
2. Condensation occurs in the pipes. The condensed water can be pumped out by using a small submersible pump.
3. Convection occurs in the pipes; no uniform temperature is achieved.
4. As the refrigerant used is air, microorganisms' growth can become one of the causes of a ventilating system coupled to the system. This causes a decrease in the quality of air.

Thus, the installation of EAHE with appropriate design parameters can be a perfect alternative to conventional systems.

1.5 Advantages and Disadvantages of GSHP

Advantages:

1. High-efficiency results in lower energy consumption cost
2. Lower maintenance cost
3. Lower life cycle cost
4. No outdoor equipment
5. Greater occupant comfort
6. All electric components can be powered by renewable energy

Disadvantages:

1. The initial cost can be significantly higher than conventional systems
2. Not all system types are feasible in all locations
3. Limit pool of qualified designers and installers in many locations

Thus, GSHP systems longer life cycle giving more returns as the payback period is below ten years.

2 LITERATURE REVIEW

The most used system to obtain comfort in residential buildings, offices is the conventional air conditioning system. The air conditioning system's working principle is to condition the air, transport it, and introduce it to conditioned space. The air conditioning system uses a large amount of energy and causing depletion of the ozone layer due to the emission of CFCs. The Kyoto Protocol given by United Nations Framework Convention on Climate Change (UNFCCC) emphasizes reducing greenhouse gas emissions.[35], [36]. Passive techniques are introduced in HVAC installations so that overall energy consumption can be reduced. One such passive technique is EAHE that uses the earth as the heat sink. Air is the transfer medium for summer cooling and winter heating. When air flows through the pipes, heat exchange between air and earth takes place. This concludes that the outlet's temperature is higher/lower than the ambient temperature [9].

Many ancient Greeks, Persians, and Iranian Architects have used this technology indirectly [21]. In the 19th century, Wilkinson designed a Barn; to cool the barn during summertime, he buried a 500ft underground passage [37]. As mentioned earlier, Iranian architects also used underground air tunnels and wind towers for passive cooling. For many decades, the EAHE system has been used in conjunction with solar chimneys or air conditioning systems. EAHE system is probably the most growing alternative renewable energy in the world. With the increasing demand for energy savings, places like Europe, Germany have grown their market widely in recent years [38]. A 10% increase has been seen in installations in about 30 countries over the last ten years. In places like South Algeria, where four-fifths of the land is desert with a desert climate, where during summer maximum temperature rises to 45°C and during winter temperature lower below 1°C, the EAHE system cannot be used all alone [39]. Under this condition, the EAHE system is made in conjunction with an air conditioning system.

Several researchers around the globe had investigated the performance of EAHE using various numerical and computational methods. The summary for various studies is tabulated in Tables 1 and 2.

2.1 Experimental studies conducted across the globe:

Fard et al. [40] in Northeast Iran made a system that comprises two parallel horizontal pipes. The project aimed to evaluate the effect of parameters such as burial depth, pipe length, air velocity, pipe material. The simulations were based on factorial design. Results show that the average relative humidity was 67% with an average temperature of 3.8°C (heating mode) and the average relative humidity is 14% with an average temperature was 36.5°C (cooling mode). With increases in burial depth, the soil temperature and pipe length increase for both heating and cooling modes. It was also observed that the differential temperature of galvanized pipe is more than PVC because the heat transfer coefficient of galvanized pipe is more than PVC. There is no significant effect seen in the pipe material's material as pipe material does not vary the temperature variation. Based on the previous data, it was found that COP cooling is 5.5, COP heating 3.5.

Ozegener et al. [9] made an experimental setup with ambient temperature 18.67°C and relative humidity of 48.16%. It was found that the average temperature for the greenhouse was 21.5°C and relative humidity 40%. Results showed that the average heating capacity obtained from the setup was 7.67 kW. Thus, it concluded that effective use of EAHE with a suitable technology is beneficial to the climate of Turkey.
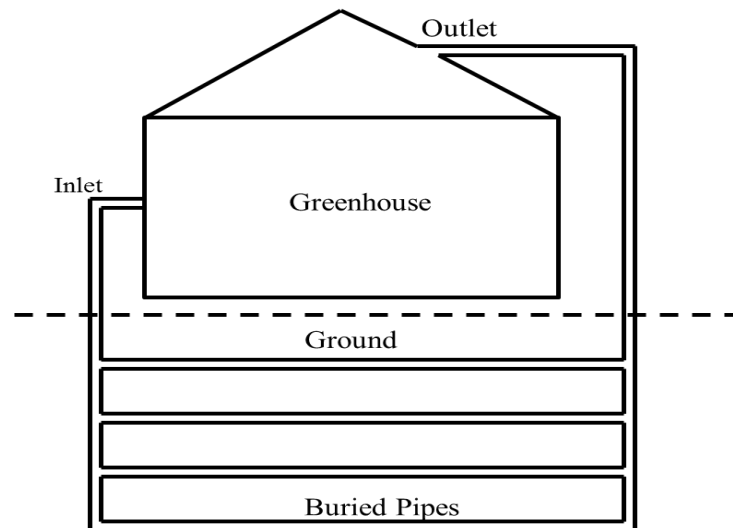
Figure 6: Schematic diagram of EAHE coupled with Greenhouse [35]

Mongkon et al [35] considered three seasons; winter, summer, and monsoon in Chaing Mai for HETS cooling in Thailand's tropical climate. The cooling performance and condensation in pipes were evaluated. The experiment was concluded with a series of pipes placed in a serpentine manner considering fully developed Turbulent Flow. The temperature difference between inlet and outlet is studied by regression analysis. A high-temperature difference during the summer season was observed. In condensation analysis, it was found that saturated temperature decreases due to the dew point temperature. The results also indicate that maximum COP was obtained during summers in comparison with the other two seasons.

Goswami et al. [41] used corrugated plastic pipe for his experimental setup conducted in Floridas. The experiment was performed considering the soil having high moisture content. The operating time for the EAHE system was 8-12 hours/day. A heat pump circulates the air at the outlet. It was observed that if the air was spread uniformly throughout the tunnel, COP was improved by 8%. The open-loop tunnel used 14 kWh of electricity during the cooling period and 52 kWh during the heating period. This indicates that the EAHE consumes less energy than conventional AC. The author also recommends the EAHE for agricultural buildings. It was also seen that the payback

period was approximately 20 years. Thus, the use of the multi-pipe system instead of using a single pipe is more cost-effective.

Vaz et al. [42] considered an experimental and numerical simulation to reduce conventional energy consumption. Vaz et al. setup the experiment in Viamas, Brazil. The numerical solution was solved based on the Finite Volume Method (FVM), and turbulence was tackled with the Reynolds stress model. The computational modeling was done using GAMBIT and FLUENT. The numerical solutions were validated against experimental results. The three ducts' temperature variation shows that the magnitude of air temperature decreases in the same soil temperature on moving along the length. There was a difference of 15% with the numerical model proposed during validation. Also, it was found that if the depth is more than 2m, the operating potential for heating and cooling was higher by 8°C and 4°C, respectively.

Bojic et al. [37] investigated the performance of ATEHE for the summer and winter seasons in Athens, Greece. Space was heated by using a heater during winters and cooled by using an air conditioning system during summers. At ambient temperature, 20°C results indicate that the energy use ratio for building increases with the increase in the pipe length. It was also observed that the energy use ratio in summer days was higher than in winters. In summers, the energy expenditure was 11d/MJ-s with 10 m long pipe, and the lowest was 7d/MJ-s on the application of two pipes for ATEHE. The author suggests that when the length of the pipe L< 17m, it is better to use four pipes instead of two, thus making the ATEHE cheaper. The temperature at the outlet was found three times higher in summer than in winters. This clearly shows that the ATEHE is more energy-saving and cheaper in summers than winters.

Mihalakakou et al. [21] predicted the thermal performance inside the tube. The model was developed within ANSYS. The influence of temperature due to ground surface temperature at any point of the pipe was analyzed. The proposed model was validated against the experimental data and was predicted the temperature of the circulated air and temperature distribution contributes to the performance of EAHE.

Silva et al. [43] modeled a computational model to predict the thermal behavior of EAHE. The results were checked for every time step for two years. The average soil temperature considered was 29.1 °C for the entire computation simulation, and the temperature variations were checked at every point from 1-5m and were plotted at the outlet. The results indicate that an increase in depth causes a decrease in temperature amplitude variation because the temperature becomes constant at 3m deep. Thus, this configuration causes a reduction of 8°C in summers and an increase of 2°C in winters.

Su et al. [44] developed a computational model with a 1D implicit transient convection-diffusion model for air temperature and humidity and a 1D explicit heat conduction sub-model for the rock temperature. The mass transfer coefficient is large (h_d) varies from 0.0001 – 0.0005 kg/m^{2}s. On analyzing, it was found that the difference in outer temperature and humidity between the two simulations is minimal.
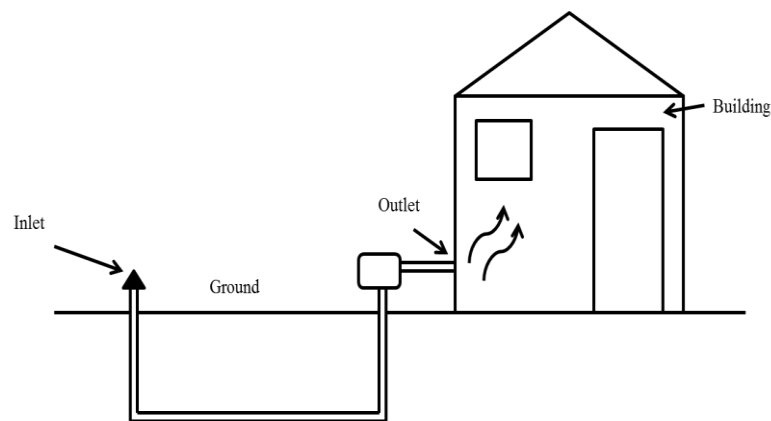
Figure 7: Schematic diagram for EAHE coupled to a building [45]

Benhammou et al. [45] studied the thermal performance in the steady-state and transient condition in Algerian Sahara during July. The author introduced a new term DF, which is a function of the buried pipe's length. The results indicate that as the length increases, DF decreases; thus, the temperature at the outlet increases. The study states that the outlet temperature is a function of the diameter of the buried pipe. Again, as the length is increased, the mean efficiency also increases but COP decreases; also, on studying the influence of pipe diameter, as the pipe diameter increases, COP decreases. This increase in pipe diameter reduces the pressure losses and increases the thermal

potential, but the cooling potential was reduced, resulting in a decrease in COP. DF is proportional to the pipe diameter. Thus, EAHE with larger pipe diameters has more heat transfer than smaller diameter pipes.

Yang et al. [46] predicted the performance of EAHE subjected to Harmonic thermal environments. The experiment was conducted in Changqing, China, considering a cylindrical coordinate system. The total time for the numerical simulation was t =1000s. It was found that with an increase in depth, the outlet temperature decreases. It was observed that the annual fluctuating amplitude decreases with depth and attains a particular value when depth exceeds 7m. Results show that the outlet temperature initially drops then increases with an increase in radius. The cooling and heating capacities are a function of outlet temperature and airflow rate; as the flow rate increases, the cooling /heating capacity increases.

Santamouris et al. [47] performed a parametric analysis performed on a glass greenhouse of a 1000 m^2 area having four buried pipes in Athens, Greece. TRNSYS software was used as a simulation tool. A relationship between change in pipe length and outlet temperature was observed. The results show that the outlet temperature increases more during July and August, but August's greenhouse temperature was higher due to the time lag of the underground temperature, which delays the temperature variation at different depths. Also, an increase in the pipe radius causes high indoor temperature and high outlet temperature because of the high convective heat transfer coefficient. It was observed that the indoor temperature increases with an increase in depth of the pipe, but the cooling capacity increases with an increase in depth. The indoor temperature also increases with an increase in the velocity of air. Thus, due to an increase in mass flow rate, the outlet temperature increases.

Yassine et al. [48] coupled EAHE with a mechanical ventilation system for thermal comfort of a typical house conducted in Lebanon. The study aimed to use regional materials such as strawboards for insulation and Hempcrete to decrease buildings' embodied and operational energy. For controlling the amount of ventilation air, the author used PID (Proportional Integral derivation). The house was divided into two

thermal zones: Living Zone and Bedroom Zone. ASHRAE recommended that the lower limit of airflow rate was 7.5 ACH (air change/hour), and the upper limit flow rate was 25 ACH. During occupancy, the PID controller was activated in winters where $T_{room} < T_{winter}$, so T_{out} of EAHE can moderate indoor temperature as $T_{out} > T_{room}$. Again, the controller was activated during summers when $T_{room} > T_{summer}$ so that outer temperature can moderate indoor temperature. The energy and mass balance equations were solved to predict the indoor air temperature for each zone. The program was developed using MATLAB and was validated against TRNSYS (2009). It was observed that there was a difference of $\pm 4\%$ between space temperature obtained numerically and space temperature predicted by TRNSYS.

Serageldin et al. [49] experimented with Egyptian weather conditions where the soil temperature distribution was studied. An unsteady, 1D quasi-mathematical model was developed for energy equation using MATLAB. A CFD analysis was done to estimate the air and soil temperature. The mathematical and simulation results were validated against experimental results. Also, a mathematical model was developed to predict the temperature profile along the length and time. An explicit finite difference method was used to solve the governing equations. The results indicate that the inlet temperature depends on ambient temperature and outlet temperature; thus, the convective heat transfer has less influence than conductive heat transfer. Thus, the soil temperature increases with an increase in the outlet temperature. Also, as the pipe length was increased, the temperature inside the pipe along with the length increases but decreases at the outlet due to heat losses to the surrounding. The CFD simulations indicate that the temperature increases with depth during winters and vice versa. Also, a parametric study was conducted to study the design parameters considered in the simulation. The results for the study show that as the pipe diameter was increased, the air temperature decreases, thus decreasing the convection heat transfer. The effect of outlet temperature variation for three different pipe materials was also considered in the same study. It showed that the outlet temperatures for all 3-pipe materials were similar. Thus, the pipe material has a more negligible effect on the performance of EAHE.
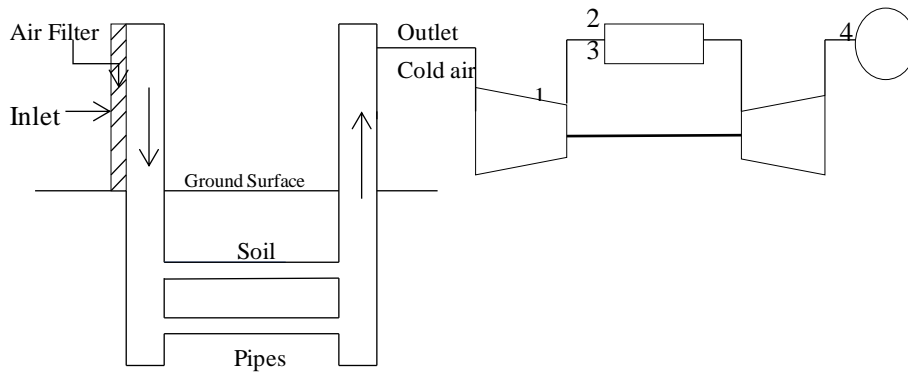
Figure 8: Schematic diagram of EAHE installed in gas turbine plant [50]

Barakat et al. [50] studied the application of EAHE as an inlet of a gas turbine. The thermal performance of EAHE, a transient 1D model, was developed using MATLAB. A mathematical model was validated against an experimental study conducted in Damietta Power Plant, North Carolina. Results showed that the outlet temperature decreases with the decrease in length. Thus, a longer pipe length provides more heat exchange. It was also seen that as the pipe diameter and velocity increase, the outlet temperature also increases and decreases, respectively. The fuel consumption was evaluated, which showed a drop of 4.4% on using EAHE as an inlet to the gas turbine. Thus, a longer tube, smaller diameter, placed deep and low inlet air velocity give lower outlet temperature using EAHE increases the power output. Uddin et al. [51] investigated the performance of EAHE to maintain thermal comfort in Bangladesh. Life cycle energy and GHG emission analysis are done using cradle to grave assessment. The experiment was conducted in an office for two seasons, winter (11°C, 91% RH) and summer (34°C, 77% RH), with an AC of 1 TR was already present in the room. A small fan of 30W was placed to ensure the flow of air through the coil. For the cradle to grave analysis, four stages were considered. Stage I: extraction of raw material, Stage II: manufacturing of heat exchanger material [PVC and MS].

Stage III: installation and use and Stage IV: disposal at the end of life. The thermal performance was estimated for both seasons, and results showed that the outlet temperature was around 23-24°C for both seasons. But the outlet humidity during

winters was 45-50%, and during summers, RH was 30-70%. In the life cycle assessment, the total life cycle energy for PVC= 307 MJ and MS= 96.4 MJ. Thus, MS pipe can be used as pipe material from a life cycle energy point of view as MS generated lesser energy than PVC. The GHG analysis observed that the magnitude of emission in MS is lower than PVC. Also, the CO_2 emission for PVC and MS was 86kgs and 20 kg, respectively. Thus, MS is preferred over PVC for the cases. As specified before, 1 TR of AC consumes 9.6 kWh of energy per day. When EAHE is coupled to AC, it saves up to 288 kWh per month during both seasons. Thus, using AC with EAHE saves more energy than single AC.

Gan et al. [52] formulated a model in FORTRAN to study the thermal performance of EAHE. A 3D mass and energy equation and two interfaces were considered to check the heat and moisture transfer: between earth and atmosphere between the heat exchanger and supply air. The simulation of the present study was run on FLUENT for two modes continuous and intermittent modes. In continuous mode, the heat is transferred from the soil to air at any given time. In intermittent mode, this occurs for a specific period when the air is preheated; only then heat transfer takes place. Simulations were done at different lengths (10 to 40 m). There was a rise in temperature from 5 - 6.6°C for ambient air. It was seen that the heat transfer rate decreases day by day with a decrease in soil temperature. Thus, with an increase in the length, the rate of heat transfer and temperature rise decreases but overall heat gain increases. Also, the author found that the thermal and moisture interaction between heat exchanger atmosphere and soil has a significant effect on the rate of heat transfer.

Rodrigues et al. [53] employed constructional design for EAHE to obtain the highest thermal potential. The numerical simulation was performed using Ansys FLUENT. The computational domains were developed in Ansys workbench and discretized in Gambit. Time was taken as a function, and the validation was done against an experimental setup constructed in 2007. Adrain Bejaan created the constructional design in 1997. In this experiment, five different configurations of EAHE were evaluated. This design is applied to employ volume fraction parameters to find the optimal installation. For installation I, the high thermal potential was reached during December. In Installation

2, a stable behavior of thermal potential was seen. In this, the horizontal spacing of the pipe was increased, so the thermal potential was also increased. In installation 3, the volume fraction concept was considered, and the highest value of thermal potential was seen in May, June, July, October, November, and December. There was no significant change in thermal potential seen during January and February. In installation 4, Thermal potential has an intermediate value. Installation 5 shows superior performance in heating and cooling. Thus, increasing the ducts and reducing the duct diameter constant air volume fraction can be maintained.
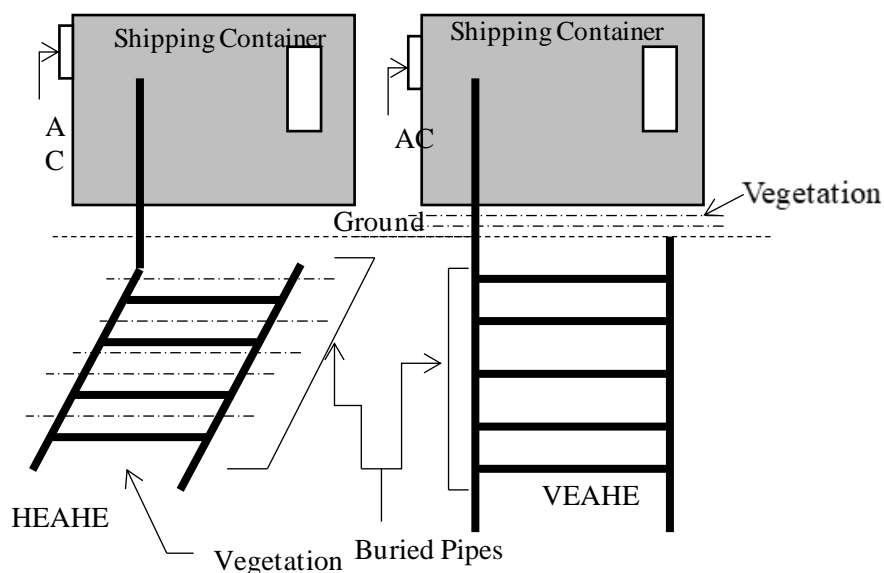
Figure 9: Schematic diagram of HEAHE and VEAHE [54]

Ahmed et al. [54] investigated the thermal potential of EAHE by experimenting at Rockhampton, Australia, using two shipping containers, one connected with Vertical EAHE [VEAHE] and the other with horizontal EAHE [HEAHE]. Fans were installed to suck the air inside the pipe inlet — twenty PVC corrugated pipes for each configuration. For increasing the cooling effect, small trees were planted to cover the underground pipe. The schematic diagram of the setup is given in figure 7. A CFD model was formulated considering the flow inside the corrugated pipe to be turbulent. The discretization was done using the PRESTO scheme. The soil temperature analysis was done for different depths and showed that the soil temperature increases with a

decrease in-depth on a summer day. For the measure of the performance of HEAHE, the VEAHE was turned off and vice versa. Simulation results show that the average room temperature for HEAHE was slightly larger than VEAHE. Thus, it concluded that VEAHE provides more reduction in temperature drop than the HEAHE. So VEAHE is preferable to use for Australian weather.

Sansui et al. [55] studied the capacity of Malaysian soil for the application of EAHE. This research aims to predict the soil temperature for different soil surface conditions. The experiment was set up at the Gombak campus of International Islamic University, Malaysia. Three different soil surface conditions were considered. The soil condition was 1. Bare and short grass 2. Sheltered by layers of recycled timber palette, and 3. Layers of used tires insulated it. A parametric analysis that estimates the soil temperature at an optimum depth was done to find the appropriate soil surface condition. The simulations for the present study were conducted in Energy Plus software. The soil temperature was investigated, and it was observed that soil temperature ranges between 21.5- 34.1°C. All three types had the minimum soil temperature for soil shaded with timber palette and insulated with used tires. Simulating all three soil surface conditions by considering the solar radiation, soil shaded with timber palette, and insulated with used tires shows the best results. Thus, low soil temperature gives better heat exchange and more cooling temperature. Hence the EAHE cooling is feasible in Malaysia's climate.

The climate of India ranges from tropical to the south and temperate to the north. The Himalayas and the Thar Desert influence the climate of India. With geothermal energy, about 6.5% of electricity generation is achieved [38], but India is at a nascent stage for power generation using geothermal energy. India's Geological Survey reported about 340 geothermal hot springs [38] that conserve geothermal energy in India. EAHE has not much influenced the Indian market.

Table 1: Summary of the various studies conducted around the world.

Author	Place/ Year	Season	Material	Length of pipe [m]	Diameter of pipe[m]	Depth of pipe [m]	Temperature range [°C]	Velocity range [m/s]	Temperature variation [°C]	Variable	Others
Goswami et al. [40]	Florida, 1993	-	-	30.48	0.3048	3.6576	23.89-33.05	-	26.67-28.33	Inlet Temperature	-
Li et al. [72]	Harbin, China, 2006	Summer	HDPE	-	0.0325	47.6	-	-	0.75	Ground Temperature	-
Ford et al. [39]	North east of Iran, 2011	Winter	PVC and galvanised mild steel	20	-	4	35-43	0.4-30	-	Material of Pipe	-
		Summer								Soil Temperature	-
Vaz et al. [41]	Viamas ,Brazil, 2011	Summer	PVC	Duct A: 0.11	-	2	30	-	25	-	-
		Winter	-	Duct B : 0.11	-	2	12.8	-	19	-	-
		-	-	Duct C: 0.10	-	5	-	-	-	-	-
Ozegener et al. [8]	Turkey, 2011	-	-	47	-	3	18.67	-	21..5	-	greenhouse temperature

Author	Place/Year	Season	Material	Length of pipe [m]	Diameter of pipe[m]	Depth of pipe [m]	Temperature range [°C]	Velocity range [m/s]	Temperature variation [°C]	Variable	Others
Mongkon et al. [34]	Thailand, 2013	Winter	Iron	38.5	0.08	1	24.5	9	20.88	-	-
		Summer					28.8		21.37	-	-
		Monsoon					28.6		26.8	-	-
Benhammou et al. [62]	Algerian Sahara, 2013	Summer	PVC	23.42	0.10-0.30	-	29	2.0-5.0	22.3-23	Diameter of pipe	-
									24	Length of pipe	
						-	-	-	27.8	Velocity of pipe	-
Yassine et al. [47]	Lebanon, 2013	Summer	-	-	-	-	28	-	26.88	Mass flow rate	-
		Winter	-	-	-	-	16	-	16.64		-
Chiesa et al. [56]	Imola, Italy, 2014	Summer	PE	2240	0.25	-	-	-	-	-	-
Sanusi et al. [57]	Malaysia, 2014	-	-	-	-	-	-	-	21.5 - 34.1	Soil type	-
Vaz et al. [58]	Viamas ,Brazil, 2014	Summer	PVC	A: 0.11	-	1.6	18.8	-	12	Burial Depth	-
		Winter		B: 0.11		0.6		-		-	-
				C: 0.10		0.5		-		-	-
		Winter		57	0.45	3	12.78	-	21-24	Configuration	Passive

Author	Place/Year	Season	Material	Length of pipe [m]	Diameter of pipe[m]	Depth of pipe [m]	Temperature range [°C]	Velocity range [m/s]	Temperature variation [°C]	Variable	Others
Yu et al. [59]	Omaha, USA 2014		Culvert Steel					-	20–27.5	Configuration	Active
Hatraf et al. [61]	2014	Summer	PVC	60	0.11	-	-	-	-	Mass flow rate	-
Li et al. [66]	2014	-	Culvert steel	57	0.45	3	-	-	14.6	Burial Depth	-
Yang et al. [45]	Changqing, China, 2015		-	-	-	-	20	0.5	1.4	Diameter of pipe	small change dia from 0.05 to 1 m
									15	Length of pipe	
		-							13	Mass flow rate	
Mohamed et al. [53]	Marrakech, 2015	Winter	PVC	72	0.15	2.2-3.2	4.2-11	-	16.7-21.2	Time	-
		Summer					44.6		24.8	Time	-
Jassim et al. [71]	Bagdad Iraq, 2015	Summer	-	-	-	-	-	-	25.3-28.2	Burial Depth	
Serageldin et al. [48]	2016	Winter	PVC	5.5m	0.0508	2	14.7	1-3.9	22	Burial Depth	-
									15.8	Velocity of pipe	
Uddin et al. [50]		Winter	PVC	14.3256	0.0381	2.43884	11	-	21.3	Time	-
		Summer					34		20.5	Time	-

Author	Place/Year	Season	Material	Length of pipe [m]	Diameter of pipe[m]	Depth of pipe [m]	Temperature range [°C]	Velocity range [m/s]	Temperature variation [°C]	Variable	Others
	Bangladesh, 2016						-		23–24	-	-
Chela et al. [33]	France, 2016	Winter	-	-	-	-	5	-	-	Configuration	Nancy
							8			Configuration	La Rochella
							10			Configuration	Nice
Mihalakakou et al. [21]	1994	Summer	Plastic	14.8	0.15	1.1	-	10.5	17-33.5	Burial Depth	-
Santamouris et al. [47]	Athens Greece 1995	-	-	50	0.2	1.5	37-42.3	8	23-36	Diameter of Pipe	-
Bojic et al. [37]	Athens Greece 1996	Winter	PVC	50	0.15	2.4	8	-	20	Length of pipe	-
		Summer					16				-
Vaz et al. [42]	Viamas, Brazil, 2011	Summer and Winter	PVC	A:0.11	-	2	30	-	20	-	-
				B: 0.11		2				-	-
				C: 0.10		5	16	-	19	-	-

27

Author	Place/Year	Season	Material	Length of pipe [m]	Diameter of pipe[m]	Depth of pipe [m]	Temperature range [°C]	Velocity range [m/s]	Temperature variation [°C]	Variable	Others
Su et al. [44]	2012	-	-	900	-	-	19	-	17.6	Error analysis	-
Silva et al. [43]	2013	Winter	PVC	25.77	0.11	1.0-5.0	-	-	2	Burial Depth	increase
		Summer							8		decrease
Vaz et al. [53]	Brazil, 2014	Summer and Winter	PVC	A:0.11	-	1.6	18.8	-	12	Burial Depth	-
				B: 0.11	-	0.6				-	-
				C: 0.10	-	0.5				-	-
Ahmed et al. [54]	Queensland, Australia, 2014	-	PVC	8	0.021	-	21.01	3.4	24.61	Configuration	VEPC
									24.58	Configuration	HEPC
									23.05	Configuration	VEPC
									23.85	Configuration	HEPC
Ariffin et al. [56]	Malaysia, 2014	Summer	PVC	30	0.076	1	36.46	0.5	30.345	Material of pipe	-
			PE						30.231	Material of pipe	-
			Steel						30.248	Material of pipe	-
			Copper						30.25	Material of pipe	-
Benhammou et al. [57]	2014	Summer	PVC	-	-	2	45	-	44.991	Crossectional area	-
									44.46	Height of tower	-

28

Author	Place/ Year	Season	Material	Length of pipe [m]	Diameter of pipe[m]	Depth of pipe [m]	Temperature range [°C]	Velocity range [m/s]	Temperature variation [°C]	Variable	Others
Xamána et al. [58]	Mexico, 2014	Winter	-	5	0.15	10	-	-	0.5	Configuration	Mexico City
									5.8	Configuration	Marida City
									3.3	Configuration	Juarez City
Carlucci et al. [59]	2014	-	-	-	-	-	-	-	no monitored results	-	-
Mendez et al. [60]	Mexico, 2014	-	-	-	-	-	-	-	-	-	-
Sansui et al. [61]	Malaysia, 2014	-	-	-	-	-	21.9-34.8	-	27.2 - 30.5	Burial Depth	-
Gan et al. [52]	UK, 2015	-	HDPE	-	0.2	1.5	10	2	17.6	-	-
Rodriguez et al. [53]	Viamao, Brazil 2015	-	PVC	26	-	-	-	-	-	-	-
Ahmed et al. [54]	Rockhamton,	-	-	-	-	-	22.4-26.4	-	22.61-25.32	Configuration	HEAHE

Author	Place/ Year	Season	Material	Length of pipe [m]	Diameter of pipe[m]	Depth of pipe [m]	Temperature range [°C]	Velocity range [m/s]	Temperature variation [°C]	Variable	Others
	Australia, 2015								23.48-26.3		VEAHE
Niu et al. [62]	USA, 2015	-	Steel	57	0.45	3	30	-	16	Soil Temperature	-
Niu et al. [63]	USA, 2015	-	-	57	0.45	3	26-34	-	15	Surface temperature	-
									13	Diameter of Pipe	-
Serageldin et al. [49]	2016	Winter	Steel and Copper (Cu)	5.5	0.0508	2	14.7	1.0-3.9	18.7	Diameter of Pipe	-
									19.9	Length of pipe	-
									19.2	Velocity of pipe	-
			PVC						19.7	Material of Pipe	-
			Steel						19.88	Material of Pipe	-
			Copper (Cu)						19.8	Material of Pipe	-
Barakat et al. [50]	2016	-	-	24.7	0.3	7	40	1.5	29	Length of pipe	-
									35.4	Diameter of Pipe	-
									30.5	Velocity of pipe	-
Ascione et al. [64]	Italy, 2016	Summer	-	50	0.3	4		-	-	-	energy demand

Many Indian types of research have been initiated to study the potential of buried pipes. The parameters for the studies are given in Tables 2 and 5. Ghosal et al. [65] conducted an analytical study in New Delhi, India. The pipes were arranged in a serpentine manner with a mass flow rate of 100 kg/h. The GHE performance was evaluated based on the length of the pipe, the air temperature inside the greenhouse for both seasons. The results indicate that with an increase in the buried pipes' length, the air temperature inside the greenhouse increases in winters and decreases in summers. Thus, it concluded that the performance of the EAHE is a function of the length and temperature of the greenhouse.

Bansal et al. [66] developed a model in FLUENT to reduce heating loads in a building. A transient and implicit model based on CFD was developed and was validated against a setup in Ajmer (winters). Two types of materials were considered Mild steel and PVC. CFD simulations were performed in FLUENT 6.3. Results show that as the air velocity increases, the outlet temperature decreases due to a rise in the materials' heat transfer coefficient. On keeping the same input conditions for both the materials, it was seen that there was a small temperature difference at the outlet of the pipe due to the high coefficient of friction. It can be concluded that convective heat transfer plays an essential role than conductive heat transfer. It can also be concluded that the performance of EAHE does not depend on the material of the pipe. Results show that EAHE saves 38% of electricity than an electric heater with an efficiency of 95%. Thus, the pipe's material is not of much concern, so that a cheaper material can be used.

Bansal et al. [15] conducted the same experiment for the summer season, considering the same input parameters. When a comparison was made, there was 0- 11.4% variation with the experimental results. It was seen that as the air velocity increases, the outlet temperature increases for both the materials, a minimal temperature difference at the outlet of the pipe. The maximum hourly energy gain was 3.1 MWh, observed at 5 m/s, in the same velocity range. The COP obtained was 1.9- 2.9. Thus, the material of the pipe does not influence the performance of EAHE.

Chel et al. [67] formulated a thermal model of vault roof building coupled with EAHE solved by Ranga Kutta approach. The adobe house has a room air temperature higher than the ambient air in winters and lowers the ambient temperature in summers by 5-15°C, which increases the energy-saving potential. The adobe house analysis was done under three conditions (Before the renovation, after renovation, with EAHE for six rooms). The total energy saving potential was obtained between 4183-10321 kWh/year for all three cases, and the CO_2 emission ranged between 7-16 tonnes/year. The average seasonal energy efficient ratio for heating was 1.8 and for winters were 2.9. Thus, it can be concluded that EAHE is more efficient for heating than for cooling.

2.2 Numerical studies conducted across the globe:

Ahmed et al. [54] focused on comparing the two different pipe systems of earth pipe cooling. The thermal performance was estimated using Ansys FLUENT. The experiment was conducted in Queensland, Australia. Two containers were considered the modeled room connected to the Vertical Earth pipe cooling system (VEPC) and the other was connected to the Horizontal Earth pipe cooling system (HEPC). There was 20 corrugated PVC pipe connected to each arrangement. For estimating the performance of VEPC, the HEPC was turned off and vice-versa. The 2D thermal model was generated in Ansys FLUENT 13.0. Simulated results show that the room temperature for the VEPC system was 23.05°C and HEPC 23.85°C. When a comparison was made with the predicted temperature, it was found that the VEPC system has 1.82°C less and HEPC system has 1.03°C less than the measured value. Thus, VEPC gives better performance than the HEPC system. On studying the VEPC and HEPC system's thermal performance on the climate of Australia, the VEPC system shows better performance than the HEPC system. The simulated results were validated with the measured data at the pipe inlet at different points.

Yu et al. [68] investigated a coupled geothermal system with an earth tube and solar chimney in Omaha, USA. Three experimental tests were conducted in a sequence [passive, active, and passive]. In this experiment, an analysis of indoor air condition, cooling capacity, and soil temperature was carried out. The design for the cooling load

was done using software TRACE 700. A solar collector was constructed with a solar chimney. This hybrid system was built to provide cooling and ventilation for the solar energy research test facility. The experiment was monitored both natural (Passive) and forced cooling modes. During the passive cooling modes, the airflow rate varied from 0 m^3/h to 500 m^3/h. Thus, a solar collector coupled with a solar chimney is capable of providing sufficient cooling force for a coupled geothermal system. For the forced cooling modes, the airflow rate was constant with a value of 2750 m^3/h. Predicted Mean Vote (PMV) and Predicted Percent of Dissatisfied people (PPD) were evaluated for the thermal comfort analysis. The results show that the indoor air condition under passive airflow conditions is more comfortable than forced airflow conditions. For the underground soil temperature analysis, the soil temperature profile at different depth was studied and was observed that during the forced airflow condition, the soil temperature increases regardless of the burial depth. Thus, the indoor condition was more stable for passive cooling modes than active cooling modes.

Ariffin et al. [56] investigated the appropriate pipe materials to predict the optimum air temperature to achieve thermal comfort. The study uses Energy Plus for the environmental simulation program. The pipe materials considered for the study were: Polyethylene (PE), PVC (polyvinyl chloride), Steel, clay, concrete, and Copper. Three pipe materials systems were performed: single pipe material, hybrid pipes, and insulated hybrid pipes system were investigated. The study uses three polyethylene pipes buried at different depths. Using Energy Plus software, a parametric study was carried of six different pipe materials: PVC (polyvinyl chloride), PE (polyethylene), steel, clay, concrete, and copper. The simulated results were validated with Sansui, Li, and Ibrahim (2012) experimental results. In the study, four types of the test were conducted which are stated as follows. Test 1: primary test, Test 2: simulation of individual material, Test 3: hybrid material (simulations of two different materials), Test 4: hybrid material and insulation (Simulation of a combination of two materials and insulation). Test 1 was performed to standardize the factors for the three simulations. Test 2: the six different pipe materials were evaluated. The pipe diameter of 50mm was not available in the Malaysian market for the pipe material clay and

concrete, so these were eliminated from the study. The results indicated that the PE (polyethylene) has the maximum temperature reduction of 6.23°C in comparison to the other three. Test 3: The simulation was run for two pipes, one inside the other. Results indicated that a combination of metal and non-metal shows a better reduction of temperature. Test 4: In this test, two types of simulation were done 4A: hybrid system + water and 4B: hybrid system + Rockwool insulation were evaluated. Results show that the best water-hybrid system is the combination of Steel and PE (ST+PE). The metal+non-metal combination shows better results, but non-metal+non-metal can also be an alternative. Thus, PE + PE pipe is recommended for selection since they are more durable and cheaper. Simulation results of 4B show the temperature reduction ranges between 6.03- 6.23°C. Thus, this combination also provides a better temperature difference.

Table 2: Summary of various studies conducted in India.

Author	Place/Year	Season	Material	Length of pipe[m]	Diameter of pipe [m]	Depth of pipe [m]	Temperature range [°C]	Velocity range [m/s]	Temperature rise/fall [°C]	Variable	Others	COP
Kumar et al. [69]	Mathura, India, 2003	-	-	80	-	-	23.8-27.9	4.9	20.2	Length of pipe	-	
									2.15°C	Mass flow rate	-	
									25.3	Radius of Pipe	-	
Ghosal et al. [65]	New Delhi, India, 2003	Summer	PVC	39	0.06	≤ 4	39-45	-	34-39	Length of pipe	-	
		Winter					4.0-9.0		7.0-8.0	Length of pipe	-	
Bansal et al. [66]	Ajmer, India, 2009	Winter	Mild steel	23.42	0.15	2.7	8.0-12.7	2.0-5.0	12.8	Velocity of pipe	-	
			PVC						12.5	Velocity of pipe	-	
Bansal et al. [15]	Ajmer India, 2009	Summer	Mild steel	23.42	0.15	2.7	8.0-12.7	2.0-5.0	12.7	Velocity of pipe	-	
			PVC						10.3	Velocity of pipe	-	
Bisoniya et al. [19]	Bhopal, India, 2014	Summer	PVC	9.114	0.1016	2	25-40	0.4-25	12.9-11.3	Velocity of pipe	-	
Mathur et al. [70]	Jaipur, India, 2014		HDPE	40	0.1		27	5	46.7-28.8	Soil Type	Soil J	
									46.2- 28.8	Soil Type	Soil F	
									46.2- 28.8	Soil Type	Soil A	

Author	Place/ Year	Season	Material	Length of pipe[m]	Diameter of pipe [m]	Depth of pipe [m]	Temperature range [°C]	Velocity range [m/s]	Temperature rise/fall [°C]	Variable	Others	COP
Chaturvedi et al. [71]	Bhopal, India, 2015	Summer	GI	9	0.05	2.0-3.0	-	-	-	Material of Pipe	-	
Thakur et al. [72]	India, 2015	Summer	Aluminum	60	0.1	-	46	3.0-9.0	25.5	Configuration	finned	
		Summer							28.3	Configuration	unfinned	
Singh et al. [73]	Punjab, India 2015	Winter	Galvanised Iron	-	0.1524	3.048	-	16.7	29.3	Crossectional area	-	
		Summer							-	-	-	
Khandelwal et al. [74]	Jaipur, India, 2015	-	PVC	-	0.1524	4	-	4	11.5	-	mathematical model	
Mathur et al. [75]	Jaipur, India, 2015	-	HDPE	-	-	-	26.39	-	27.27	Burial Depth	-	
Singh et al. [13]	Chandigarh, India, 2015	-	-	-	-	-	-	-	-	-	-	
Kaushal et al. [76]	India, 2015	-	-	3	0.1m	-	7	1.0-3.0	21-24	Configuration	Hybrid EAHE	
									12	Configuration	EAHE	
		-	HDPE	90	0.025	-	90	-	±1.61	Material of pipe	-	

| Author	Place/Year	Season	Material	Length of pipe[m]	Diameter of pipe [m]	Depth of pipe [m]	Temperature range [°C]	Velocity range [m/s]	Temperature rise/fall [°C]	Variable	Others	COP
Jakhar et al. [77]	Rajasthan, India, 2016		GI							Material of pipe	-	
			Steel							Material of pipe	-	
			HDPE						22.5-27.7	Burial Depth	-	
									31.9	Length of pipe	-	
									31.8	Diameter of Pipe	-	
Chel et al. [67]	New Delhi, India, 2009	Winter	PVC	78	0.06	1.5	-	13	-	-	Before renovation, after renovation, EAHX for six rooms	2.9
		Summer					-		-			1.8
Dubey et al. [78]	India, 2013	-	GI	17	0.064	1.5	-	4.1-11.6	12.7-15.7	Velocity of pipe	-	6.4-3.6
Misra et al. [79]	India, 2014	Summer	PVC	-	-	3	34-44	-	20-22	Time	-	-
Jakhar et al. [31]	-	Winter	PVC	60	0.1	3.7	15-18	5	17.7°-21.1	Configuration	Mode I	-
									17.5-22.3	Configuration	Mode II	1.54

| Author	Place/Year	Season	Material	Length of pipe[m]	Diameter of pipe [m]	Depth of pipe [m]	Temperature range [°C]	Velocity range [m/s]	Temperature rise/fall [°C]	Variable	Others	COP
	Ajmer India, 2015								17.6-24.1	Configuration	Model III	4.57
Soni et al. [80]	Bhopal, India, 2016	Monsoon	Galvanised steel	11	0.05	2	37.5-46	-	35.5-42	Burial Depth	-	-
		Summer									-	-
Jakhar et al. [81]	Ajmer, India, 2016	Winter	PVC	60	0.1	3.7	13.9- 20.4	2.5,3.5,5	24.3-24.7	Velocity of pipe	-	2.8-3.1

Hatraf et al. [82] studied the soil ground temperature profile to estimate the pipe's depth. The physical characteristics of the soil were studied, and a mathematical model was formulated. A comparison was made between the simulated and experimental results by considering different flow rates at 100, 150, and 200 m^3/s. The airflow affects the performance. The Nusselt number increases with the increase in Reynolds number. Thus, the soil properties have a significant impact on the performance. The depth of the pipe depends on the diffusivity of the pipe.
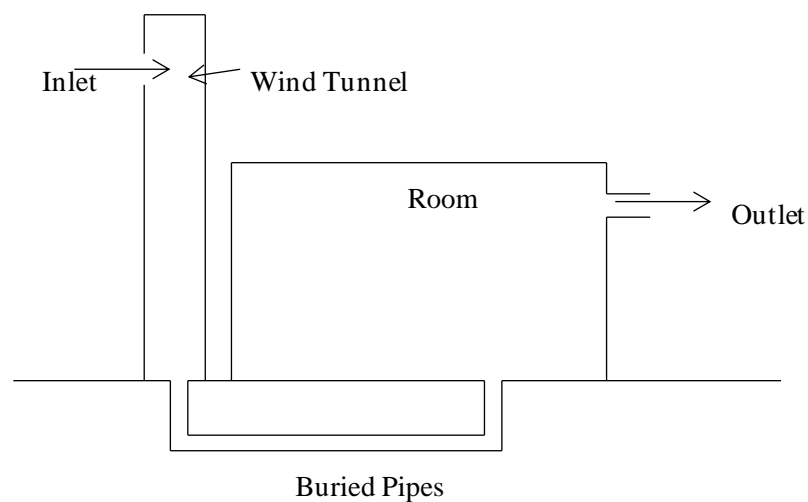
Figure 10: Schematic diagram of EAHE coupled to wind tunnel [57]

Benhammou et al. [57] made an analytical design model to investigate the influence of design parameters on the performance of EAHE. The outlet of the EAHE is placed inside the building, and the inlet is connected to a wind tower, considering that the wind direction was unidirectional. The schematic diagram of the setup is given in figure 8. A mathematical model was developed for the thermal analysis of EAHE. The model was validated against the experimental data collected by Dhaliwal and Goswami [83]. The soil temperature of the burial depth was 18.89°C. The variation of the air velocity inside the pipe was studied, and results show that with an increase in the pipe diameter, there is an increase in the air velocity. When diameter was increased, the air velocity was increased, the air velocity decreases as the pipe's length increases. The influence of wind tower cross-sectional area is also discussed. When the cross-section increased by a very small difference, there was a change of 0.009°C in temperature. Again, when

the tower height was increased, air velocity was raised, and the temperature was decreased. Thus, the cross-section does not affect the performance of the system. The cooling effect of the system was also evaluated. Results show that the air temperature is lower for the system coupled with a wind tower compared to the air temperature of a wind tower on a wet surface. This comparison was made considering a similar work done by Bouchahm et al.
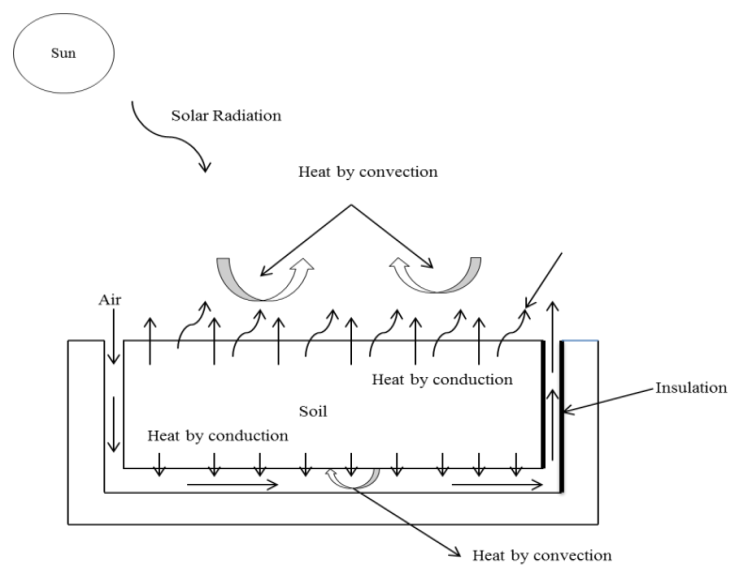
Figure 11: Schematic of EAHE with thermal Insulation [58]

Xamána et al. [58] predicted the thermal performance of EAHE for the three cities of Mexico. The effect of thermal insulation at the outlet was investigated. This study considers two configurations of the EAHE system. The configurations were: EAHE without insulation and EAHE with thermal insulation (polystyrene) at the outlet. The schematic diagram of the setup is given in figure 11. The results were obtained for Re=1500 for three Mexico cities (México City, Mérida, and Cd. Juarez) with soil conditions of silt, clay, and sand soil. Thus, adding insulation to the EAHE system, EAHE for México and Mérida city was profitable during the summer season and for Cd. Juarez city thermal insulation was helpful during the winter season.

Carlucci. et al. [59] considered an EAHE coupled with an HVAC system and coupled system to estimate the system's thermal potential. The pipes were laid on an L-shaped

pattern. The selection of soil has also been monitored. To investigate the temperature profiles, various sensors were installed at different depths. For the installation of EAHE, the first phase is excavating up to a depth of 0.3 m. The pipe bed was filled with FSC soil. The EAHE consist of 3 pipes that are connected to the inside of the tower, and the other end was connected to the conveyor box. A planned monitoring system was also installed to monitor the results whether the non-zero objective is reached or not. In this study, only the systems were installed, the results were not monitored. Three soil types have been used to cover the pipes: a mixture of fine sand and clay, scoriaceous lava, and topsoil.
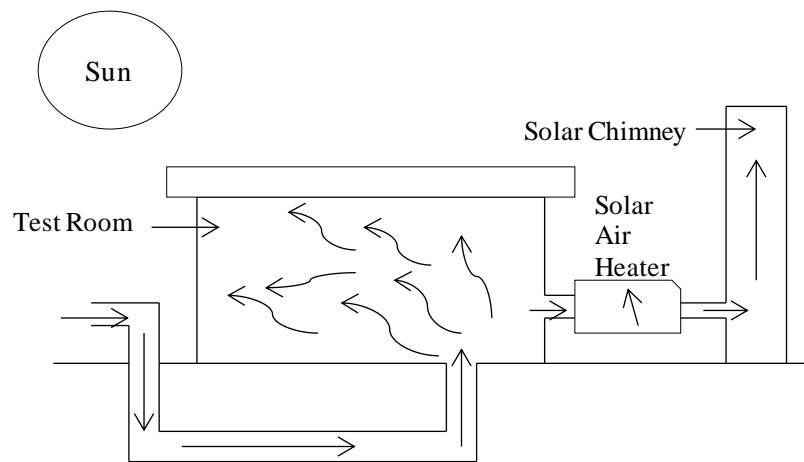
Figure 12: Schematic diagram of EAHE coupled to solar chimney [84]

Li et al. [84] studied a Hybrid EAHE coupled with a solar chimney. The solar collector is used to connect the solar chimney to the building. The system consists of an EAHE pipe exposed to the outside and the other end to the inner side. The experimental setup was made on a testing facility at the University of Nebraska. The solar chimney was designed in such a way that the pressure losses from EAHE were compensated. The schematic diagram of the setup is given in figure 12. The parameters examined are time and date, the indoor relative humidity (%), outdoor relative humidity (%), supply air relative humidity (%), supply airflow rate (m^3/s), solar collector airflow rate (m^3/s), average indoor temperature (°C), supply air temperature (°C), and outdoor air temperature (°C). The underground soil temperature was monitored at different depths;

fewer temperature fluctuations were observed for deeper depth. The maximum temperature difference was observed at 2.9 m depth.

Mendez et al. [60] studied the PID controller's uses, which is generally used for thermal processes. This study shows the usage of PID in improving the performance of EAHE than conventional heat exchange. Simulation of PID was created in LabVIEW. The results show that PID controllers show better control of temperature in comparison with the traditional controller. The PID controller reduces energy consumptions after a steady temperature is achieved. The average energy consumption on energy consumption was 0.017kWh. There was about 87% energy saving in comparison to conventional controllers. A simulation runs on a PID controller; results show that energy consumption can be reduced if a PID controller is applied. It increases the efficiency and the sustainability of the EAHE system and has lower emissions compared to conventional methods.

Sansui et al. [61] investigated the soil temperature at different depths up to 5m to estimate the potential of EAHE in Malaysia. The experiment's site location was the International Islamic University campus in Malaysia, which was generally exposed to solar radiation. The soil type is sandy and covered with short grass. The study was carried out in 2 phases: In the first phase, the temperature measured up to 5 m, and the second phase focuses more on the temperature at shallow depths. It was seen that there was a slight change in temperature for shallow depths. The results indicate that the application of EAHE in the building is possible only if the air temperature increases beyond 34°C. Also, the optimum temperature for the undisturbed soil temperature was at a depth of 1m.

Niu et al. [62] studied the 2D heat transfer mechanism through the transient control volume method. The computational domain was divided into control units, and thermal balance was applied. A self-recovery temperature analysis was done using continuous and intermittent modes. The data was validated against an experimental setup already present in Omaha, USA. The measurements were done to record the cooling capacity of the system. The simulations were done using MATLAB 8. Results indicate that the

outlet temperature increased when the soil air temperature was increased. It was observed that there was a good agreement with the experimental results during validation. It was observed that the soil temperature near the tube fluctuated more than the far one. Thus, the temperature difference between soil and air is higher than the outlet. During the night, lost energy is recovered. Two modes were considered to analyze the recovery analysis: continuous modes and intermittent mode. In intermittent mode, the soil temperature was recovered during non-working time. The recovery ability decreases with time and distance. As the supply air temperature increases in continuous mode, the recovery temperature varies between 19.5- 21.7°C.

Niu et al. [63] predicted the cooling capacity of EAHE using regression analysis. The study considers both heat and mass transfer between tube and air. A mathematical model was formulated to estimate the underground soil temperature. The results were validated with results already present in a test facility. For the heat transfer analysis, sensible and latent heat transfer were considered. A simulation model was developed in MATLAB 8. The data was validated with the experimental data already present in a test facility in Omaha, USA. The results, when compared, show a good agreement with the present data. Thus, the formulated equation for soil temperature can be used. For the EAHE, there was a rise in outlet temperature. To predict the soil temperature, temperature profiles were checked along the length. The results indicate that as the surface temperature increases, the outlet temperature increases. Also, as the tube diameter increases, there is a decrease in the outlet temperature. The cooling capacity for the system was also investigated. The cooling capacity increases with an increase in the inlet air temperature. On calculating the cooling capacity, the sensible cooling capacity was 0.31 kW/°C, and the latent cooling capacity was 0.7 kW/°C. Thus, the total cooling capacity was 1.1 kW/°C.

Jassim et al. [85] investigated the performance of windcatchers in EAHE to reduce the energy consumption in hot, dry areas like Iraq. A wind Catcher is a device designed for pulling and expelling the air. Generally, wind catcher towers are connected to a building to cool the building. The thermal performance was studied in two phases. Phase 1: The temperature was measured using data loggers. Phase 2: Simulation is done using CFD.

The model was a 2-storied building with a wind catcher of a 2 m^2 area. A CFD model was formulated and was validated against the experimental setup. Results indicate that a higher fluctuation in temperature was seen in August. But these fluctuations were decreased in June, but the relative humidity was increased. This result also indicates that the soil temperature also depends on the soil type and water table. It was observed that if the windcatcher space was increased in phase 1, thermal comfort was not achieved. But in phase 2, if space is increased, the temperature is reduced by 18°C. It was also observed that when the velocity was increased, the COP was increased to 5.24. Thus, this new design for self-cooling reduces energy consumption.

Li et al. [86] constructed an experiment in the Harbin area of an air-conditioning system for cold areas, which directly supplies the cold energy stored in the ground. The operation time was in summer in 2006. Performance parameters such as cooling seasonal performance factor (CSPF) and the average heat rejection rate unit depth of borehole were investigated. The system consists of the ground heat exchanger and indoor fan coil. The circulating fluid considered was water. To reduce the building's thermal influence on the ground, the borehole was made 7 m exterior to the walls. The heat rejection rate per unit depth of the borehole ranged between 40-100 W/m. The cooling characteristics are divided into seasonal cooling characteristics and daily cooling characteristics. Daily, maximum cooling capacity occurred on the 2nd day. The ground temperature rises rapidly initially but becomes stable at a later stage. There was an increase of cooling 0.75°C on the last 45 days. On an hourly basis, maximum cooling capacity occurred on 1st hour, and minimum cooling capacity happened on the tenth hour, having a ratio of 0.81. Thus, the increase in ground temperature is initially low at different depths and gradually becomes faster.

Chlela et al. [33] carried out a numerical study to evaluate two different ventilation systems' energy performance and earth air heat exchanger for three French climates. The building considered is a dwelling called "Mozart" having floor area 101m^2. The simulations were carried out for three French cities: Nancy [5°C], La Rochelle [8°C], and Nice [10°C]. Two ventilation systems were considered: mechanical extract ventilation system and balanced ventilation system. The soil type proposed was clay.

The thermal behavior of the building was carried out using SIMBAD. The results were validated with other building data [El Khouryet et al., 2005]. Yearly simulations were done to evaluate the thermal performance of EAHE and balanced ventilation systems for all three cities. The heating demands of the three cities' ventilation system were evaluated, and there was a reduction in heating demand. The house's heating demand in Nice was 13.2 kWh/m^2, which was almost equal to the annual heating demand. There was a decrease in heating demand for EAHE with a mechanical extract ventilation system. Thus, the balanced ventilation with heat recovery unit is more efficient than EAHE. During the summer season, the heat exchanger of the balanced system was bypassed. The cooling potential for the three cities modes was evaluated on three modes. Thus, EAHE has a good prospect for cooling.

Ascione et al. [64] study the Net Zero Energy buildings[NZEB], the main strategy to reduce energy consumption and CO_2 emission in buildings. It analyses a case of a two-storied building in Palero, Italy, having an area of $520m^2$. The NZEB is a new concept introduced by European Directive 31/2010/UE. This concept came from nearly Zero Energy Building [nZEB], which implies that the non-renewable energy demand is equal to 0 kWh/m^2 annually. For the analysis, the computational software used in EnergyPlus. The results obtained were validated with the climate data available at International Weather for Energy Calculations. A PV system made of monocrystalline silicon panels titled to an angle of 15° [essential to obtain NZEB]. A mechanical ventilation system [MVS] was considered to estimate the thermal performance. Energy Plus was used to evaluate the heating, cooling potential considering two modes. Results show the primary energy use per floor [PE] for summer [PE_c] and winter [PE_h]. Thus, during summers, PE_c reduces with an increase in airflow and vice-versa in winters. The annual electricity demand for MVS was 35455 kWh, and for EAHE + MVS, the demand was 31200 kWh. But the PV panels produced only 31300 kWh. Thus, more PV panels are to be installed to satisfy the demand. Thus, NZEB is possible using renewable energy is possible. In the case of only MV, the electrical demand is more so a higher number of PV must be sued to compensate the demand than in the other case.

Table 3: Thermophysical Properties of Materials used.

Material	Density (Kg/m³)	Specific Heat Capacity (J/KgK)	Thermal Conductivity (W/mK)
PVC [66]	1380	900	0.161
Copper*	8933	385	401
Aluminium*	2702	903	237
Galvanised Iron[GI] [75]	-	-	-
Steel* [AISI304]	7900	477	14.9
Galvanised steel [76]	-	-	-
Mild Steel[MS]*	7854	434	60.5
Galvanised mild steel [40]	-	-	-
Polyethylene [PE]**	-	2000	0.45
High density Polyethylene (HDPE)**	940	2000	0.45
Iron*	7870	447	80.2
Plastic [76]	-	-	-
Culvert steel [67], [60]	-	-	-
Reinforced concrete [74]	-	-	-
Bamboo + Cement Plaster [27]	-	-	3.14
Air*	1.225	1006	0.024
Water*	1000	4190	0.55

*Thermo-physical properties of Materials at 300K [87], **Thermo-physical Material properties at 296K.

Bisoniya et al. [19] investigated the cooling demand in a building for Bhopal's hot and dry climate considering the quasi-steady-state model, developed in CFX 12.0. The simulated results were validated against an experimental setup in Bhopal. The observations were made for different flow velocities assuming $T_{surface} = T_{ambient} = T_{inlet}$ to evaluate the total hourly energy gain. Results indicate that the temperature drop was

faster at the pipe's initial length and became moderate for the rest of the length. Also, a comparison was made with experimental data and simulated data at different velocities; there was a deviation of 0-8.86% of the experimental results. It was observed that the maximum hourly cooling energy gain was 1.8 MWh at 5m/s. Thus, it was concluded that EAHE could be used efficiently to reduce the building's cooling load in hot and dry summer compared to AC.

Dubey et al. [78] considered an open-loop EAHE having 3 horizontal pipes connected in parallel to the find cooling rate during the summer season. The pipes were in parallel connection with a typical intake and exhaust manifold of the air passage. Results indicate that there was a decrease in the temperature and COP of the system as the velocity was increased. Thus, the velocity of airflow affects the performance of the system.

Chaturvedi et al. [71] investigated the performance of EAHE in Bhopal having multiple pipes in parallel during the summer season. It was seen that the material of the pipe does not affect the output. Results show that the temperature difference at inlet and outlet is less if the length of the pipe is small and blower voltage is high. Thus, it can be concluded that the material of the pipe does not affect the performance of the system.

Kumar et al. [69] studied the finite difference method's numerical techniques and FFT (MATLAB) model. The results were validated against the experimental data of a similar tunnel in Mathura (India). It was observed that when the length and flow rate was decreased, the outlet temperature increases and decreases, respectively. Also, when the pipe radius was increased, the outlet temperature was raised, but the convective heat transfer coefficient is lowered. Thus, it can be concluded that a longer tunnel length is efficient for more cooling energy saving. Results indicate that the cooling potential for the setup was 456kWh. By increasing the pipe radius above a critical value, the outlet temperature can be improved, affecting the heating/cooling potential. Thus, it was concluded that by using a larger diameter pipe large outlet temperature can be achieved.

Singh et al. [73] designed a metallic EAHE to determine the classroom's heating and cooling loads. The ducts were laid in a zigzag pattern with PVC and Iron, a square cross-section for the metallic pipe, and around cross-section for PVC. The cooling load was found using the CLTD method. The central duct was divided into three parts; the inlet and outlet were made of PVC, and the remaining sections were made of galvanized iron. The simulations were run in ANSYS. Results show that there was a change in the temperature profile at the outlet of the metallic section. The central portion's air is warmer than the air near the boundary layer by 2°C as the inner part gets less convected. After all the variables were considered, the final layout of the earth-air tunnel was made through CATIA software. The prototype was run in different seasons. The prototype showed a maximum C.O.P of 3.9 in the summer season, which was more than COP of 2.1 in the winter season. It was seen that the maximum cooling effect of the prototype was 2.6 kW. Thus, it can be concluded that the EAHE is more useful during the summer season than in the winter season for the climate of Punjab.

Thakur et al. [72] developed a model in Pro–e to study the effect of the finned model of EAHE. This was compared with a finless model of EAHE. The meshing tool used was ANSYS Workbench, complex heat transfer, and airflow process studied using FLUENT. The computational model was validated against an experimental study conducted by Misra [88]. The simulations were run at different pipe inlet velocities. On comparing the data with the existing experimental data, it was seen that there was a variation of 7.64%. The simulation results for the finned and finless EAHE system were studied. The results concluded that with the addition of fins, the system works efficiently even if the soil has poor thermal conductivity. Also, concluded that smaller lengths of pipes could perform satisfactorily, thus lowering the initial cost.

Soni et al. [80] experimented with reducing the power consumption of a 1.5TR air conditioner coupled to EAHE. For the experiment, three different arrangements were considered. The economic analysis techniques such as simple payback period, discounted payback period, etc., were also evaluated. From the arrangements, it was observed that in arrangement II, the condenser tube temperature was reduced by 10% than the arrangement III condenser tube temperature. The power consumption in all

three arrangements was also calculated, and a comparison was with the base model. The results indicate that arrangement III was helpful in terms of power reduction during summer days. At a velocity range between 5- 7 m/s, the EAHE arrangement gave optimum results. For the energy matrices, the EPBT for arrangement II is 604.3 days and arrangement III are 362.6 days, and the CO_2 emissions for arrangement II are 5425.92 kg, and arrangement III is 9043.2 kg. Thus, arrangement II is profitable to use to reduce CO_2 emissions.

Jakhar et al. [81] estimated the performance of EAHE with and without Solar air heating duct (SAHD) during the winter season and was formulated using TRNSYS 17. The results were validated against an experimental setup in Ajmer, India. For the solar air heating purpose, galvanized iron ducts were used. In the study, three cases were considered to investigate the performance of EAHE. The results show that EAHE coupled with SAHD increased the outlet by 6- 9°C when the air velocity was varied. Also, it was observed that the heating capacity of EAHE was improved when coupled with a solar air heating duct. In the error analysis, it was observed that there was an error of 3.9%.

Jakhar et al. [77] investigated the operating temperature of Photovoltaic panels (PV) which was responsible for life span and performance using TRNSYS v17.0. Water was used as the working fluid. The simulated system was compared with the existing ones in the literature for a given cooling setup of Concentrating Photovoltaic (CPV). In the study, three types of pipe material are considered for the study. The temperatures along with the depth for all three pipes were evaluated, keeping the pipe length, flow rate, diameter constant. On considering the pipe material, it was observed that there was a temperature variation ± 1.61°C. For the analysis, HDPE was considered cheaper. It was observed that as the depth increases, the average temperature also increases. Thus, it was concluded that 3.5m was considered as the optimum depth for further simulation. Also, it concluded that the pipe material does not affect the performance of EAHE. But when the mass flow rate was increased, the outlet temperature, Reynolds number, and Nussult number were increased. Thus, the mass flow rate affects the outlet temperature.

Mathur et al. [75] focus on the soil's thermal saturation and self-recovery ability between different (continuous and intermittent)modes of the EAHE system set up in MNIT Jaipur, India. The numerical simulations were performed using Ansys FLUENT v14.5. It was seen that there was a good agreement between the measured and simulated results. After the validation of the CFD model, a comprehensive analysis was done to analyze the soil temperature's impact on EAHE. Results indicate that the soil temperature along the length decreases. Thus, ambient air temperature is also an essential factor in soil temperature. For the study of heat penetrating the soil, the temperature profile in the radial direction was simulated. Results showed that the soil temperature decreases as it moves away from the EAHE surface, but the pipe's soil temperature varies with ambient air temperature. The ambient temperature goes down in continuous operation and cools the heated subsoil, recovering its cooling ability. In intermittent operation mode through the soil layers' heat conduction, the soil temp can be retrieved during non-working hours.

Jakhar et al. [31] predicted the thermal performance of EAHE when coupled with a solar air heating duct in Ajmer, where the temperature ranges from 15-18 °C in winters. The inlet of the solar air heating duct is connected to the outlet of the EAHE. In this study, three modes were considered to estimate thermal performance. The three modes were evaluated in four periods 14-16 January, 26-28 January, 1-3 February, and 13-15 February. The results show that using EAHE with a solar heating duct increases temperature 1.1- 3.5°C inside the room. The heating capacity and COP for mode II was 665.52 kW and 1.54; for mode III, heating capacity was increased to 1976.02 kW and COP 4.57. Thus, it was concluded that the solar heating duct increases the heating capacity and the COP of the system for the same power consumption.

Singh et al. [13] studied Chandigarh city for the installation of EAHE. Chandigarh is situated at latitude 30.74°N, longitude 76.79°E, and at an altitude of 321 m. It receives rainfall of 1110.7 mm. The cooling period is from April to October, and the heating period is from November to March. The soil type is sandy in Chandigarh up to 3m with a water table of 5-15 m. The electricity demand in summers and winters is 350 MW, but availability is only 324 MW. The soil diffusivity varies from 0.084 to 0.14 m^2/day. Thus, Chandigarh city is suitable for the installation of EAHE.

Khandelwal et al. [74] studied the heating and cooling load of a Library of MNIT, Jaipur. A simple excel model was developed. The library consists of 4 rooms conditioned with split AC to which EAHE was connected. For the cooling load estimation, total sensible and latent heat was considered, including infiltration load. On the survey, it was found that the comfort temperature was 28.6°C. Results show the maximum temperature drop was 11.5°C and the length of the pipe was 72 m. Cost analysis results in Rs. 1149380 was estimated for its installation. The cooling load was 77 kW, including ventilation load and the cooling capacity of EAHE was 60781 kW.
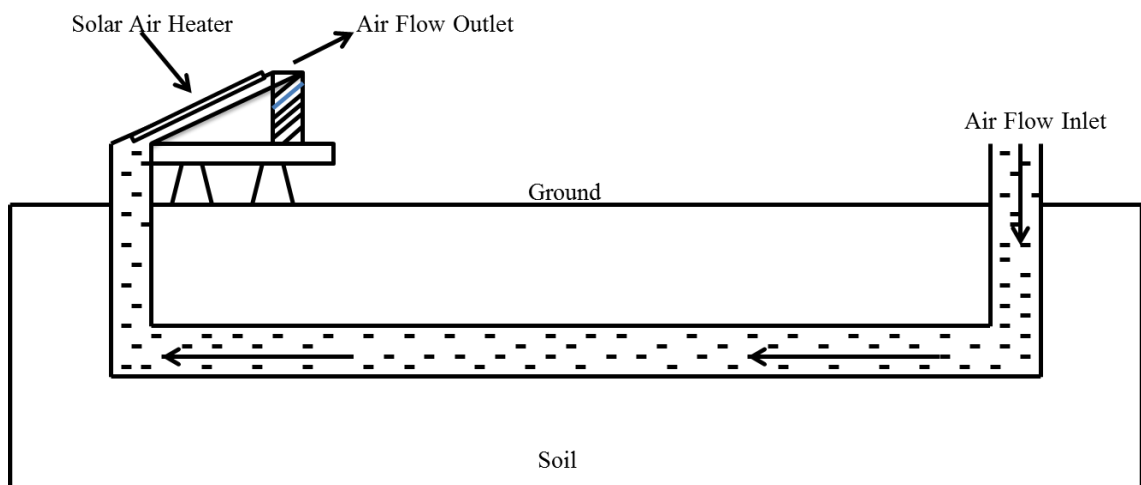
Figure 13: Schematic diagram of EAHE with SAHD [76]

Kaushal et al. [76] used FVM to investigate the thermal potential of hybrid EAHE. This study also used the response surface method is used to optimize the process parameters using Ansys Fluent. The numerical results are compared to individual EAHE. The EAHE is made hybrid by coupling it with a solar air heater. The schematic diagram of the setup is given in figure 14. The temperature contours along the length were studied, which shows that temperature increases with an increase in length. The results of only EAHE were validated against the data reported by Bansal [66]. The results of HEAHE were validated against the experiment set up. Response surface methodology uses f test and ANOVA technique to estimate the factors affecting the input variables. Results show that the potential or solar heat gain decreases with an increase in temperature. Results show that hybrid EAHE shows maximum temperature drop. Thus, HEAHE delivers good performance than EAHE.

Misra et al. [79] emphasize the use of low-cost materials like PVC to the cooling potential. The author focused on the design of the duct system. The experimental setup was made as a prototype model where the model's base was a metal tray. As noted earlier, the performance of EAHE depends on the air velocity and the material of the pipe. Thus, a cheaper material can be used for the analysis. It was observed that the minimum EER for the system was 3.78, which was almost equal to an energy star5 rating. Thus, EAHE also consumes less energy than convention systems. This study suggests that the prototype model can be used in tiny houses to maintain the room temperature lower than the outside temperature during the summer season. The author recommends that the EAHE to use domestically in homes to achieve thermal comfort. Thus, EAHE is an energy-efficient system when compared with the energy star rating system.

Bisoniya et al. [89] developed a model to study the different design parameters pipe length, radius, depth of burial, and airflow rate to estimate the thermal potential of EAHE. For one dimensional model, a relation was derived between inlet and outlet temperature by describing pipe. This shows the performance of EAHE as a steady-state 1D model. 2D

models are used to calculate the ground temperature at the surface at five different depths. Finite element methods are used to solve the conduction problems. 3-D models are developed to analyze the performance analysis also provides room for all types of grid geometry. For solving the 3D heat transfer and energy equation, CFD is used. For complex fluid flow and heat transfer processes in any heat exchanger, CFD software like Ansys FLUENT, STAR-CD, CFX, FIDAP, CFD2000, PHOENICS, ADINA can be used.

Choudhury et al. [27] investigated an experimental study of EAHE design using low-cost material like Bamboos and hydra form to reduce energy consumption. An open-loop EAHE system was used to predict the potential of EAHE. The experiment was conducted in Arunachal Pradesh. The study mainly focuses on the use of locally available materials. Out of all locally available materials, bamboo was selected for the pipe material. The thermal conductivity of bamboo was increased by using hydra form plaster. PVC pipes were used to install sensors for the measurement of the temperature gradient. The inlet and outlet were formed using PVC pipes and bricks. Results show that the maximum humidity recorded was 98%. Irrespective of the inlet temperature, the outlet temperature range between 25-26°C. Results also show the variation of outlet temperature with the airflow velocity. It was seen that using bamboo with hydra form plaster in the tunnel reduces the outlet temperature by 10- 15°C, which reduces the electricity consumption. Thus, this type of tunnel configuration is very effective for agricultural and residential buildings. EAHE supplies fresh air ventilation and is safe for the environment. It also reduces CO_2 emission, which helps in environment management.

Mathur et al. [70] studied the thermophysical properties of soil on the performance of EAHE. The study was validated using the 3D transient numerical model for 3 different soil types. A CFD model was formulated and solved using Ansys FLUENT 6.3. For the creation of geometry Gambit, 3.3 was used. The model was validated against the numerical model developed by Mishra,2013 [88]. The three soil types selected for the study are Soil J, F, and A. The results also imply more heat penetration in the surrounding soil for J and F soil

type as they have high thermal conductivity than soil type A. Thus, soil types J and F's performance were similar because soil with high thermal conductivity has a high heat transfer rate.

2.3   Essential studies on GSHP systems

Conge do et al. [90] carried out a CFD simulation to study three different geometries of HGHE: linear, helical, and slinky, considering the climatic conditions of South Italy both in summers and winters. It is observed that the most crucial parameter is the thermal conductivity of the ground and the most effective ground type was of the highest thermal conductivity of 3 W/mk. The second key parameter was the velocity of working fluid inside the tubes. However, the depth of installation of HGHEs didn't count as an effective parameter. Results show that the helical coil arrangement was the best performing configuration.

Benli [91] conducted an experimental study and compared HGSHP and VGSHP for greenhouse heating. The results were obtained from November to April author founded that the COP_{hp} (coefficient of the heat pump) and COP_{sys} (coefficient of overall system) were ranging from 3.2-3.8 for VGSHP and 3.1-3.6 for HGSHP and 2.9-3.5 for VGSHP and 2.7-3.3 for HGSHP, respectively. It was observed that the utilization of the GSHP is effective for greenhouse heating in the district.

Bakirci [92] evaluated the performance of VGSHP under the cold climatic conditions of Turkey from October to May. It was observed that the COP of the heat pump and overall system were approximately 3.0 and 2.6. Results show that the experimental setup system could be used for the heating purpose of residential buildings in Turkey's cold climatic region.

Kayaci et al. [93] conducted a comparative study by comparing the experimental results and the numerical model to improve the performance of GSHPs. For testing work, they

54

buried a horizontal network of parallel pipes under the foundation of about 2400 m^2. It was observed that COP of the ground source heat pump, when buried in the soil under the foundation, is more significant than when buried in the building's foundation. Results show that maximum differences between the numerical calculation and experimental setup readings for daily average inlet and outlet fluid temperatures were estimated as 8.36% and 5.58%, respectively, and they conclude that the simulation results show a good agreement with experimental data.

Luo et al. [94] investigated a GSHP system's thermal performance continuously for 4 years, which was installed in an office in Southern Germany. The coefficient of performance (COP) for a typical winter day is founded to be 3.9, and the Energy efficiency ratio was founded to be 8.0 for a typical summer day. However, it was observed that the system's seasonal energy efficiency ratio is founded to be increased by 8.7%, while the COP of the system is reduced by 4% over a long-term period of 4 years. They found that the GSHP system's performance follows the opposite trend as per the building's uneven cooling and heating load.

Sivasakthivel et al. [95] worked to optimise GHE parameters for space heating application implementing Taguchi and utility methods. These crucial parameters include borehole radius, U tube radius, heating load, entering water temperature, the grout conductivity, distance between U tubes, thermal conductivity of U tube, and mass flow rate. The length of the ground heat exchanger, COP, and thermal resistance is taken as the essential functions. Results were obtained using an optimized set of parameters. A reduction of 15.17% and 17.1% is observed in length, and thermal resistance of GHX, whereas the COP is improved by 2.5%. The implementation of utility methods to achieve a best-suited set of optimum parameters resulted in a decrease in COP and thermal resistance of 1.2% and 13.23%, while the length of GHX is increased by 3.2%.

The performance of GHE can be integrated with various cooling and heating technologies such as evaporative cooling technology, solar thermal collectors, Zero Energy Buildings (ZEB), etc. Emmi et al. [96] investigated the Solar Assisted Ground Source Heat Pump (SAGSHP) system in the cold areas using the TRNSYS tool. The effect of the depth of the borehole on the energy efficiency of GSHP was analyzed. It was founded that the efficiency of a solar-assisted heat pump is 10% higher than the GSHP system without solar assistance.

Girard et al. [97] investigated the performance of the GSHP system compared to the SAGSHP system in 19 European cities using numerical simulations. It was observed that solar-assisted systems have a higher performance value between 4.4 and 5.8 while between 4.3 and 5.1 for the GSHP system. Results show that solar thermal collectors are best suited for regions with a cool climate and higher irradiance.

Zhu et al. [98] investigated the performance of the GSHP system and SAGSHP system and developed a mathematical model to analyze the COP of both systems. They installed solar collectors over 1500 m^2 and 580 sets of GHE at a depth of 120 m. Results show that the overall COP of the heat pump and the system is improved by 2.4% and 3.4%, respectively.

Yoon et al. [99] investigated the heat transfer rates of horizontal slinky, spiral coil, and U tube GHE systems installed in a steel box (5 m $\times$ 1 m $\times$ 1 m). Results show that the spiral coil type heat exchanger gives a greater heat exchange rate per unit length of pipe of about 30- 40% than the horizontal slinky GHE. However, U- type heat exchanger gives the highest heat transfer rate per unit length of pipe than the slinky and spiral coil GHEs. A cost-efficiency analysis was conducted, which revealed that U-type GHE has high economic efficiency of about 20% better than the horizontal slinky and spiral coil type GHE.

Tarnawski et al. [100] investigated the performance of GSHP with HGHE using computer simulation operating in cooling and heating mode for a residential house with a living space of 200 m^2. They installed a 5.5 KW GSHP unit of length of 300 m buried in a serpentine

manner at a depth of 0.5 m. It was observed that the overall COP of the system is 3.26, and the system will require 19.7 GJ of total electric consumption annually. It was concluded that the system would offer an enormous saving from consuming high-grade energy, and the system is founded feasible for residential and commercial use.

Kim et al. [101] analyzed the effect of the GSHPs design factors such as length of GHE, shape, and the storage tank's capacity on the system's performance. It was observed that when the GHE type, size, and storage capacity were optimized, the primary factor affecting the heat exchange rate and COP of the heat pump was heat storage capacity as by using storage tanks, the heat exchange rate, and the heat pump performance is increased by 17% and 7%. However, the factor affecting the system's performance was heat exchanger length, as it was observed that when the length is increased from 1050 m to 1500 m, the COP of the system is increased by 4%.

Chen et al. [102] analyzed the heat exchange rate per unit depth of VGHE using numerical simulation and multiple regression models. They formed a regression equation considering the heat exchange rate and depth of the heat exchanger as variables and observed that as the depth increases by 1 m, the heat transfer rate per unit length decreases by 0.153 W/m, whereas if the length of the heat exchanger increases by 1 m, then the heat transfer rate decreases by 0.031 W/m. They concluded that this difference varies due to the ground's experimental environment and characteristics as per ground depth.

Fujii et al. [103] performed numerical modeling of horizontal slinky coil type GHE for optimum design. They used a commercial simulator, FEFLOW, to simulate the performance of the heat exchanger. Results show a good agreement between the simulated values and the measured values of ground temperature and heat medium, taking thermal conductivity of the heat exchange pipes between 0.025 and 0.045 W/mk. They concluded that the numerical model presented by them could be an influential tool in the optimum design of horizontal slinky coil-type heat exchangers.

Esen et al. [104] analyzed the energy and exergy of the GCHPs of two HGHE for the heating season, taking trenches' depth as a variable. They took two HGHE, one buried at 1 m depth (HGHE1) and the other at 2 m depth (HGHE2). Results show that the COP of GCHP systems was 2.5 and 2.8 while the exergy efficiency was 53.1% and 56.3% for HGHE1 and HGHE2, and the irreversibility of HGHE2 is 2.0% less than the HGHE1. It was observed that COP and exergy efficiency of the system increases by the increase in ground temperature during the summer season, whereas with an increase in environmental temperature, exergic efficiency decreases for both heat exchangers.

Dasare et al. [105] developed a numerical model to present designing the GHE to meet high energy demand applications. It was observed that soil conductivity is the primary parameter responsible for heat exchange. Also, the velocity of heat exchanging fluid, i.e., the mass flow rate, was founded to be an important parameter affecting the thermal performance of GHE. However, it was established that the depth of installation has a negligible effect on the performance of GHE. They suggested a double layer helical geometry of pitch 0.3 m, spire diameter of 0.2 m, and the distance between consecutive layers as 1.2 m was best-suited HGHE, as the installation cost and material cost were observed to be optimum.

Asgari et al. [106] conducted a comparative study of different arrangements of HGHEs. They considered three different arrangements as linear, spiral, and slinky to evaluate the performance of GHEs. They designed a 3D numerical model to simulate the performance of GHE. Results show that the linear arrangement with a quadruple layer provides an even heat distribution and thus, has the highest heat transfer rate per unit land area, nearly 34% more than the traditional single-layer arrangement. However, for slinky and spiral ground heat exchanger types, the best arrangement was founded to be a staggered double layer, which has nearly 22% and 7% higher heat transfer rate per unit land area than the conventional ones. It was also founded that the heat transfer rate in soil with thermal conductivities 0.75 and 1.75 W/mk was 38% lower and 38% higher than that of soil with thermal conductivity of 1.24 W/mk.

P.C.M. Kumar et al. [107] determined the heat transfer rate and friction factor for a helically coiled heat exchanger. They took Al_2O_3 water-based nanofluid at different volume fractions and considered a laminar flow. It was observed that the Nusselt number, inner heat transfer coefficient, and overall heat transfer coefficient are 28%, 25%, and 24%, respectively, greater than water when volume concentration was 0.8% particle of nanofluid. It was concluded that the friction factor increases with the volume concentration of particles in the nanofluid.

Diglio et al. [108] examined borehole heat exchanger using nanofluid. They presented a numerical study to evaluate the best nanofluid (copper, aluminum, silver, copper oxide, alumina, silicon oxide, and graphite) with low volumetric concentration (0.1 to 1%) minimum change in pressure drop. It was observed that copper gives the highest reduction in borehole thermal resistance of about 3.8% when volumetric concentration was 1%; however, it provides the highest pressure drop.

Naili et al. [109] conducted an experimental analysis to evaluate the geothermal resources for air conditioning in Northern Tunisia. Results show that a test room's average temperature is reduced by about 2°C during a day using a horizontal ground heat exchanger. They calculated the COP of the heat pump and COP of the whole system as 4.46 and 3.02, proving that the GSHP system is a beneficial solution in Tunisia.

Wu et al. [110] performed experiments and numerical simulation for slinky type HGHE considering the UK's climate. They investigated the system's performance for different slinky intervals distances and coil diameters using a 3D model. Results show that the average COP of the system was 2.5 and the numerical calculations show no significant difference in the extraction of the heat of heat exchanger at different coil diameters while the larger diameter coil was founded to give higher extraction per unit length pf soil. However, it was observed that heat extraction per unit length of soil was decreased with an increase in coil interval distance.

Wu et al. [111] analyzed the performance of HGSHPs both numerically and experimentally in the UK's climate. They studied the numerical simulation of a 2D transient model considering different parameters such as ambient air temperature, refrigerant properties, wind speed, and soil thermal conductivity. Results show that the specific heat extraction increased with soil thermal conductivity and ambient temperature, decreasing the increase in refrigerant temperature. It was observed that the effect of wind speed was negligible.

Naili et al. [112] analyzed the performance of HGHE experimentally and analytically to evaluate optimum parameters of GHE. They examined the effects of different parameters such as an inlet temperature of GHE, the mass flow rate of working fluid, length, and buried depth of GHE. Also, they investigated water to water ground source cooling systems implementing HGHE. It was observed that the COP of the heat pump and COP of the system ranged between 3.8 - 4.5 and 2.3 - 2.7 for the GSCS. Results show that the utilization of GSHP in Tunisia is suitable for cooling buildings.

N. Kayaci et al. [113] developed a numerical model to validate their experimental results carried out using GSHP. They conducted an hourly simulation of a 200 m^2 office, and the variation of ground soil temperature, fluid inlet and outlet temperatures are examined for ten years. It was observed that higher temperature fluid at the inlet is best suited for GSHP operation. However, higher distances (more than 2 m) between the pipes have no remarkable effect on soil temperature.

Naili et al. [114] analyzed the performance of horizontal ground heat exchanger experimentally for space cooling. The total cooling requirements were tested for a surface of 12 m^2 and it was observed that the system's energy efficiency ranges between 14 -28%. Results show that the GHE with a length of 25 m and burial depth of 1 m covers 38.5% of the tested surface area's overall cooling requirement.

P.C.M. Kumar et al. [107] conducted CFD analysis to determine heat transfer rate and pressure drop for a helically coiled heat exchanger. The simulations were carried out for a

laminar flow considering 0.1%, 0.4%, and 0.8% volume concentrations of nanoparticles. It was observed that the Nusselt number (Nu) and maximum pressure drop are 30% and 9% higher than the water. They founded that the average relative error between the experimental and CFD simulation results for pressure drop and Nu was 9.5% and 8.5%, respectively.

Selamat et al. [115] examined the methods to optimize the design for HGHEs by using different pipe materials and layouts. It was observed that there is an improvement in the performance of the system of about 16% when the copper pipe is used in replacement of traditional HDPE pipes. Results show that the system's effective period can be improved by 14% when the GHEs are installed in the vertical orientation.

A.Flaga-Maryanczyk et al. [116] presented experimental and simulation results for a ground source heat exchanger operating in a cold climate. It was observed that the simulated results show a good agreement with experimental results. The results give an RMS error of 0.62%, which indicates a difference of 1.7 degrees only. It was found that the results obtained were satisfactory and could be used for operating a passive ventilation system in a cold climate.

Table 4: GSHP research summary.

Author	Place/Year	Season	Material	Length of Pipe [m]	Diameter of Pipe [m]	Velocity range [m/s]	Temperature range [°C]	Depth of Pipe [m]	Variable	COP/others
Congedo et al. [95]	Lecce, Italy, 2010	Summer & Winter	--	--	--	0.25-1.0	--	1.5 2.0 2.5	Configuration	Helical
Benli [91]	Turkey, 2012	Summer & Winter	--	--	--	--	40 - 56	2 60	Burial Depth	COP_{sys} (HGHE) = 3.0 COP_{sys} (VGHE) = 3.3
Bakirci [92]	Turkey, 2009	Summer & Winter	--	--	0.032	--	15	53	--	COP_{sys} = 2.6
Kayaci et al. [93]	Turkey, 2020	--	HDPE	85	0.026	--	30 - 50	1.45	NPT	Increases
Luo et al. [94]	Nuremberg, Germany, 2014	Summer & Winter	--	--	0.121 0165 0.180	--	16	80	--	Decreased by 4.0% over 4 years period
Girard et al. [97]	2015	--	--	--	--	--	30-60	--	Geographical Location	COP (GSHP) = 4.4-5.1 COP (SGSHP) = 4.4-5.8
Zhu et al. [98]	Tianjin, China, 2015	Summer & Winter	--	--	--	--	25.9-35	120	--	Increased by 3.4%
Kim et al. [101]	Korea, 2020	--	HDPE	--	--	--	22-45	150	Configuration, Material	Increases
Asgari et al. [106]	Tehran, Iran, 2020	--	--	900	--	--	--	1-2	Pipe Arrangements	Soil Thermal conductivity
Dasara et al. [105]	Mumbai, India, 2015	--	--	--	--	0.25 -1	--	1.5 2.5	Mass flow Rate	Soil Thermal conductivity
Esen et al. [104]	Turkey, 2007	--	PVC	100	0.016	--	7-18	1 2	Burial Depth	Increase in COP_{sys} (HGHE)
Fujii et al. [103]	Japan, 2012	--	PVC	--	0.024	--	7.1-27.5	1.5	--	Numerical Model

Author	Place/Year	Season	Material	Length of Pipe [m]	Diameter of Pipe [m]	Velocity range [m/s]	Temperature range [°C]	Depth of Pipe [m]	Variable	COP/others
Kim et al. [117]	The Republic of Korea, 2016	--	--	18	0.02	0.251	18-23	1	Soil Thermal Conductivity	Spiral Coil (HGHE)
				24	0.02	0.211				Slinky (HGHE)
Selamat et al. [115]	Japan, 2016	--	HDPE	17	0.0127	--	--	1	Configuration & Orientation	16% improvement for copper pipe
			Copper	39	0.0127					

S.A.M Said et al. [118] investigates a model for examining the heat transfer using horizontal heat exchanger pipes. The simulated model was presented considering thermal properties of soil, ground surface temperature, the distance between the borewells, and the gap between the pipes in every borehole. Results show that change of ground surface temperature works as a deciding factor for the overall length of the pipes, and it was observed that the pumping power decreases with an increase in the number of parallel loops used for GHE, working under the same climatic conditions and for the same length.

The temperature difference (ΔT) of ambient air and earth temperature is the cause of heat transfer. This temperature difference varies slightly throughout the day, thus keeping ΔT always maximum. The surface area or contact area of the pipe with the ground has to be maximized optimally to achieve maximum heat transfer. However, a long pipe means more cost. If we can control the heat transfer rate effectively, then the overall cost can be reduced. When turbulence is generated within the fluid, a thermally resistant, static boundary layer is formed near the transfer surface [119]. This type of effect can be reduced by the spirally corrugated design.

From the literature survey, it can be concluded that the performance of the GSHP or an EAHE system depends on the material type of the pipe, length of the pipe, diameter of the pipe, pattern of the pipes laid on the ground, underground soil temperature, soil properties, soil thermal conductivity, inlet flow velocity, geographical and climatic conditions. For the computational formulation selection of suitable software like FLUENT, TRNSYS, EnergyPlus, REHAU. The performance parameter affected is the pressure drop, temperature drop at the inlet and outlet, convective heat transfer coefficient, Reynolds Number, Friction factor, overall heat transfer coefficient, heat capacity and the total heat generated by the system. In the case of coupled GSHP system, the coefficient of performance is greatly affected. The significance of Boundary layer formation inside the pipes has not been brought into focus. An attempt can be made by comparing different duct geometries with varying duct materials considering the pipes' boundary layer formation. Computational software such as ANSYS

FLUENT, STAR-CD can be used as the simulation tool to evaluate the performance parameters mentioned above.

2.4 Discussions

The results of various studies conducted are shown in Tables 1 to Table 6. It has been analyzed from the tables that results mainly focus on the variation of outlet temperature. It should be noted that according to the working principle of GSHP, the outlet temperature depends on the location, season, depth, length and diameter of the pipe, ambient temperature, the thermal conductivity of the pipe, airflow velocity, and configuration. It has been varied from the results of various studies in the literature. Following are parameters that influence the performance of GSHP with summarized suggestions.

1. Underground Soil temperature: The underground soil temperature depends on the aboveground temperature. The soil characteristics also influence the underground soil temperature. The soil temperature increases with an increase in depth [49], but soil temperature should be lower than the surface temperature. The decrease in soil temperature decreases the heat transfer rate [52]. At a certain depth, the soil temperature becomes stable.

2. Depth of pipe and pipe orientation: Burial depth is directly proportional to soil temperature. As the depth of the pipe goes deeper into the earth, the soil temperature increases. But the burial depth is inversely proportional to the outlet temperature. Depth of pipe affects the thermal potential. It was seen in the literature that temperature increases with depth in winters and decreases in summers [49]. Hatraf et al. suggest that the depth of pipe burial depends on the diffusivity of the pipe. The cooling capacity increases as depth increases. Generally, the burial depth considered for the studies varies between 2-5m. The pipe orientations used in the literature are open-loop, closed-loop. The pipes were also laid in a parallel and serpentine manner. These configurations have not much effect on thermal performance.

3. Diameter of pipe: The diameter of the pipe is directly proportional to the outlet temperature. As the diameter of the pipe is increased, the outlet temperature also increases. But increase in the pipe diameter reduces the convective heat transfer coefficient, which in turn reduced the system's heating capacity. Generally, diameters vary between 0.1- 0.6 m, as suggested in the studies.

4. Length of the pipe: The length of the pipe is directly proportional to outlet temperature. As for length increases, the outlet temperature also increases. This enhances the healing potential of the system. The optimal length depends on the climatic conditions.

5. Pipe Material: The pipe material does not affect the performance of EAHE. Thus, a cheaper pipe material such as PVC can also be used. This makes the system more economical. But in the case of GSHP, since the heat-carrying capacity of working fluid is more, pipe material plays a significant role.

6. Airflow velocity: Airflow velocity is directly proportional to outlet temperature. Any slight change in the airflow velocity causes a decrease in the outlet temperature. High air flow velocities are not considered as it is not energy efficient. Generally, the airflow velocity varied between 2-5 m/s, as suggested by the studies.

7. COP: As suggested in the literature, the COP in winters is lower than COP in summers. Thus, GSHP systems can be used in both the season for space heating and cooling.

As noted from the literature survey, EAHE or GSHP saves up to 50% more energy than conventional systems. Depending on the current scenario GSHP is the perfect alternative to conventional systems employed in commercial, residential, and agricultural buildings to achieve thermal comfort.

2.5 Conclusion

Minimizing high-grade energy and promoting renewable energy to save the earth from hazardous effects have become important aspects in today's world. Heating/cooling air with EAHE is a passive way to reduce heat losses due to ventilation and thermal

comfort. GSHP is an emerging technique that can be efficiently used for pre-heating in winters and vice versa in summers. Computational software like FLUENT, EnergyPlus, TRANSYS, etc., is used in the studies to predict the thermal performance of the GSHP system. The literature concludes that the soil temperature is lower in summers and higher than the outside air in winters after a certain depth. Generally, a depth of 2.5 m -3 m is recommended for constant soil temperature. While analyzing the performance of GSHP, soil properties such as moisture content, soil type must be considered. The design parameters such as the pipe's material, the pipe's diameter, length of pipe, and air velocity inside the pipes have found a significant effect on its performance. Thus, while designing GSHP, consideration of design parameters and soil properties play an essential role in evaluating the performance.

Literature shows that EAHE or GSHP is installed in different locations such as the hot and humid climate of Sahara, the cold weather of Australia, Brazil and Tunisia's tropical climate, the Mediterranean climate, and a moderate climate India, that makes GSHP feasible to use. EAHE systems are also made in conjunction with a ventilation system and other cooling techniques to obtain the optimal inner room temperature. GSHP enhances the use of low energy cooling techniques to eliminate air conditioning systems in buildings. Using hybrid EAHE other than EAHE has become very prominent in today's research as it promotes more energy saving. It must be noted that EAHE saves about 5% more energy than conventional systems. Thus, GSHP or EAHE is an efficient energy technology that can replace the existing approach to reduce today's energy crisis. Understanding the actual behavior of GSHP or EAHE simulation along with data interpretation is very useful. But the crucial parameters that influence the performance of GSHP must be investigated and selected with care and understanding to get the optimal temperature difference.

2.6 Research Gap:

From all literature discussed above, we can conclude that although so much research has been conducted to improve the performance of the GSHP by using various

secondary fluid and pipe layout [79-94], no significant step has been taken to improve the thermal performance by varying primary working fluid and basic geometry.

All the studies conducted till now, only air, water mixed with some antifreeze like methyl alcohol or ethyl alcohol have been used as the primary working fluid. We must look after a new working fluid that is more effective and durable as compared to the conventional fluid.

2.7 The objectives of this study:

The objectives of the proposed study are as following:

1. Performance evaluation of conventional GSHP system using experimental setup and Numerical model.
2. Design and performance evaluation of modified GSHP system and Validation of Numerical model.
3. Design modification and testing of GSHP with microencapsulated phase change material for summer cooling and winter heating using Numerical Model.
4. Design modification and testing of GSHP with water-nanoparticle fluid for summer cooling and winter heating using Numerical Model.

3 PROBLEM SETUP

3.1 Introduction

This current study aims to understand the impact of pipe geometry and working fluid on the performance of GHE. A plane pipe has been compared to the novel spirally corrugated pipe for the present study, generating swirling flow. Also, the working fluids which are studied are water, Al_2O_3- water nanofluid, and micro-encapsulated phase change material (MPCM) slurry. The computational fluid dynamics (CFD) analysis

Literature review of various parameters of Ground Source Heat Pumps and their impact on performance.

Modelling and designing Experimental setup of base pipe geometry with water as working fluid.

Validation of the CFD model with existing experimental model.

Design modification and then numerical analysis with base fluid. Results will be compared for plain pipe and novel pipe geometry.

CFD model of microencapsulated phase change slurry will be developed, and simulation will run with modified design and plain pipe.

CFD model of water based Nanofluid will be developed, and simulation will run with modified design and plain pipe.

Effect of different working fluid will be compared. Also, the effect of modified design will be studied.

was conducted using Ansys, Fluent 14.0. This software gives us greater flexibility and control to simulate the conditions accurately. The results are expected to be in the form of outlet temperatures from the GHE, which will then be utilized for performance analysis.

To achieve the proposed objectives of work, a methodology is prepared. We will design and model a base fluid and base geometry (Objective 1). The results of this numerical analysis will be compared with an experimental study conducted in India for validation purposes. Once our model is validated, we will work on proposed modifications in the geometry of pipe and various working fluid combinations to evaluate the system's performance (Objective 2 to 4).

3.2   Spirally Corrugated Pipe

To improve the performance of heat exchanger, there are various techniques which are employed. Using inserts to or corrugation are part of passive techniques to enhance the heat exchanger performance. In spirally corrugated pipes, the fluid induces nonaxial velocities, thus enhancing secondary recirculation flow [120]. This enhancement comes with some loss of pressure. This pressure loss is due to the surface curvature pass and secondary flow swirls [121].

Table 5: Research conducted on the spirally corrugated tube.

	Author	Findings
[122]	Mimura and Isozaki	Effect of corrugation height and depth was studied by comparing friction factor and heat transfer
[123]	Withers	Heat transfer and pressure drop relationship was developed
[124]	Asako and Nakamura	Studied thermohydraulic characteristics of a rounded corner corrugation

[125]	Garimala et. al.	Studied laminar, transitional, and turbulent flow in a spiral flute tube
[126]	Rainieri et. al.	Studied thermal characteristics for variable pitch values in a spirally corrugated tube
[127]	Pethkool et. al.	Found higher thermal performance in the spirally corrugated pipe when compared to a smooth pipe
[128]	Z. S. Kareem et. al.	Evaluated thermophysical properties of two-start spirally corrugated tube

Previous research (Table 5) on the spirally corrugated pipe has also suggested better performance, and results found were close to reality. Thus, a novel six-start with a smooth profile or round edges was studied. The design can be seen in Fig. 14 and 15.

3.3 Geometry and Meshing

The 3-D geometry of the GHE pipe was created using Creo Parametric. The aim behind creating these geometries is to maintain a constant hydraulic diameter of 0.04 m for both geometries. Further details related to design can be found in Table 6.

Hydraulic diameter and length of pipe are equal for both geometries.

Table 6: Boundary condition considered for the current study.

Inlet Condition	Reynolds Number	
	5000, 7500 and 10000	
Outlet Condition	Pressure (atm)	
	1	
Wall Condition	Temperature (^{0}C)	Wall Thickness (m)
	25	0.001
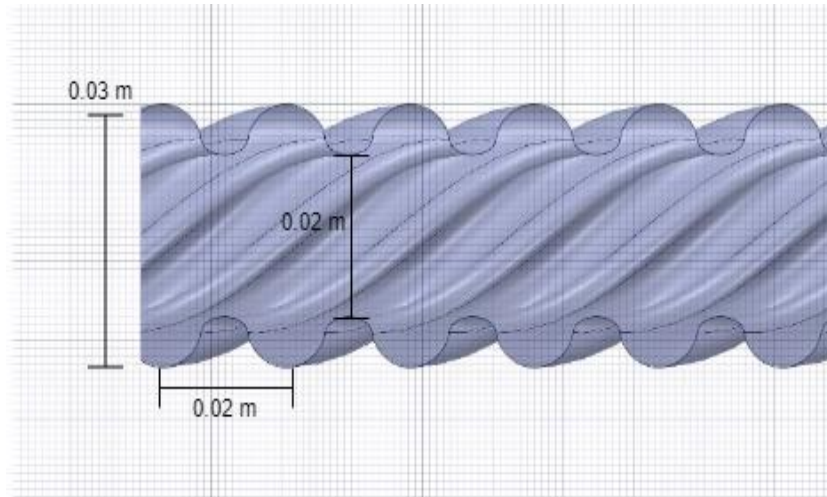
Figure 14: Novel pipe design (pitch = 0.02 m)
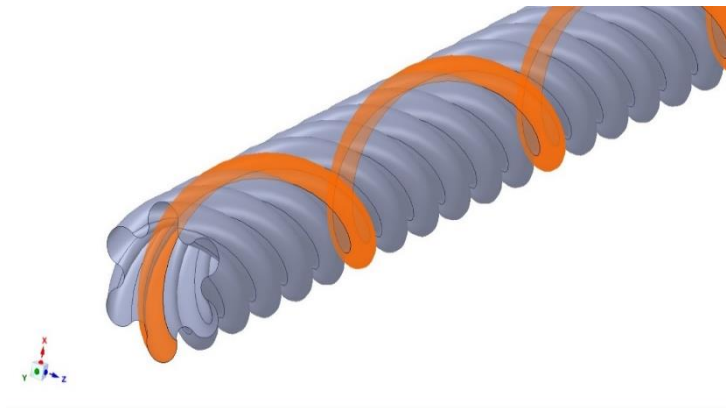
Figure 15: Novel Spirally corrugated pipe design

The pipe design is inspired by already tested spirally corrugated pipes by various researchers across globe. The major difference in this design is rounded corrugations which helps in reducing losses during fluid flow.

3.4   Mathematical Modelling

3.4.1   *Governing equations in generalized form:*

Continuity equation:

$$\frac{\partial \rho}{\partial t} + \nabla.\left(\rho \vec{v}\right) = S_m \quad \frac{\partial \rho}{\partial t} + \nabla.\left(\rho \vec{v}\right) = S_m \tag{1}$$

The above equation is in the general form of a mass conservation equation. It is valid for compressible as well as incompressible flow. The source S_m is the mass added to the continuous phase from the dispersed second phase (e.g., due to vaporization of liquid droplets) and any user-defined sources.

Conservation of momentum:

$$\frac{\partial \left(\rho \vec{v}\right)}{\partial t} + \nabla.(\rho \vec{v} \vec{v}) = -\nabla p + \nabla.\left(\overline{\overline{\tau}}\right) + \rho \vec{g} + \vec{F} \tag{2}$$

P is the static pressure, $\overline{\overline{\tau}}$ the stress tensor (described below), and the gravitational body force and external body forces (e.g., that arise from interaction with the dispersed phase). $\vec{F}$ also contains other model-dependent source terms such as porous media and user-defined sources.

The stress tensor $\overline{\overline{\tau}}$ is given as

$$\overline{\overline{\tau}} = \mu \left[\left(\nabla \vec{v} + \nabla \vec{v}^T\right) - \frac{2}{3} \nabla.\vec{v} I\right] \tag{3}$$

Where μ is the molecular viscosity, I is the unit tensor, and the second term on the right-hand side is the effect of volume dilation.

Conservation of energy:

$$\frac{\partial}{\partial t}(\rho E) + \nabla.\left\{\vec{v}(\rho E + p)\right\} = \nabla.\left(k_{eff} \nabla T - \sum_j h_j \vec{J_j} + (\overline{\overline{\tau}}_{eff}.\vec{v})\right) + S_h \tag{4}$$

Where k_{eff} is the effective conductivity ($k + k_t$, where k_t is the turbulent thermal conductivity defined according to the turbulence model being used), and $\vec{J_j}$ is the diffusion flux of species j. The first three terms on the right-hand side represent energy transfer due to conduction, species diffusion, and viscous dissipation. S_h includes the heat of chemical reaction and any other volumetric heat sources if defined.

3.4.2 Governing equations for spirally corrugated pipe flow:

Continuity equation:

$$\frac{\partial u_r}{\partial r} + \frac{u_r}{r} + \frac{1}{r}\frac{\partial u_\theta}{\partial \theta} + \frac{\partial u_x}{\partial x} = 0 \tag{5}$$

Momentum equation *r* component:

$$\rho\left(u_r \frac{\partial u_r}{\partial r} + \frac{u_\theta}{r}\frac{\partial u_r}{\partial \theta} - \frac{u_\theta^2}{r} + u_x \frac{u_r}{x} \right) = -\frac{\partial P}{\partial r} + \mu\left(\frac{\partial^2 u_r}{\partial r^2} + \frac{1}{r}\frac{\partial u_r}{\partial r} - \frac{u_r}{r^2} + \frac{1}{r^2}\frac{\partial^2 u_r}{\partial \theta^2} - \frac{2}{r^2}\frac{\partial u_\theta}{\partial \theta} + \frac{\partial^2 u_r}{\partial x^2} \right)$$

$$\text{(6)}$$

Momentum equation θ component:

$$\rho\left(u_r \frac{\partial u_\theta}{\partial r} + \frac{u_\theta}{r}\frac{\partial u_\theta}{\partial \theta} + \frac{u_r u_\theta}{r} + u_x \frac{\partial u_\theta}{\partial x} \right) = -\frac{1}{r}\frac{\partial P}{\partial \theta} + \mu\left(\frac{\partial^2 u_\theta}{\partial r^2} + \frac{1}{r}\frac{\partial u_\theta}{\partial r} - \frac{u_\theta}{r^2} + \frac{1}{r^2}\frac{\partial^2 u_\theta}{\partial \theta^2} + \frac{2}{r^2}\frac{\partial u_r}{\partial \theta} + \frac{\partial^2 u_\theta}{\partial x^2} \right)$$

$$\text{(7)}$$

Momentum equation x component:

$$\rho\left(u_r \frac{\partial u_x}{\partial r} + \frac{u_\theta}{r}\frac{\partial u_x}{\partial \theta} + u_x \frac{\partial u_\theta}{\partial x} \right) = -\frac{\partial P}{\partial \theta} + \mu\left(\frac{\partial^2 u_x}{\partial r^2} + \frac{1}{r}\frac{\partial u_x}{\partial r} + \frac{1}{r^2}\frac{\partial^2 u_x}{\partial \theta^2} + \frac{\partial^2 u_x}{\partial x^2} \right) \tag{8}$$

Energy equation:

$$\rho c_p \left(u_r \frac{\partial T}{\partial r} + \frac{u_\theta}{r} \frac{\partial T}{\partial \theta} + u_x \frac{\partial T}{\partial x} \right) = k \left(\frac{1}{r} \frac{\partial}{\partial r} \left(r \frac{\partial T}{\partial r} \right) + \frac{1}{r^2} \frac{\partial^2 T}{\partial \theta^2} + \frac{\partial^2 T}{\partial x^2} \right) \qquad (9)$$

3.4.3 Heat Equation:

The primary mode of heat transfer in a GHE is conduction. The governing equation can be given as:

$$\nabla^2 T = \frac{1}{\alpha} \frac{dT}{dt}, \alpha = \frac{C_p}{\lambda} \qquad (10)$$

Where,

λ is the thermal conductivity of medium (W/m-K)

C_p is the heat capacity (J/(m^{3}K))

α is the Thermal diffusivity (m^2/s)

3.5 Assumptions

Looking into the complex nature of GHE systems, some assumptions and simplifications are used in the current analysis.

  I.   The pipe of GHE is in continuous contact with the soil, and there are no air gaps in between.
  II.   The ground will be treated as a source or sink depending on whether we are extracting heat or rejecting heat and the temperature of the ground is constant.
  III. The pipe wall's outer temperature will remain constant along the pipe length and act as a thermal reservoir.
  IV.   The soil properties are homogeneous, and variation is ignored.

V. The undisturbed temperature along the pipe of GHE is assumed to be constant. This assumption can be considered because the temperature variation beneath the ground is significantly less.

VI. No heat losses are considered, and the whole system is isolated.

3.6 Parameters Considered

Table 7: List of Parameters considered for the model.

Parameter	
Pipe Length	1 m
Depth of burial	1.5 m
Internal pipe diameter	0.0254 m
Thermal conductivity of the soil	1.41 W/mK
Thermal diffusivity of soil	0.0036 m^2/h
Thermal conductivity of water	0.567 W/mK
Thermal conductivity of HDPE pipe	0.38 W/mK
Specific heat of the water	3.9 KJ/kgK
Velocity	0.5 m/s
Pumping Power	0.37 kWh

The study intends to compare two pipe geometries methodically. For this study, plain circular pipe and spirally corrugated pipe are considered. Enhancement in heat transfer while using a six-start spirally corrugated pipe has been highlighted by many authors [129][130][131][132].

3.7 Experimental Setup

To validate our numerical problem, an experiment was also conducted. The sole purpose of conducting this experiment was to test our model and its results. The setup configuration can be seen in figure 16.
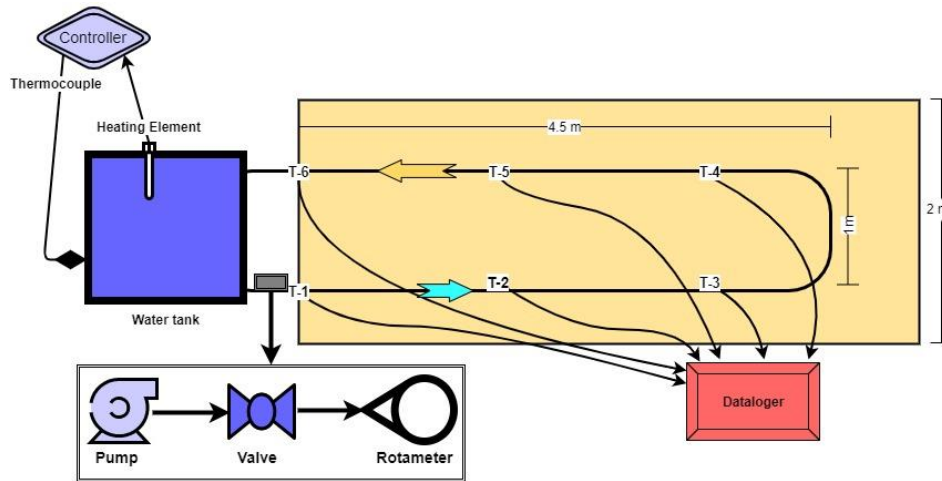
Figure 16: Experimental Setup

3.8 List of equipment

Table 8: List of equipment used in the experimental setup.

S. No.	Name of equipment	Image
1	Datalogger (8 channel) Thermotec L-2002	

S. No.	Name of equipment	Image
2	Controller – Honeywell DC1010 For maintaining inlet water temperature	
3	Digital Thermometer TP3001 (-50^0C - $+300^0$C) resolution of .01^0C and error $+-0.05^0$C.	
4	Rotameter (0-20LPM) resolution of 0.5 LPM	
5	RTD PT100 (6", 6mm) resolution is 0.02^0C and error $+-0.05^0$C. To be used as feedback for the controller. It will be attached to the water tank.	

S. No.	Name of equipment	Image
6	J-Type thermocouple PT100 (1.5", 3mm) resolution is 0.02^0C and error +- 0.05^0C. Time Constant = 0.45 sec To be used for measuring fluid and soil temperature.	
7	J-Type thermocouple PT100 (surface type) resolution is 0.02^0C and error +- 0.05^0C. To be used for measuring pipe surface temperature.	
8	Kalsi Shining Star Self Priming Monoblock Pump, 0.5 hp	
9	HDPE pipes, 1" dia.	

S. No.	Name of equipment	Image
10	Flow control valve	

3.9 Ground temperature

The average ground temperature for a depth of 1.5 m was calculated to be $25\,^0C$. Also, some sample reading for the temperature variation for a single day is given in the following table.

Table 9: Ground temperature variation on 22 September 2019.

Time	At 1m depth (^0C)	At 1.5 m depth (^0C)	Ambient temperature (^0C)
9 AM	26	25.02	30
10:30 AM	26.04	25.05	32
12 Noon	26.09	25.08	33
1:30 PM	27	25.09	34
3 PM	26.08	25.07	34
4:30 PM	26.06	25.06	32
Avg. Temp. Difference	**6.28**	**7.43**	
Max Temp. Difference (3 PM)	**7.92**	**8.93**	

Ambient conditions: T_{max}= $34\,^0C$, T_{min}= $23\,^0C$, Humidity= 57%

3.10 Equations used for calculating various parameters.

3.10.1 Fluid Velocity

$$V = \frac{m}{\rho W H} \tag{11}$$

3.10.2 Hydraulic Diameter

The hydraulic diameter of the pipe is measured by the formula given below:

$$D_h = \frac{4 A_c}{P} \tag{12}$$

3.10.3 Reynolds Number (Re)

The formula for this is as given below in equation:

$$\mathrm{Re} = \frac{\rho V D_h}{\mu} \tag{13}$$

3.10.4 Friction Factor (f)

Darcy's equation is used for finding the Friction factor.

$$f = \frac{2(\Delta P) D_h}{4 \rho L V^2} \tag{14}$$

3.10.5 Coefficient of Heat transfer (h)

The heat transfer coefficient is calculated as

$$h = \frac{Q_u}{A_p \left(T_p - T_f \right)} \tag{15}$$

3.10.6 Heat Transfer Rate

The rate of transfer of heat (Q) is given by,

$$Q = mC_p \left(T_o - T_i \right) \tag{16}$$

3.10.7 Nusselt Number (Nu)

Nusselt number is calculated for finding the coefficient of heat transfer.

$$Nu = \frac{hD_h}{k} \tag{17}$$

Also, Churchil and Ozoe [133] developed a relation covering both entrance and fully developed region, which is as follows:

$$Nu_x = \left[4.364 \left(1 + \left(\frac{Gz}{29.6} \right)^2 \right)^{\frac{1}{6}} \right] \left[1 + \left[\frac{Gz/19.04}{\left[1 + \left(Pr/0.0207 \right)^{2/3} \right]^{1/2} \left[1 + \left(Gz/29.6 \right)^2 \right]^{1/3}} \right]^{3/2} \right]^{1/3}$$

$$\tag{18}$$

Where,

$$Gz = \frac{\pi}{4x} = \left[\left(\pi \, Re_{d_n} . Pr \right) \Big/ 4 \left(x/d_n \right) \right] \tag{19}$$

3.10.8 Coefficient of Performance (COP)

$$COP = \frac{Q}{W_{in}} \tag{20}$$

3.10.9 Time constant (Response Time)

It is a term used to understand the responsiveness of a sensor. It is time taken by sensor to read the 63.2% of its total step change in measurand. For the thermocouple used in our study the time constant $\mathcal{T} = 0.45$ sec.

3.11 Working Fluid

Working fluid is the heat carrier in an heat exchanger system. It is also one of the most critical factors which influence the performance of any heat exchanger. We will study and compare three working fluid types: water, water-based nanofluid, and MPCM slurry. The details of the property of these fluids are in Table 10.

Table 10: Working fluid properties.

	Mass/ volume Fraction (%)	Density (kg/m³)	Viscocity (mPa-s)	Effective Thermal Conductivity (W/m-⁰C)	Specific Heat (J/kg-K)
Water	-	998.2	1.003	0.6	4182
MPCM Slurry CT02 [134]	6	982.4	1.76	0.589	1700
Al₂O₃ / water [135]	0.6	1068.99	1.89	0.451	3485.30

MPCM slurry: When tiny or small particles of phase change material are encapsulated in homogeneous or heterogeneous capsules is known as Microencapsulation. This technique helps in handling flowing materials efficiently [136]. These particles are manufactured or fabricated by two processes: a) Chemical Process and b) Physical process. The particle size must be less than 100 µm; a chemical process is used. Otherwise, the physical process is used. Then this microencapsulated PCM is added to water or any other base fluid. From previous studies, it has been found that MPCM has enormous potential to be used as a working fluid in various heat transfer applications.

Nanofluid: Due to nanofluids' enhanced thermal properties even at low concentration, it makes it an ideal working fluid for heat transfer applications [137]. As the concentration of nanoparticles in the base fluid increases, the heat-carrying capacity also increases but simultaneously, the viscosity also increases. Al_2O_3 – water nanofluid is the commonly used nanofluid due to its cost-effectiveness and no adverse impact on the environment.

3.12 Numerical Setup

The simulation tool used for analysis is Ansys Fluent 14.0. It provides excellent control and options to simulate our problem close to the actual. Once the model was designed and geometry was created using Creo parametric, Fluent was used to generate the mesh. The mesh on the geometry can be seen in the following figure 17.

For the current study, three Reynolds Number, i.e., 5000, 7500 and 10000, were considered as they lie in the turbulent region. The corresponding velocities were calculated (as in Table 11). Also, three different inlet temperatures were taken for the Summer and Winter season.

Table 11: Velocities for all fluids at different Reynold No.

Re	Water (m/s)	Nanofluid (m/s)	MPCMs (m/s)
5000	0.197	0.348	0.352
7500	0.296	0.522	0.528
10000	0.394	0.696	0.705
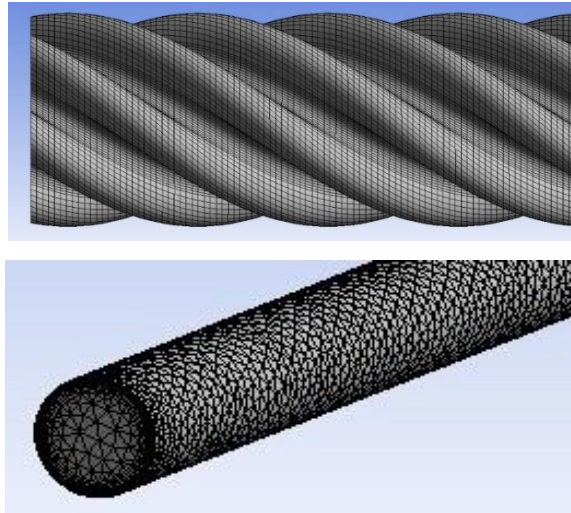
Figure 17: Meshing on Spirally corrugated pipe (top) and plain pipe (bottom).

3.12.1 Grid independence test

To refine our meshed model a grid independence test was done for the Nusselt number and the results can be seen in the following chart. An unstructured tetrahedral mesh was used because it captures the curved surfaces significantly better.
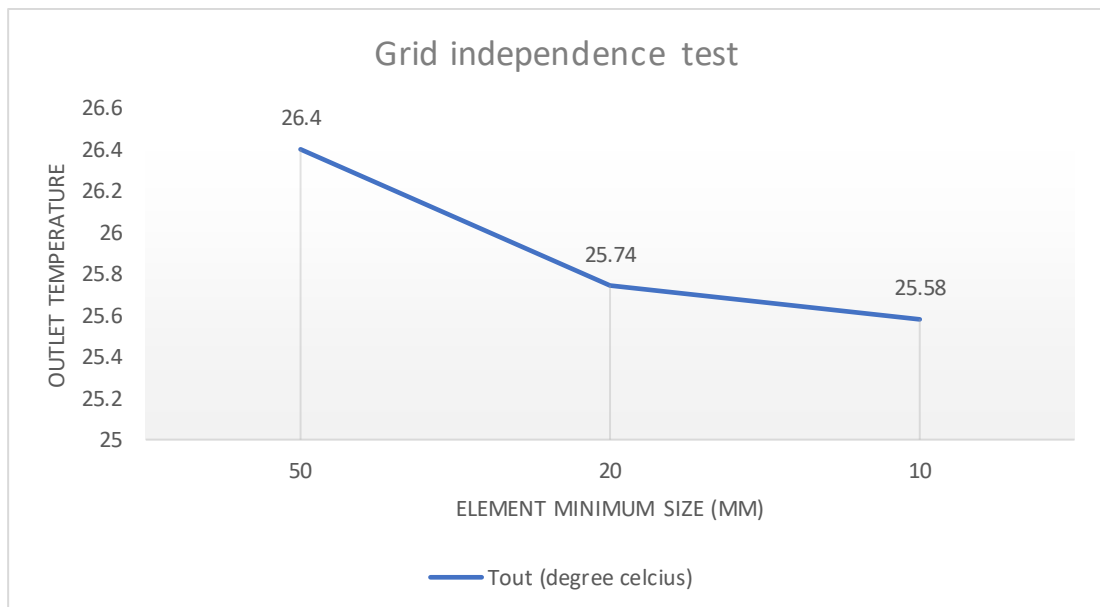
Figure 18: Grid independence test

The Y+ value signifies the mesh quality at the boundary; thus, it was kept within the range of $30 < Y+ < 500$. The difference in the value of Nusselt number for element size 10 mm and 20 mm is very less from the chart. Thus, to save computation time without losing the accuracy, an element size of 20 mm was chosen.

3.12.2 Ansys Fluent setup

The following options were chosen for performing the numerical simulation.

3.12.2.1 Models

The standard k-ε turbulence model was selected along with scalable wall functions (these shows better results when the flow is also rotating). The energy equation was turned on as heat transfer is involved.

3.12.2.2 Materials

In this section, materials are assigned to the model. Pipe walls are assigned HDPE properties, and fluid is defined and created as per the fluid properties. Then as per requirement, the desired fluid is selected for the simulation.

3.12.2.3 Cell zone conditions

Here the fluid domain is assigned.

3.12.2.4 Boundary conditions

Here inlet and outlet boundary conditions are assigned. For summers, the fluid inlet temperature is taken at 40^0C, and in winters, it is 15^0C. The pipe wall temperature is kept constant at 25^0C. Also, the fluid flow velocity is assigned. Inlet is taken as velocity inlet whereas outlet as pressure outlet with gauge pressure 0.

3.12.2.5 Solution

Under solution, the SIMPLE method is considered. A 1st order upwind scheme was applied for momentum and turbulent kinetic energy as it is more than enough for applications without chemical reaction. A 2nd order upwind scheme was used for pressure and energy equations.

3.12.2.6 Residuals

All the residuals are set to an order of 1e-06. Convergence was observed when the outlet temperature of the pipe stabilizes.

3.13 Validation of Numerical Model:

Our Numerical model was validated with the readings of the experimental setup. Our numerical model, which was compared to the experimental setup, is shown below.
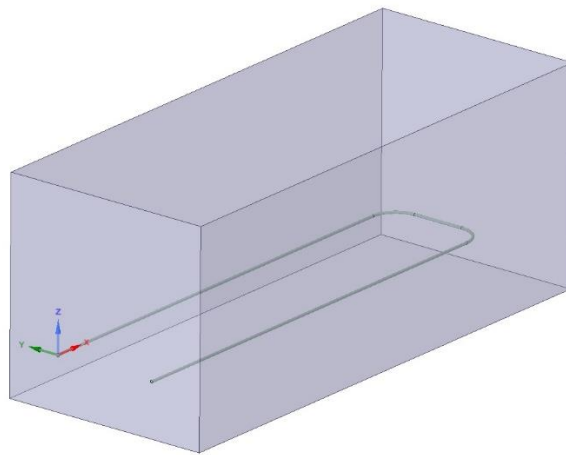
Figure 19: Model for numerical analysis.
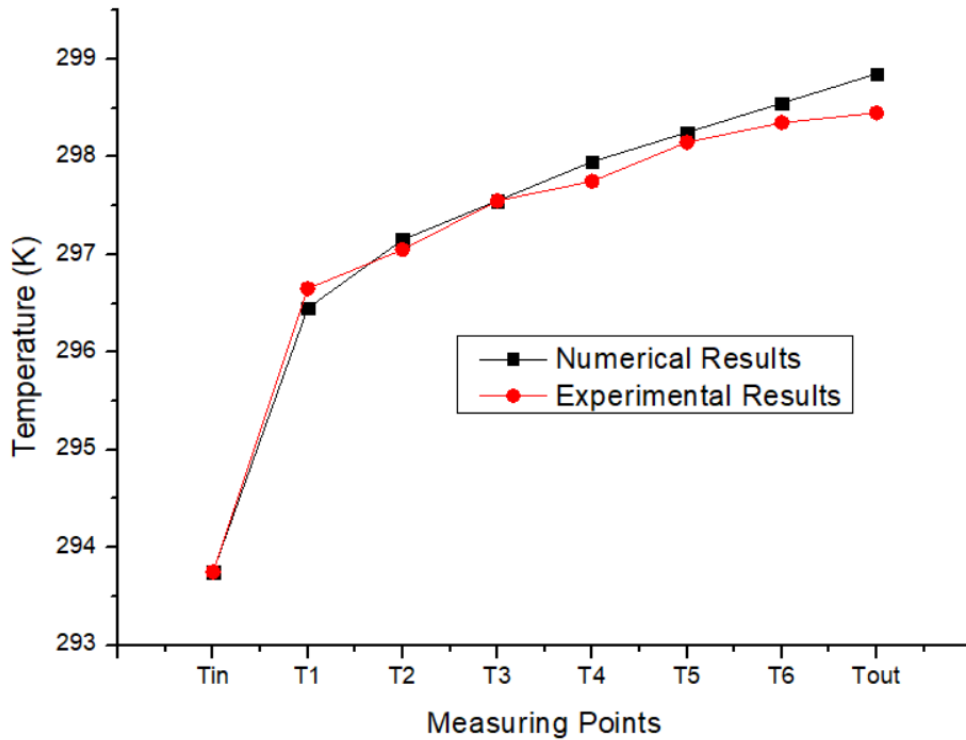
Figure 20: Temperature output as compared to the experimental results.

The variation of 1.58% (maximum) can be seen due to the heat loss while the fluid moves in the pipe. Also, the comparison is made for the plain pipe only. The numerical model is compared for the k-ω turbulence model and k-ε turbulence model. There is a minimal variation (up to a magnitude of 10^{-4}). So for further study, k-ε turbulence model will be used. Then the same design modeling will be used for the novel spirally corrugated pipe of 1m length to save computation time.

As the focus of the current study is to see whether the use of our novel pipe design helps in improving the performance. For that purpose, a pipe of a length of 1m (as shown in figure 21) is considered for further study.
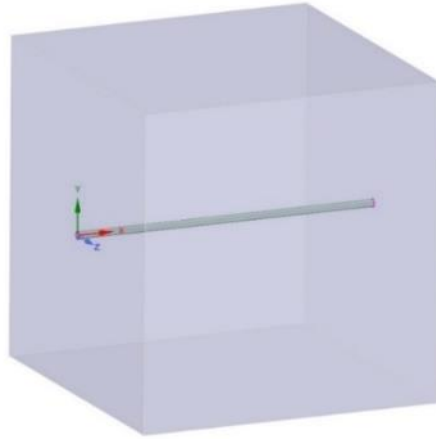
Figure 21: 1 m section of plain pipe in soil domain.

A similar six-start spirally corrugated – plain pipe hybrid was studied by Chen et al. (2019) [138]. The numerical modeling approach is kept the same as that of their study. The author also verified the model with analytical values, and the errors were found to be well within the range of 5%. Thus, our modified geometry model can be used for further analysis.

4 RESULTS AND DISCUSSION - 1

4.1 Summer Season

From figure 22, the variation of temperature at five different planes, i.e., Z = 0, 0.25, 0.5, 0.75, and 1 m, can be seen for both the pipes. As the fluid takes a spiral path, it breaks the laminar sub-layer present at the surface. This reduction in the laminar sub-layer helps increase turbulence, thus further increasing the heat transfer at the surface.
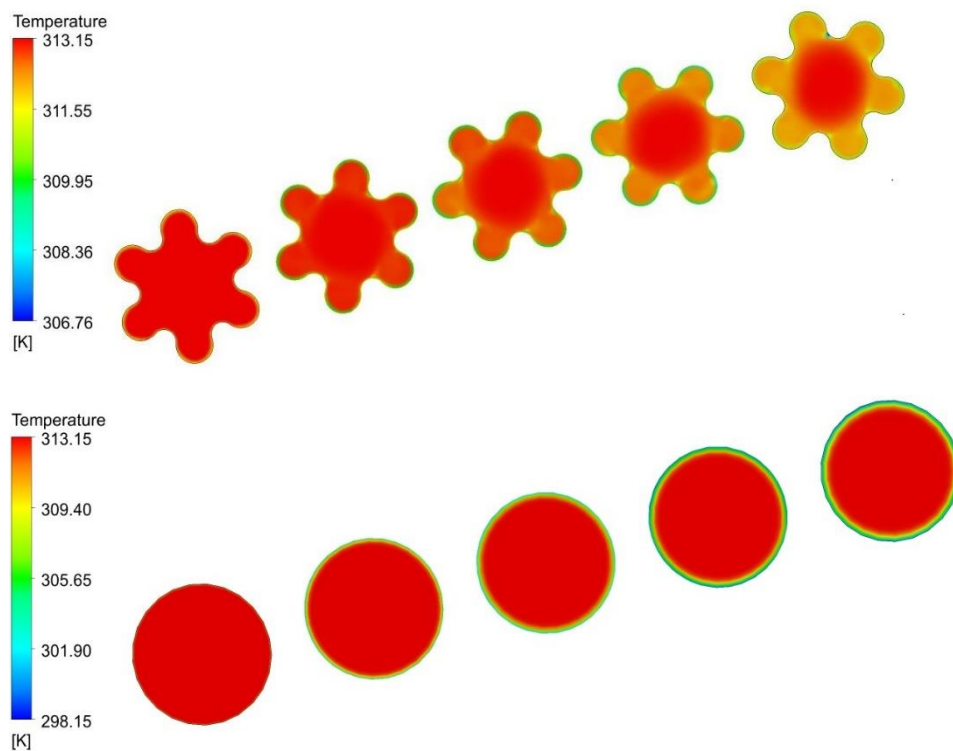
Figure 22: Temperature distribution spirally corrugated pipe and plain pipe in summer (at Z = 0, 0.25, 0.5, 0.75 and 1 m).

Three different inlet temperatures were considered as follows:

$T_{s1} = 35^0C$;

$T_{s2} = 37.5^0C$; and

$T_{s3} = 40^0C$.

90

4.2 Comparison of thermal performance in the spirally corrugated

4.2.1 For Re = 5000, (Spirally Corrugated pipe).

When the inlet temperature is T_{s1}, the maximum temperature drop is for MPCM slurry, i.e., 1.031^0C (Fig. 23). Nanofluid had the minimum temperature drop. The reason for nanofluids having less temperature drop is primarily due to low-temperature differences. As the time is not sufficient for the heat to transfer into suspended nanoparticles, it is less efficient. Similar results were found to be other inlet temperatures of 37.5^0C and 40^0C (Fig. 24 and 25). In these cases, MPCM slurry showed a maximum temperature drop of 1.289^0C and 1.546^0C for inlet temperatures of T_{s2} and T_{s3}, respectively.
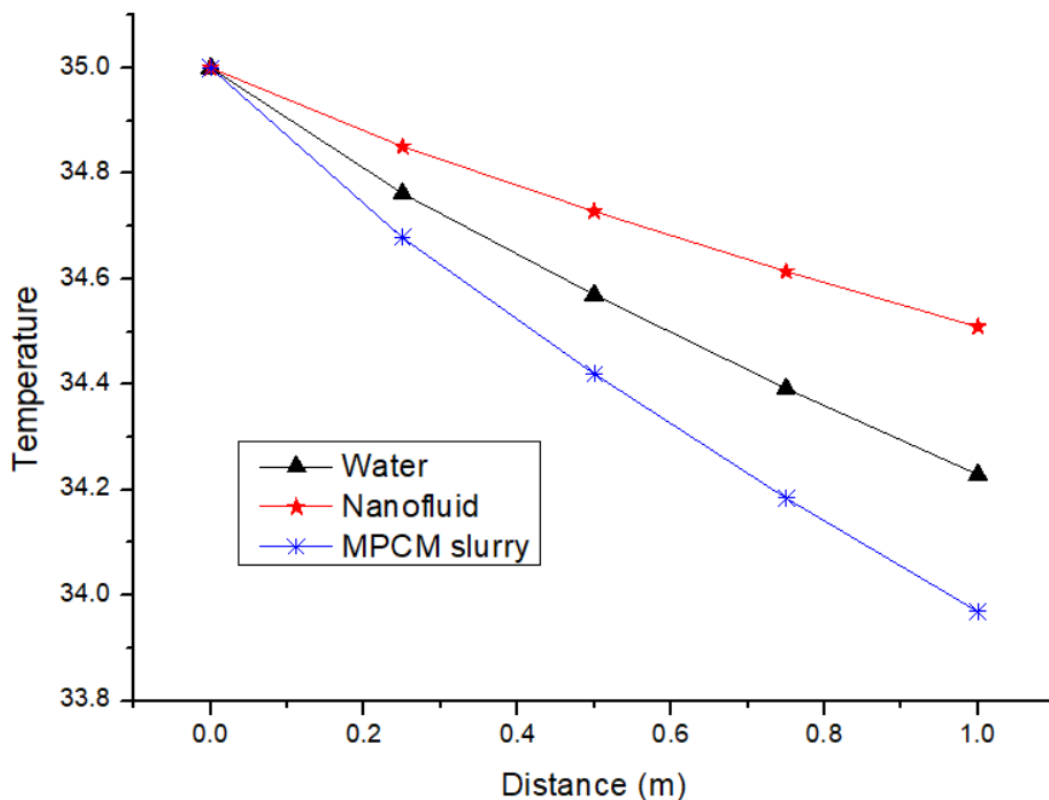
Figure 23: Temperature drop for Spirally corrugated pipe (Inlet temperature = 35^0C).

91
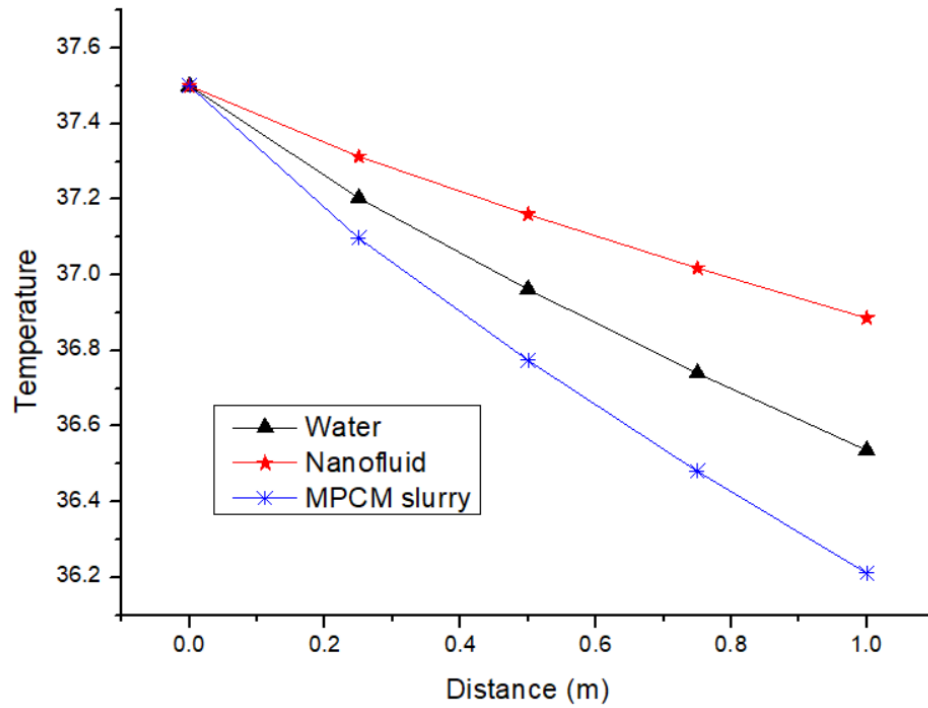
Figure 24: Temperature drop for Spirally corrugated pipe (Inlet temperature = 37.5⁰C).
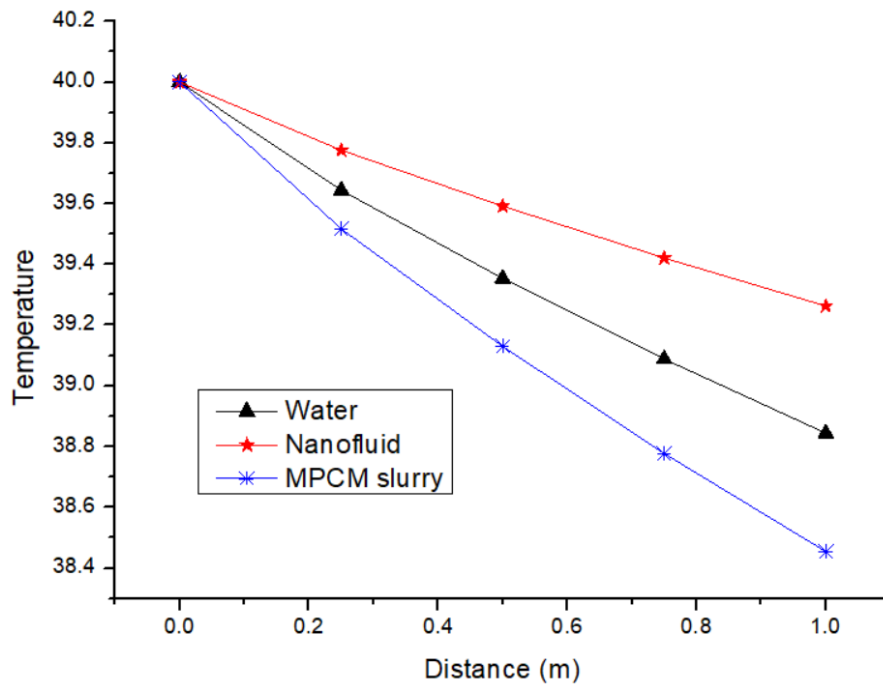
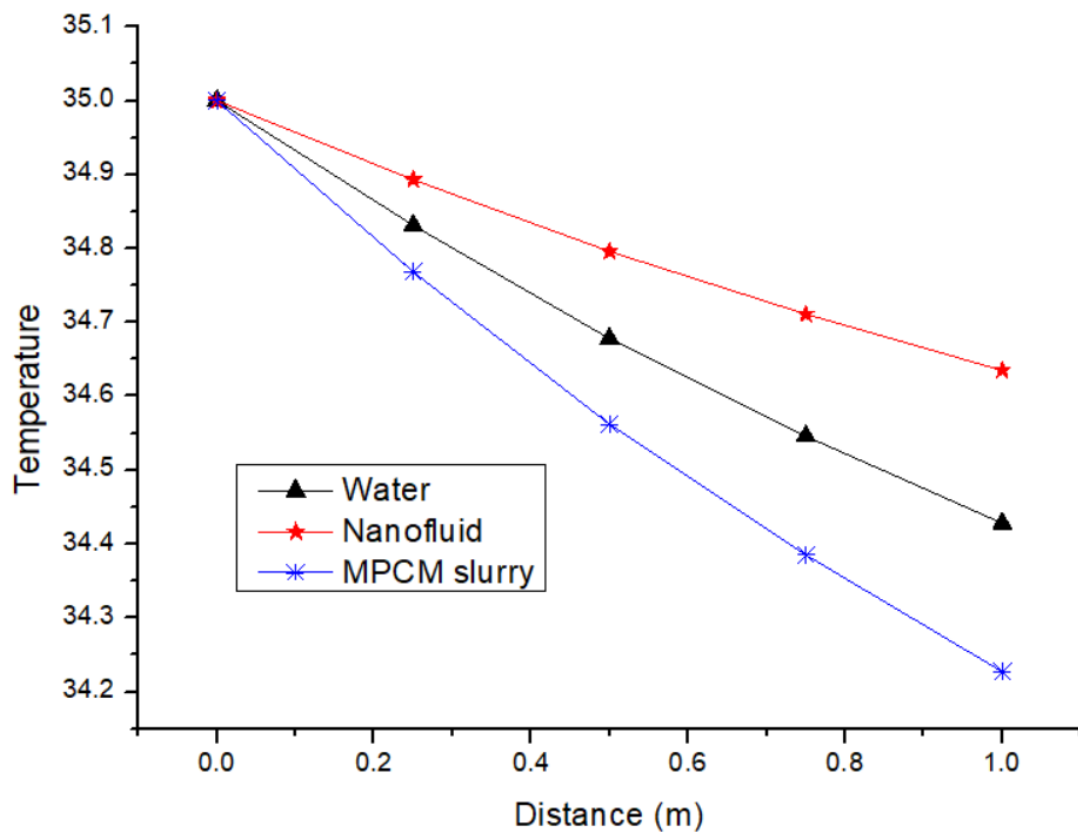**Figure 25: Temperature drop for Spirally corrugated pipe (Inlet temperature = 40⁰C).**

92

4.2.2 For Re = 5000, (Plain pipe)

From Fig. 26, when the inlet temperature is T_{s1}, then the maximum temperature drop for MPCM slurry, i.e., 0.421^0C. Similarly, for inlet temperatures of T_{s2} and T_{s3}, MPCM slurry got the maximum temperature drop of 0.527^0C and 0.632^0C, respectively. The results are shown in Fig. 27 and 28.
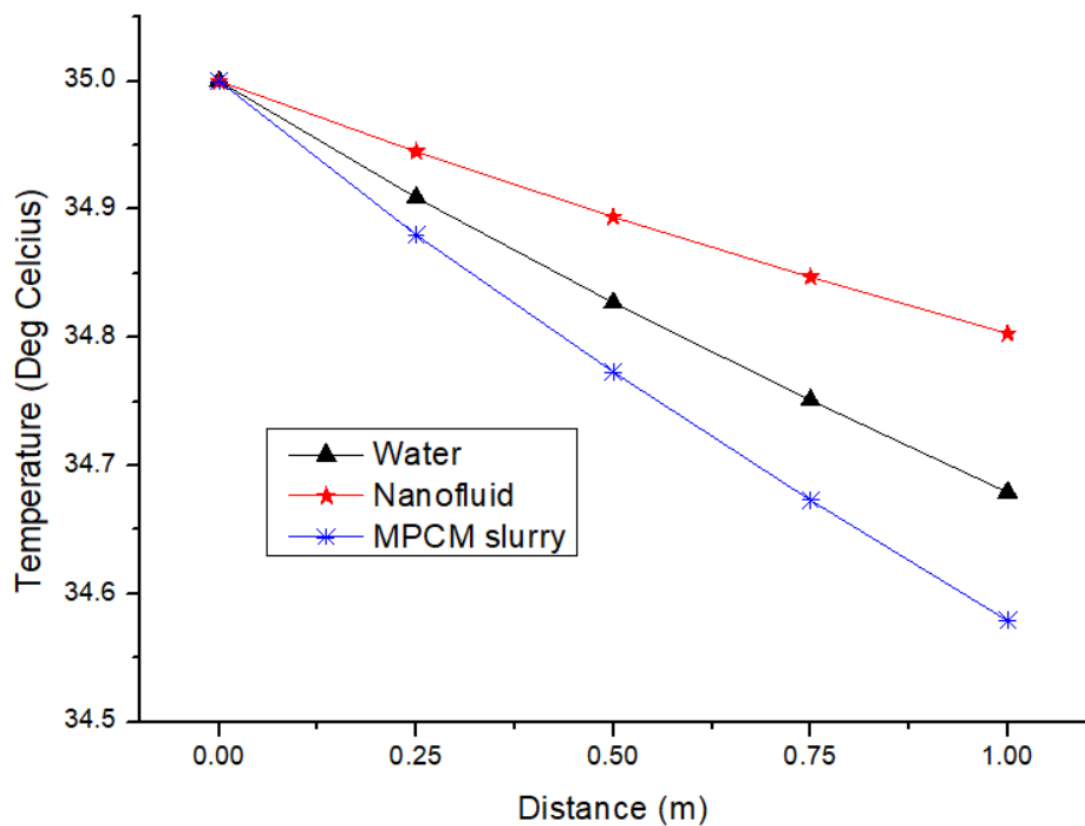
Figure 26: Temperature drop for plain pipe (Inlet temperature = 35⁰C).
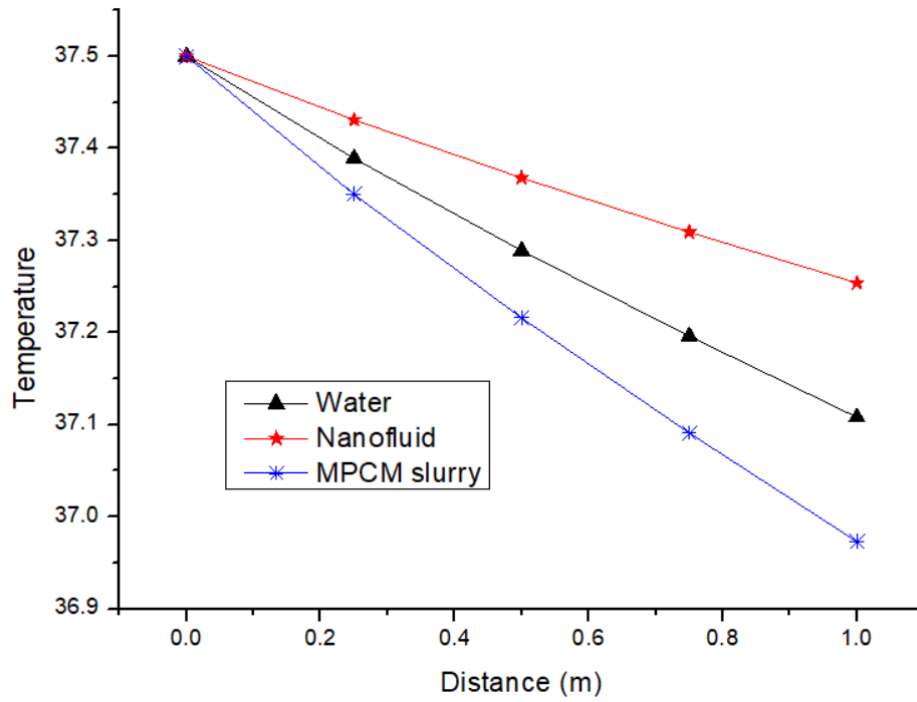
Figure 27: Temperature drop for plain pipe (Inlet temperature = 37.5⁰C).
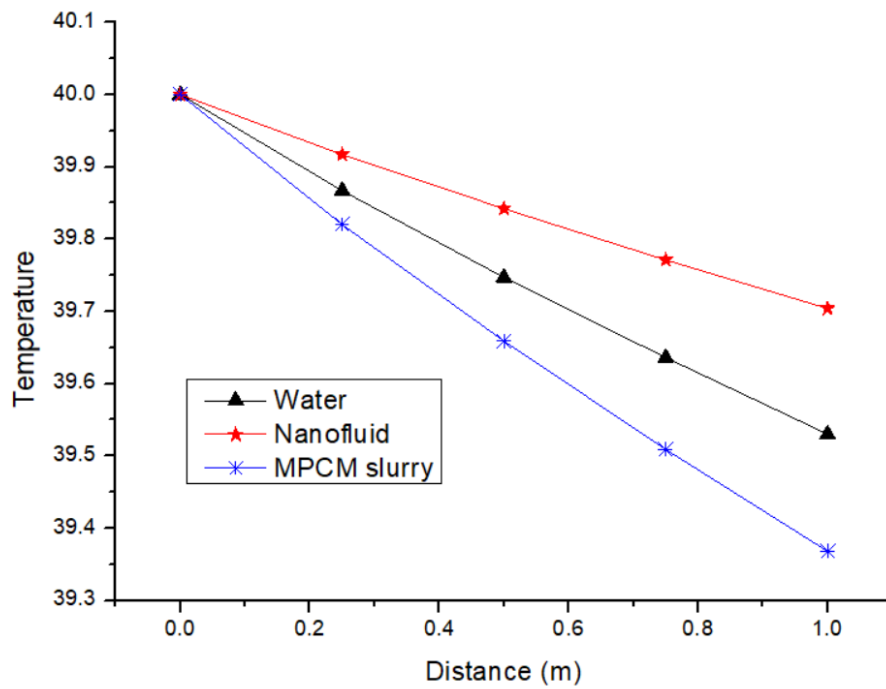
Figure 28: Temperature drop for plain pipe (Inlet temperature = 40⁰C).

4.2.3 For Re = 7500, (Spirally Corrugated pipe).

When the inlet temperature is T_{s1}, the maximum temperature drop is for MPCM slurry, i.e., $0.773\,^0C$ (Fig. 29). The difference in temperatures of water and MPCM slurry is $0.201\,^0C$. Similar results were found to be other inlet temperatures of $37.5\,^0C$ and $40\,^0C$ (Fig. 30 and 31). In these cases, MPCM slurry showed a maximum temperature drop of $0.966\,^0C$ and $1.16\,^0C$ for inlet temperatures of T_{s2} and T_{s3}, respectively. Again nanofluid had a minor temperature drop.

Figure 29: Temperature drop for spirally corrugated pipe (inlet temperature = $35\,^0C$).
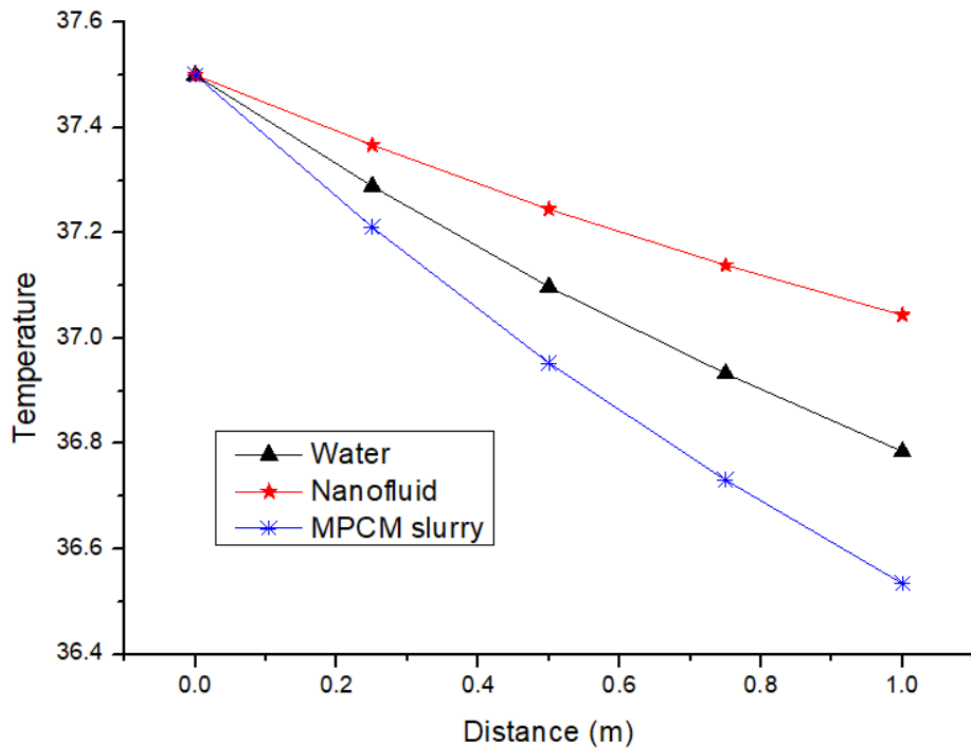
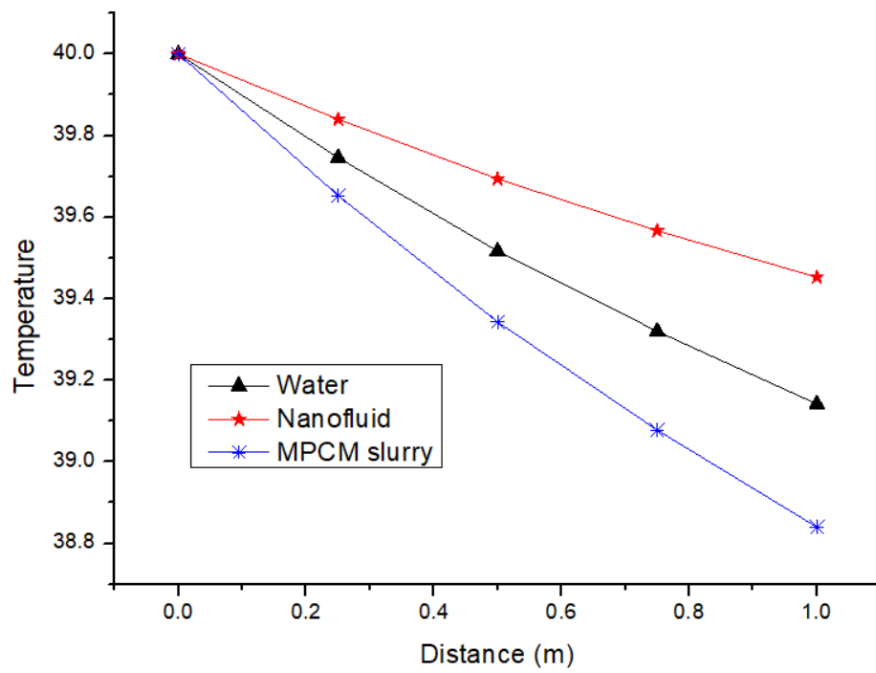**Figure 30: Temperature drop for spirally corrugated pipe (inlet temperature = 37.5⁰C).**

Figure 31: Temperature drop for spirally corrugated pipe (inlet temperature = 40⁰C).

4.2.4 For Re = 7500, (Plain pipe)

The difference in outlet temperature of all three fluids can be seen in Fig. 32. When the inlet temperature is T_{s1}, the maximum temperature drop is for MPCM slurry, i.e., 0.315^0C. Similarly, for inlet temperatures of T_{s2} and T_{s3}, MPCM slurry got the maximum temperature drop of 0.347^0C and 0.472^0C, respectively. The results are shown in Fig. 33 and 34.
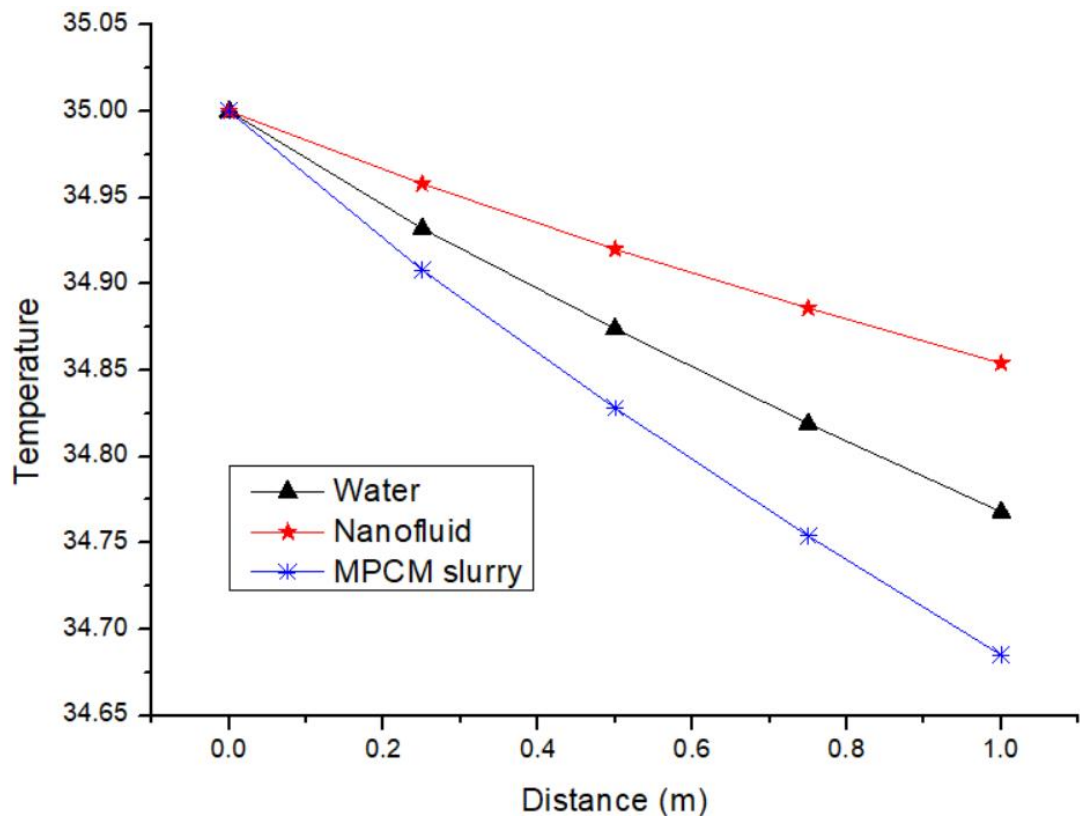

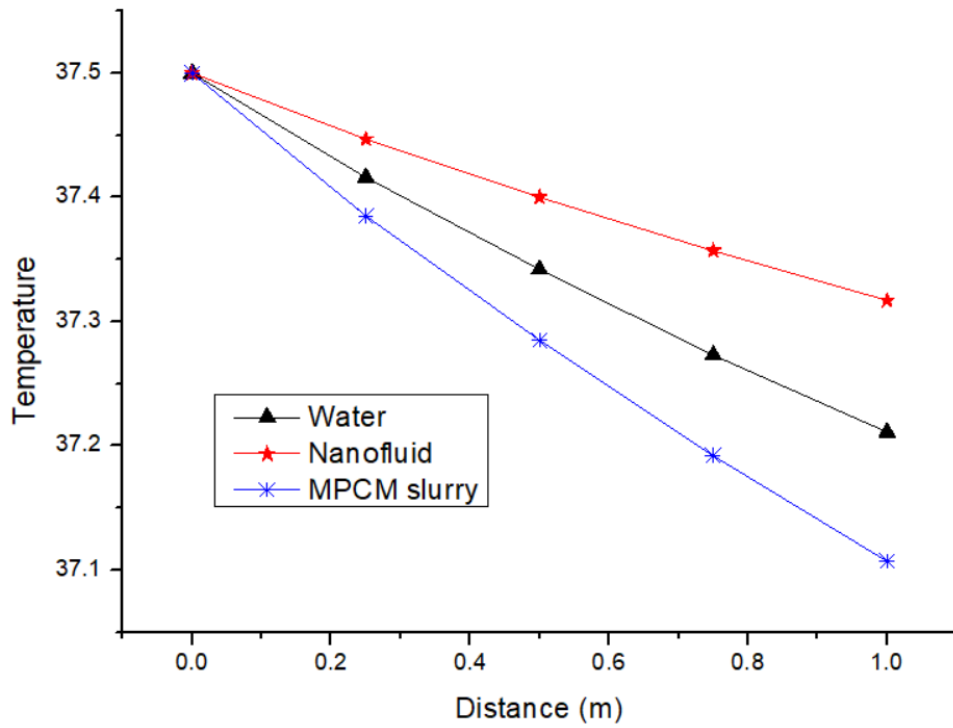**Figure 32: Temperature drop for plain pipe (inlet temperature = 35^0C).**

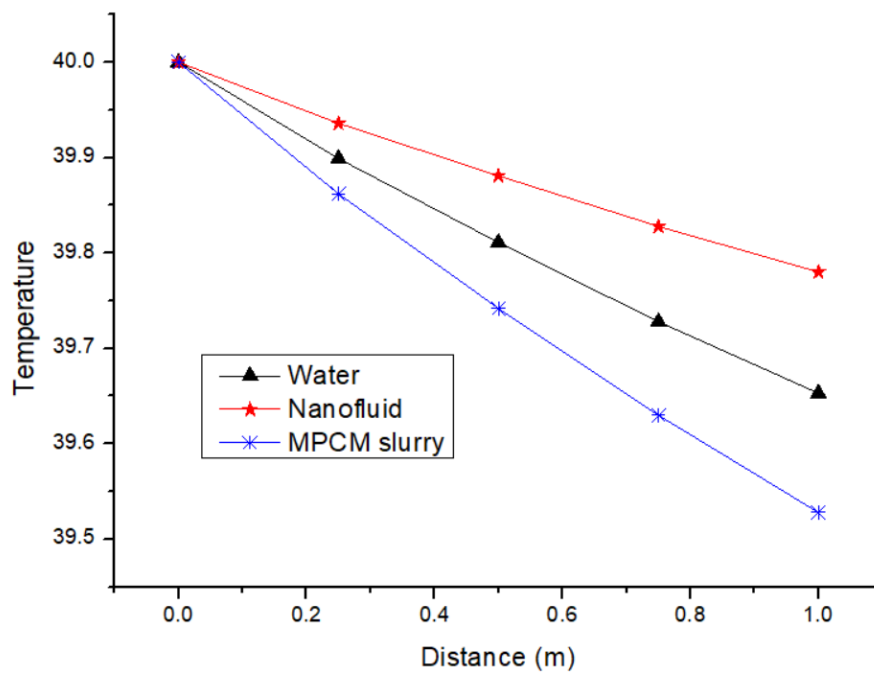**Figure 33: Temperature drop for plain pipe (inlet temperature = 37.5⁰C).**

Figure 34: Temperature drop for plain pipe (inlet temperature = 40⁰C).

98

4.2.5 For Re = 10000, (Spirally Corrugated pipe).

The difference in outlet temperature of all the three fluids can be seen in Fig. 35. When the inlet temperature is T_{s1}, the maximum temperature drop is for MPCM slurry, i.e., 0.627^0C. The difference in temperatures of water and MPCM slurry is 0.165^0C. Similar results were found to be other inlet temperatures of 37.5^0C and 40^0C (Fig. 36 and 37). In these cases, MPCM slurry showed a maximum temperature drop of 0.783^0C and 0.94^0C for inlet temperatures of T_{s2} and T_{s3}, respectively.
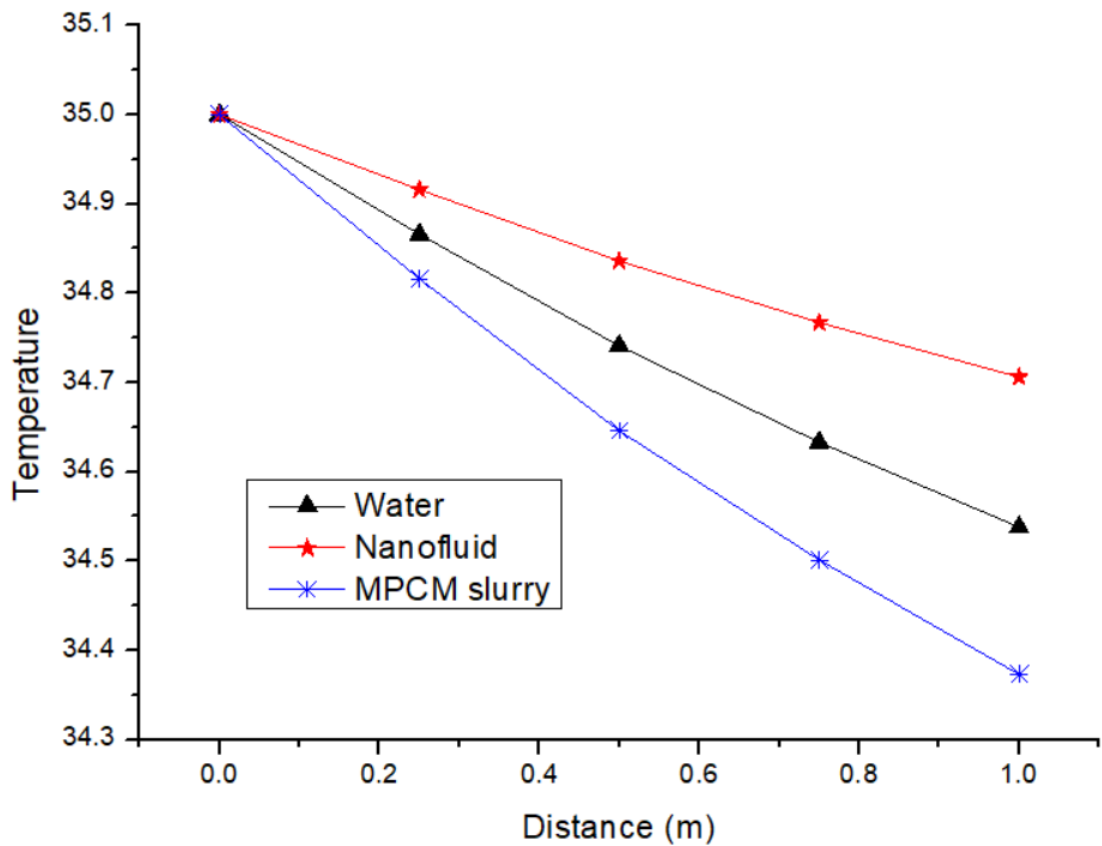

Figure 35: Temperature drop for spirally corrugated pipe (inlet temperature = 35^0C).
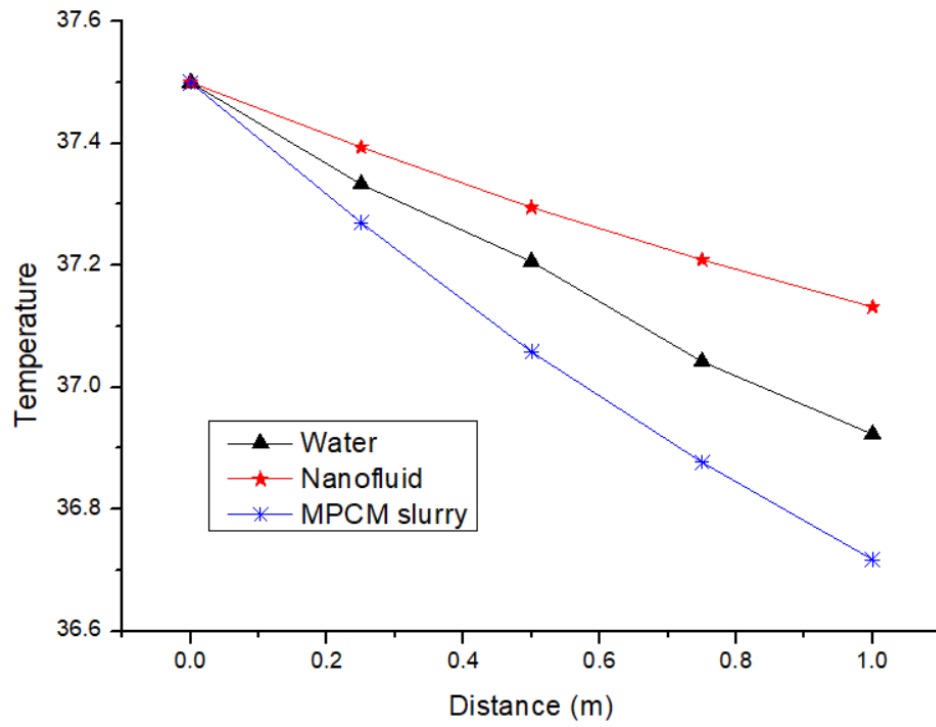
Figure 36: Temperature drop for spirally corrugated pipe (inlet temperature = 37.5⁰C).
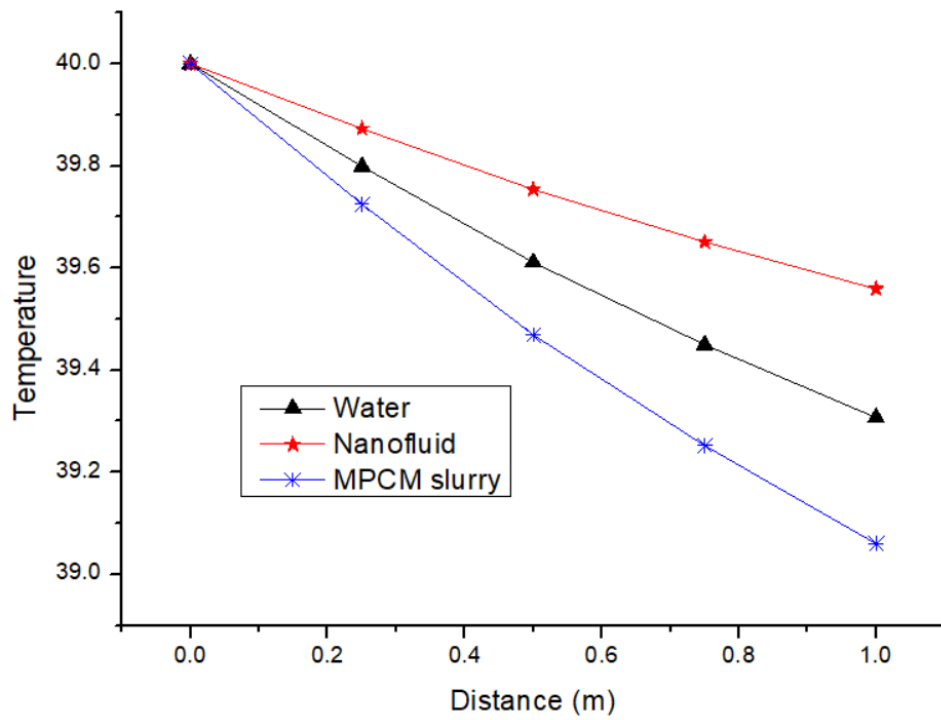

Figure 37: Temperature drop for spirally corrugated pipe (inlet temperature = 40⁰C).

100

4.2.6 For Re = 10000, (Plain pipe)

When the inlet temperature is T_{s1}, then the maximum temperature drop is for MPCM slurry, i.e., 0.183^0C (Fig. 38). Similarly, for inlet temperatures of 37.5^0C and 40^0C, MPCM slurry got the maximum temperature drop of 0.347^0C and 0.472^0C, respectively. The results are shown in Fig. 39 and 40.
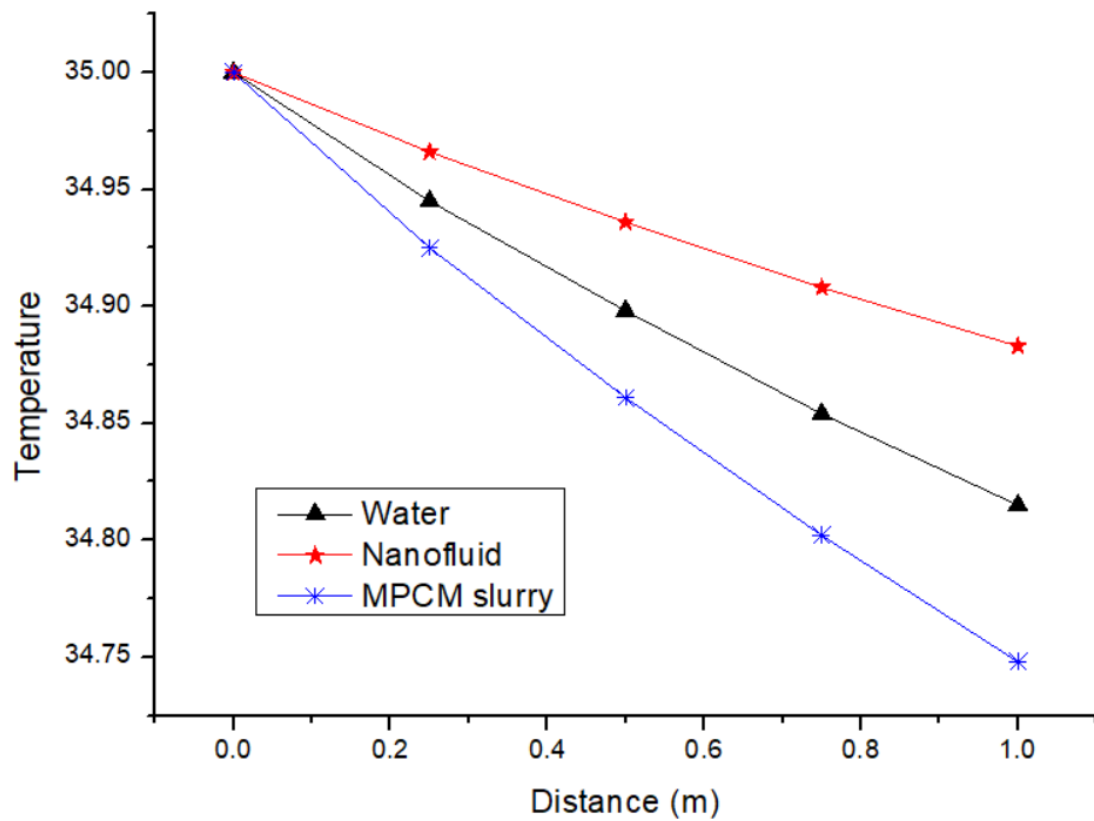

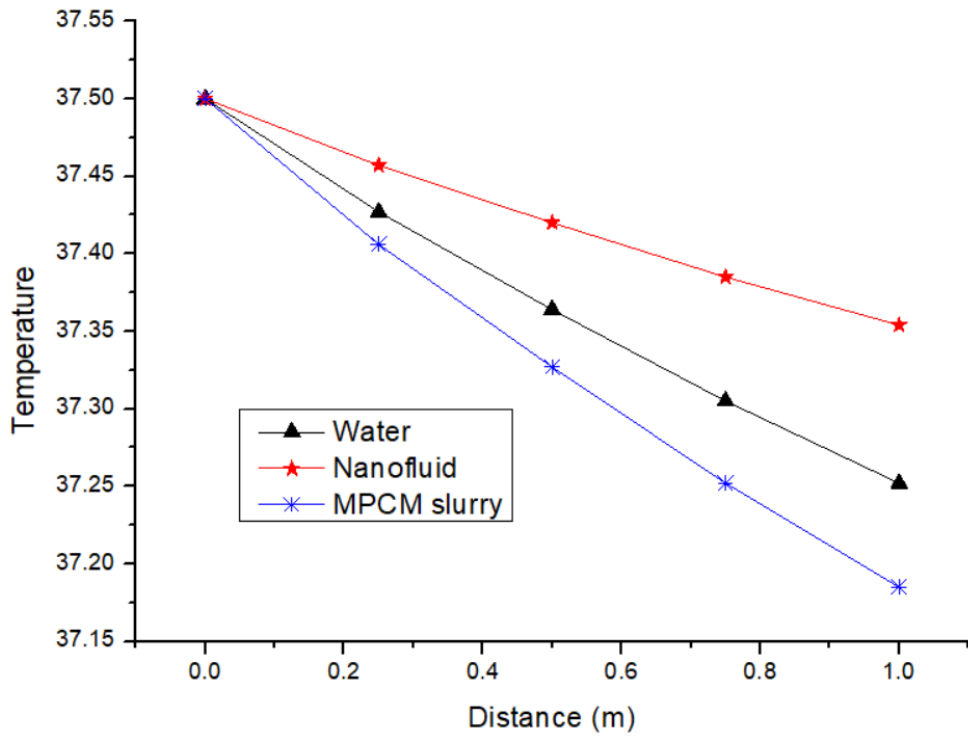**Figure 38: Temperature drop for plain pipe (inlet temperature = 35^0C).**

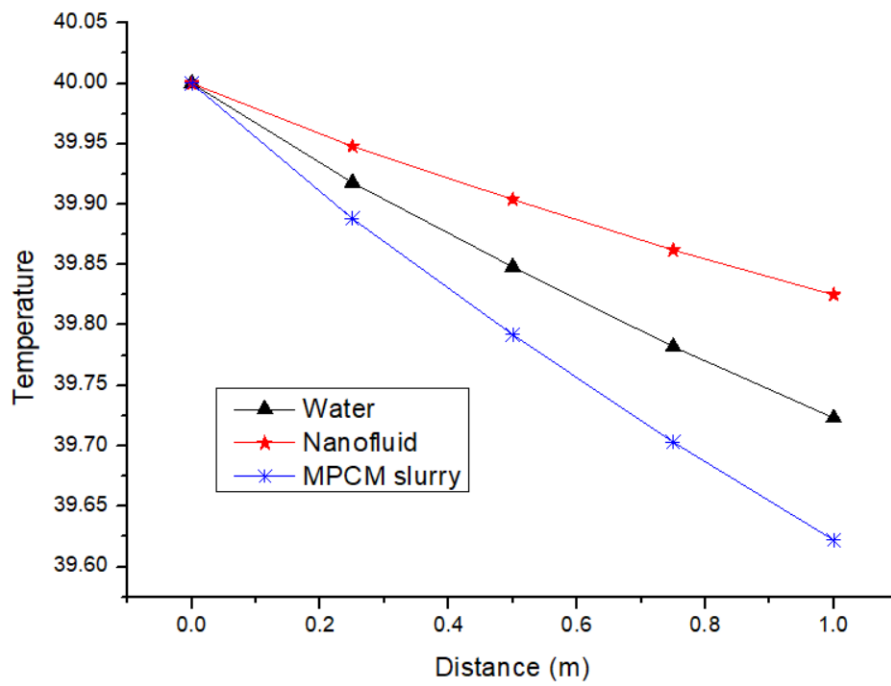**Figure 39: Temperature drop for plain pipe (inlet temperature = 37.5⁰C).**

Figure 40: Temperature drop for plain pipe (inlet temperature = 40⁰C).

The average COP of the system for the summer season can be seen in Table 12. If we compare the COP of water for plain pipe and spirally corrugated pipe, we can see a percentage increase of 3.4%. If we compare the COP of all three fluids for plain pipe, then we can see that COP of MPCM slurry is the highest again. The difference between COP of water and MPCM slurry is almost three times. Also, the difference between COP of water and Nanofluid is 1.18 times more or slightly higher than double.

Also, when we compare the Spirally corrugated pipe, we find that COP of MPCM slurry is 3.6 times higher when compared to the water. Also, the COP of nanofluid is found to be 1.65 times higher than that of water.

We can see that the difference in COP of nanofluid for the plain pipe and spirally corrugated pipe is 33%, and the difference in COP of MPCM slurry for the plain and spirally corrugated pipe is 27% high.

Table 12: COP of fluids for the summer season.

Summer	Plain pipe	Spirally Corrugated pipe
Water	1.76	1.79
Al_2O_3 - water nanofluid	2.8	3.27
MPCM slurry	4.42	5.02

4.3 Pressure Drop

Pressure drop means the amount of pressure head lost while moving from one section of the pipe to another. The reason for the decline in pressure is primarily due to friction. Other factors like surface roughness or pipe fittings also have a minor effect. If the flow is laminar, then these losses are less as compared to turbulent flow—the flow velocity in the current study results in a high Reynolds Number (Re).

4.3.1 Plain Pipe:

The maximum temperature drop of 182.86 Pa was observed for Nanofluid when Re = 10000. The higher the turbulence, the more pressure drop was observed (Fig. 41 to 43). The pressure drop calculations for a plain pipe can be found in table 13.
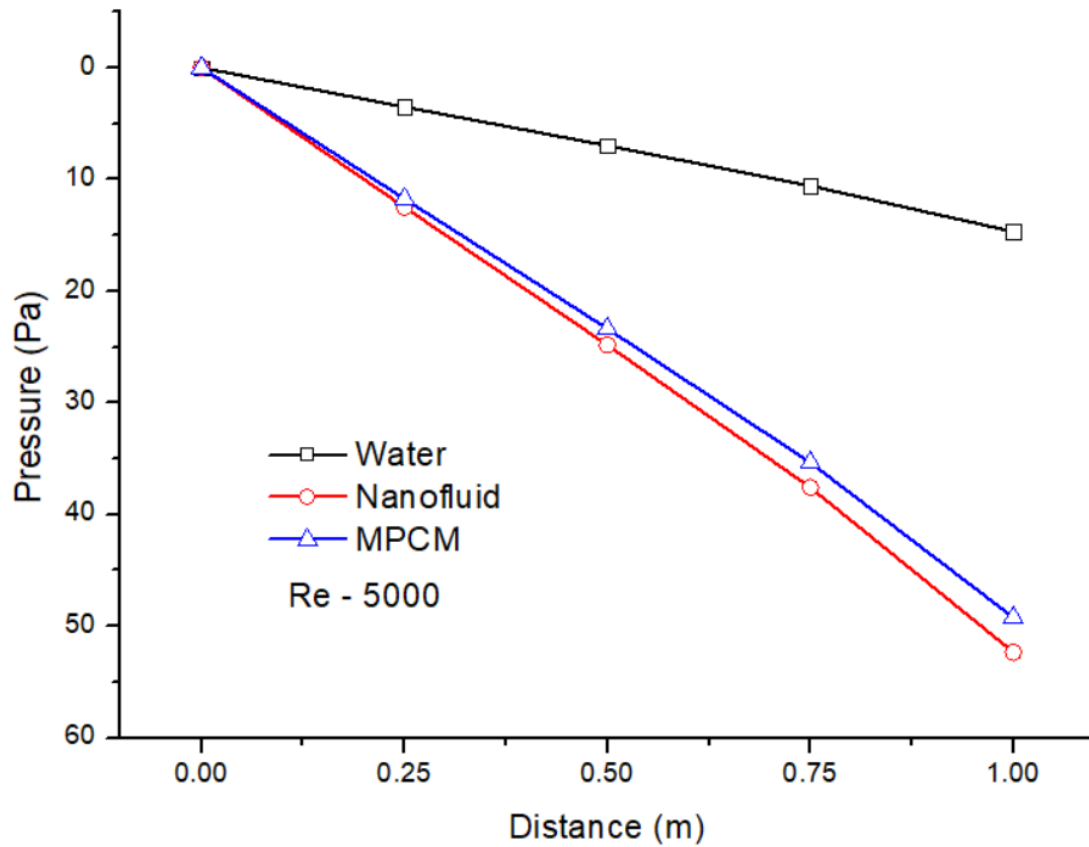
Figure 41: Pressure drop for plain pipe at Re = 5000.
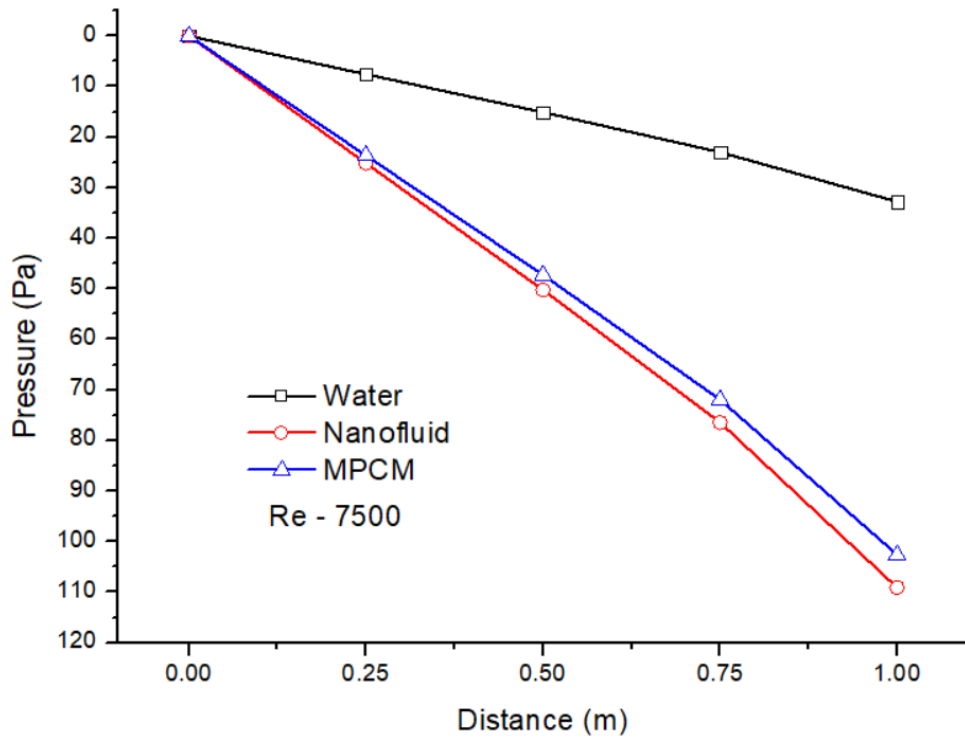
Figure 42: Pressure drop for plain pipe at Re = 7500.
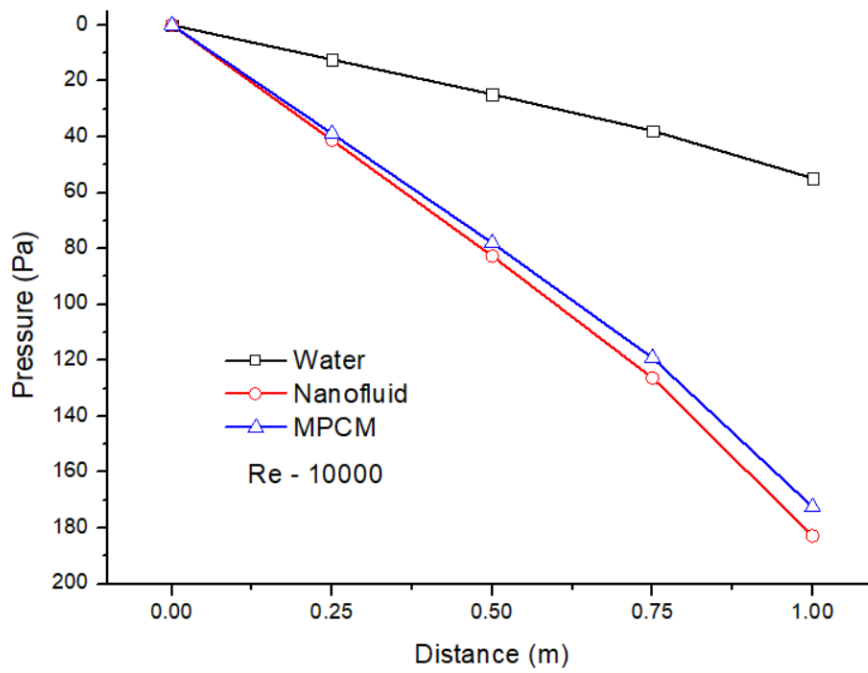
Figure 43: Pressure drop for plain pipe at Re = 10000.

105

4.3.2 Spirally Corrugated Pipe:

The maximum pressure drop of 966.53 Pa was observed for Nanofluid when Re = 10000. The higher the turbulence, the more pressure drop was observed. The pressure drop calculations for a spirally corrugated pipe can be found in table 13. Fig. 44 to 46 shows the pressure variation at various Re.
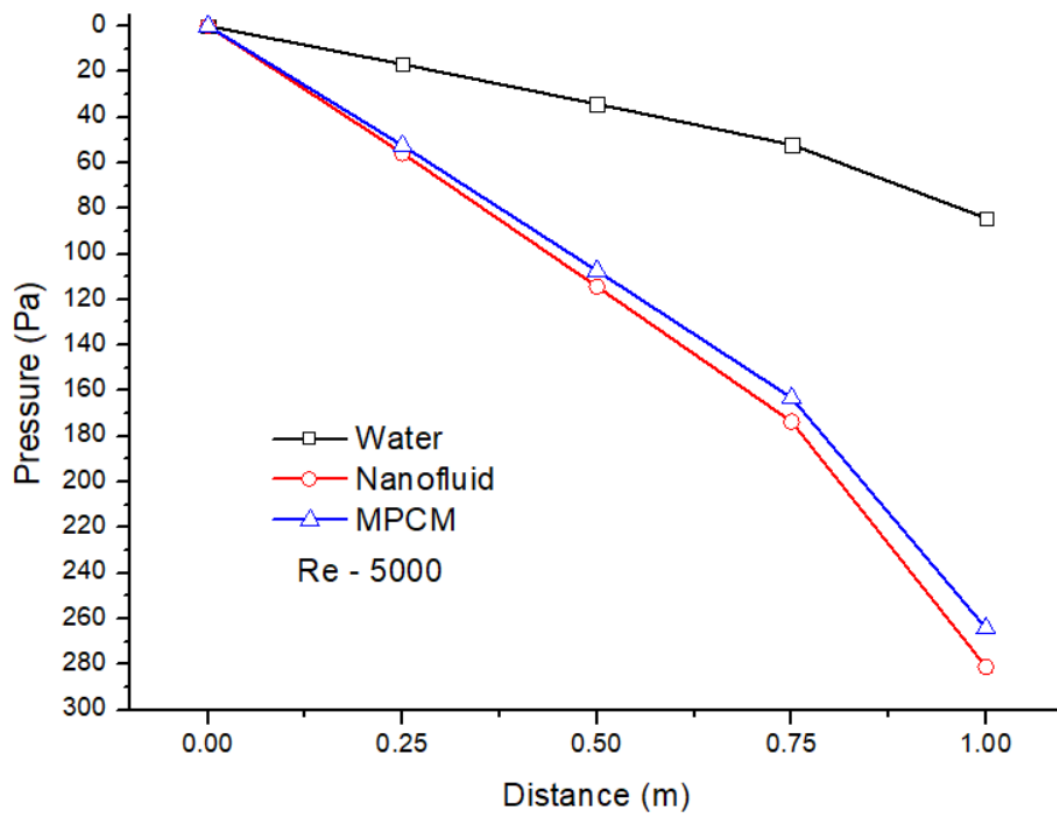
Figure 44: Pressure drop for spirally corrugated pipe at Re = 5000.

If we compare the pressure drop for both the pipes, it can be seen that pressure drop increases as Re increases for both pipes. Thus, a lower fluid velocity is suggested.
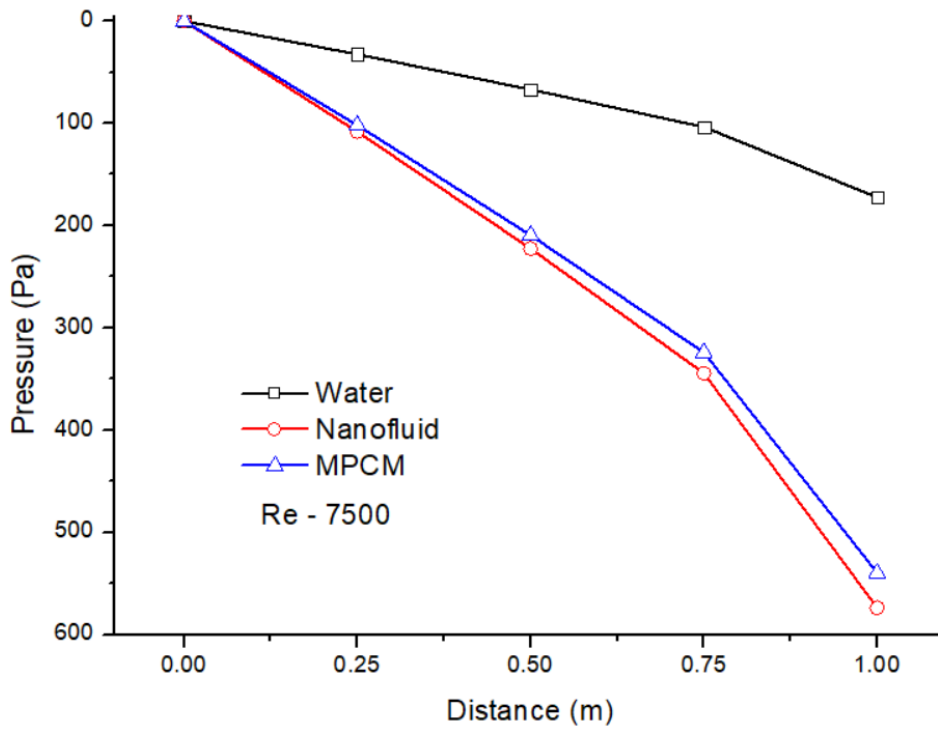
Figure 45: Pressure drop for spirally corrugated pipe at Re = 7500.
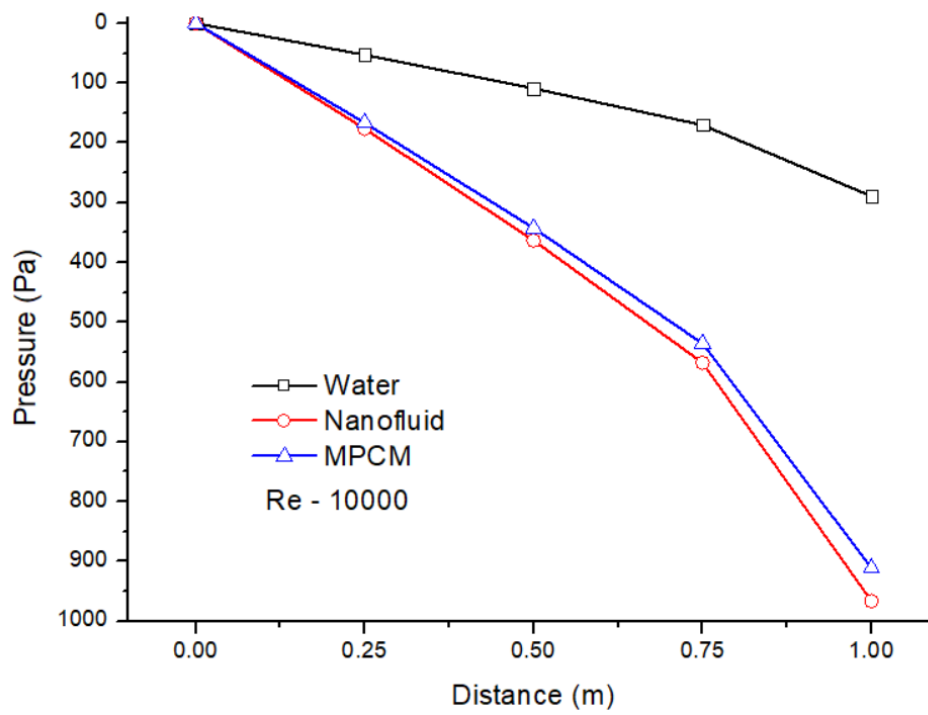
Figure 46: Pressure drop for spirally corrugated pipe at Re = 10000.

107

As the fluid velocity increased with increasing Re, the pressure drop also increases. The spirally corrugated pipe has maximum pressure drop because, with increasing flow rate, the secondary flow starts to obstruct the primary flow. To decrease the pumping power, low Reynold No. is recommended.

Table 13: Pressure drop for plain pipe and spirally corrugated pipe.

| Re	Distance (m)	Plain pipe			Spirally corrugated pipe		
		Water	Nanofluid	MPCM	Water	Nanofluid	MPCM
5000	0	14.672	52.342	49.23	84.218	281.178	264.194
5000	0.25	10.565	37.59	35.362	52.008	173.579	163.118
5000	0.5	6.982	24.83	23.357	34.246	114.281	107.333
5000	0.75	3.511	12.484	11.74	16.725	55.819	52.418
5000	1	0	0	0	0	0	0
7500	0	32.773	109.105	102.622	172.374	573.779	539.754
7500	0.25	22.978	76.487	71.949	103.493	344.411	324.08
7500	0.5	15.096	50.248	47.268	66.877	222.487	209.42
7500	0.75	7.553	25.141	23.65	32.509	108.128	101.793
7500	1	0	0	0	0	0	0
10000	0	54.764	182.86	172.435	289.362	966.532	911.396
10000	0.25	37.835	126.307	119.108	170.093	568.052	535.691
10000	0.5	24.764	82.67	77.959	108.789	363.258	342.572
10000	0.75	12.331	41.166	38.82	52.812	176.365	166.311
10000	1	0	0	0	0	0	0

5   RESULTS AND DISCUSSION - 2

5.1   Winter season

The variation in temperature drop for both the pipes in winters can be seen in Fig. 47.
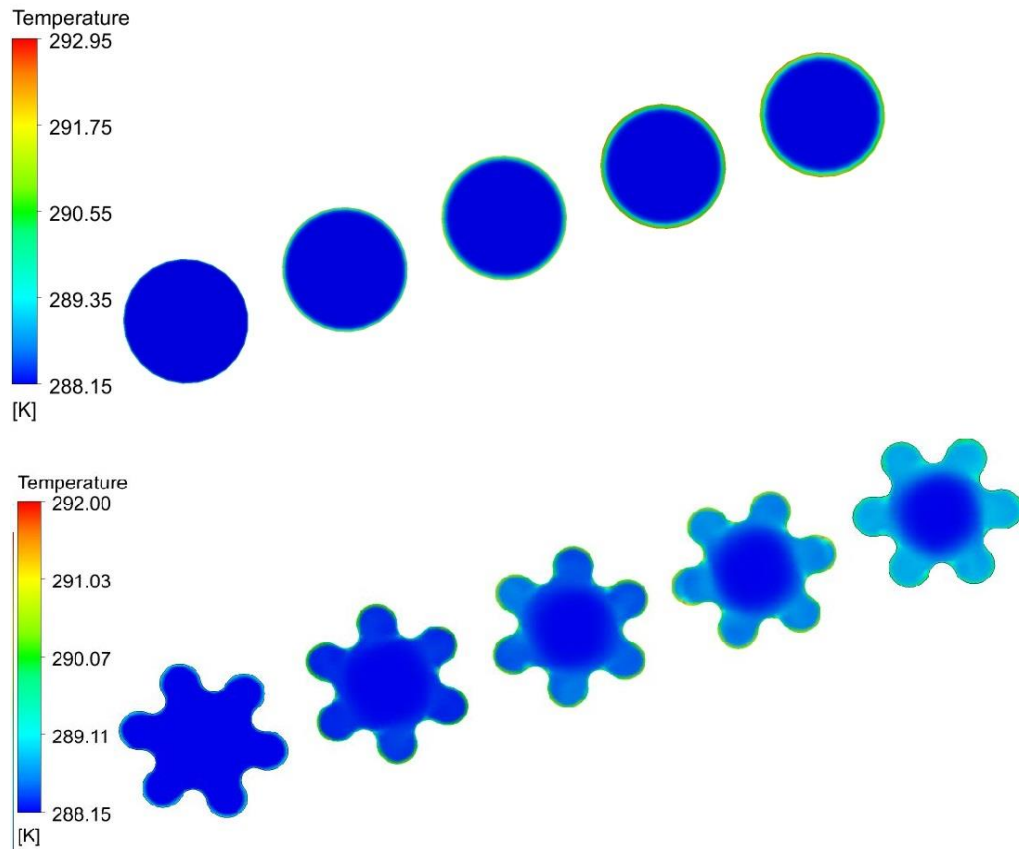
Figure 47: Temperature distribution spirally corrugated pipe and plain pipe in winter (at Z = 0, 0.25, 0.5, 0.75 and 1 m).

The inlet temperature considered for the study are as follows:

$T_{w1} = 10^0C$;

$T_{w2} = 12.5^0C$; and

$T_{w3} = 15^0C$.

5.2 Comparison of thermal performance in the plain pipe for different working fluids in winter season

5.2.1 For Re = 5000, (Spirally Corrugated pipe).

The difference in outlet temperature of all the three fluids can be seen in the Fig. 48. When the inlet temperature is T_{w1}, then the maximum temperature rise is found to be for MPCM slurry i.e., 1.547^0C. Nanofluid saw the minimum temperature rise of 0.398^0C. Similar results were found to be other inlet temperatures of 12.5^0C and 15^0C (Fig. 49 and 50). In these cases too, MPCM slurry showed maximum temperature rise of 1.289^0C and 1.031^0C for inlet temperatures of T_{w2} and T_{w3} respectively.

Figure 48: Temperature rise for spirally corrugated pipe (inlet temperature = 10^0C).

Figure 49: Temperature rise for spirally corrugated pipe (inlet temperature = 12.5⁰C)

Figure 50: Temperature rise for spirally corrugated pipe (inlet temperature = 15⁰C).

111

5.2.2   For Re = 5000, (Plain pipe)

When the inlet temperature is T_{w1}, then the maximum temperature drop is found to be for MPCM slurry i.e. 0.632^0C (Fig. 51). Similarly, for inlet temperatures of T_{w2} and T_{w3}, MPCM slurry got the maximum temperature drop of 0.246^0C and 0.421^0C respectively. The results are shown in the Fig. 52 and 53.

Figure 51: Temperature rise for plain pipe (inlet temperature = 10^0C)

Figure 52: Temperature rise for plain pipe (inlet temperature = 12.5 ^{0}C).
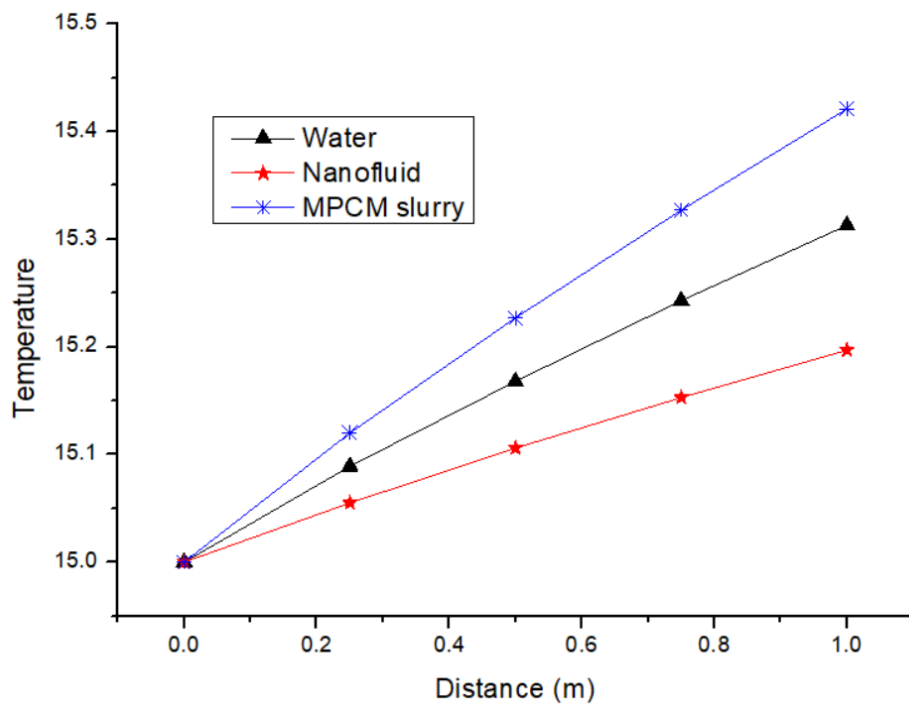
Figure 53: Temperature rise for plain pipe (inlet temperature = 15 ^{0}C).

113

5.2.3 For Re = 7500, (Spirally Corrugated pipe).

The difference in outlet temperature of all the three fluids can be seen in Fig. 54. When the inlet temperature is T_{w1}, the maximum temperature rise is for MPCM slurry, i.e., $0.858\,^0C$. The difference in temperatures of water and MPCM slurry is $0.302\,^0C$. Similar results were found to be other inlet temperatures of $12.5\,^0C$ and $15\,^0C$ (Fig. 55 and 56). In these cases, MPCM slurry showed a maximum temperature rise of $0.966\,^0C$ and $0.773\,^0C$ for inlet temperatures of T_{w2} and T_{w3}.
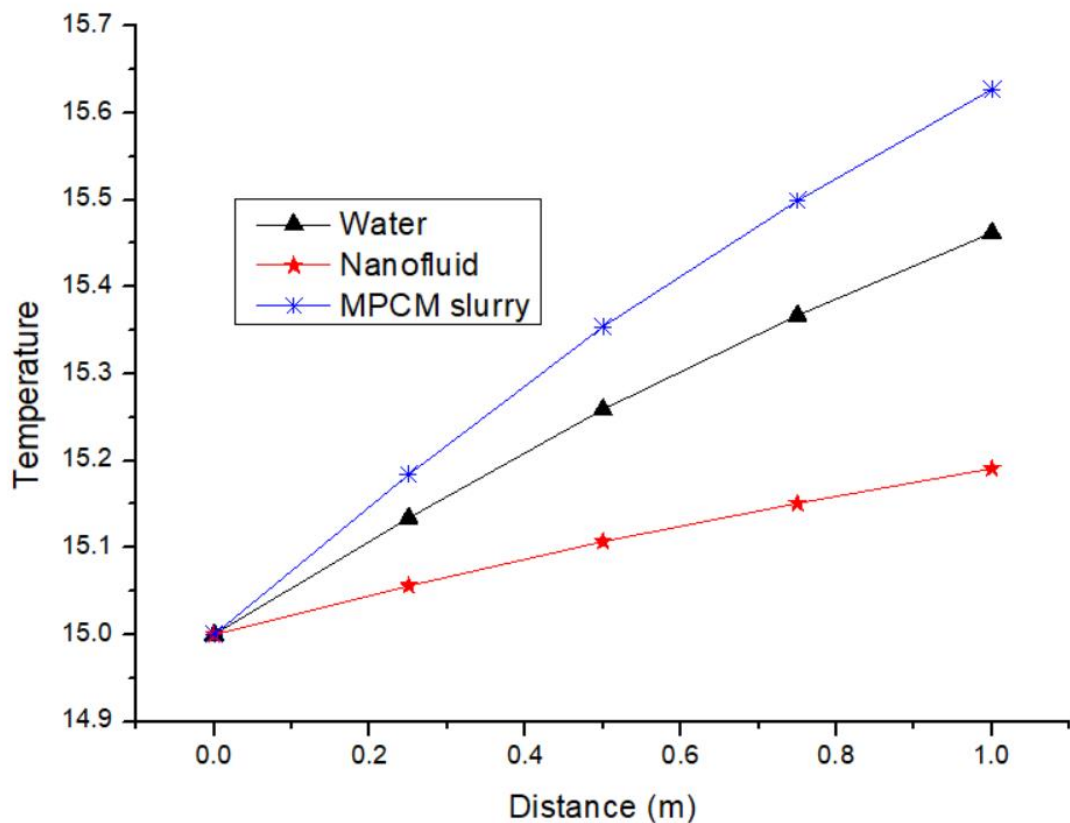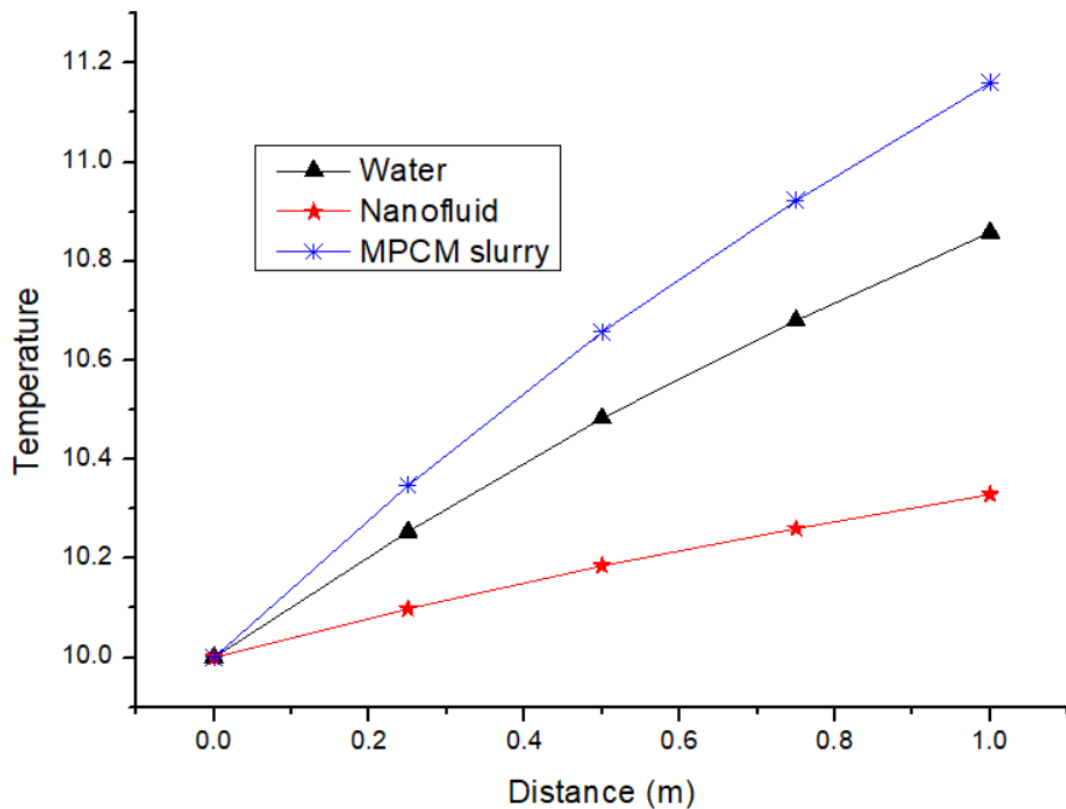

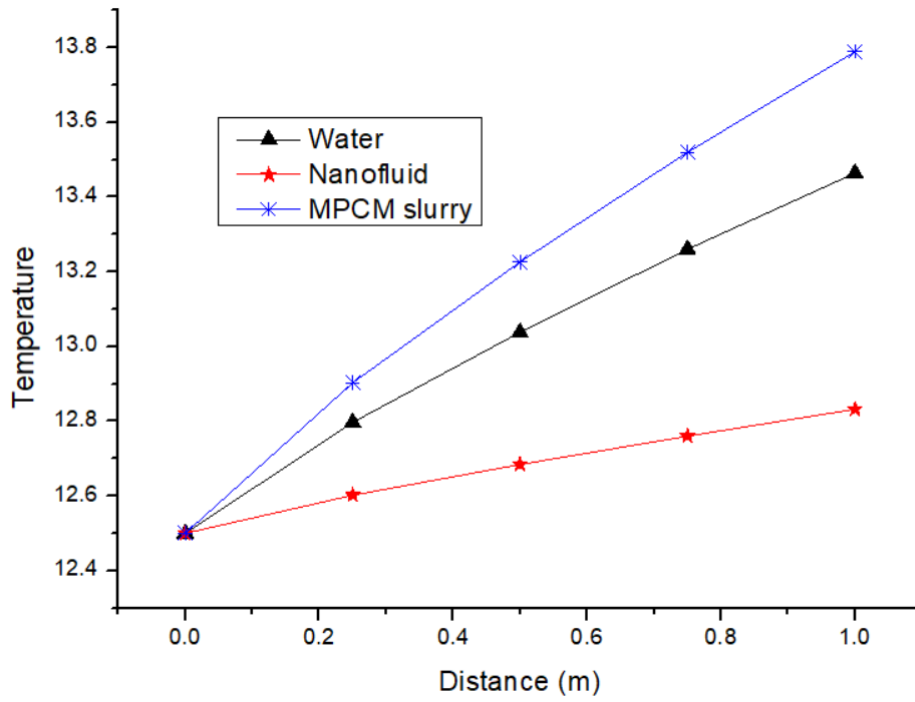**Figure 54: Temperature rise for spirally corrugated pipe (inlet temperature = $10\,^0C$)**
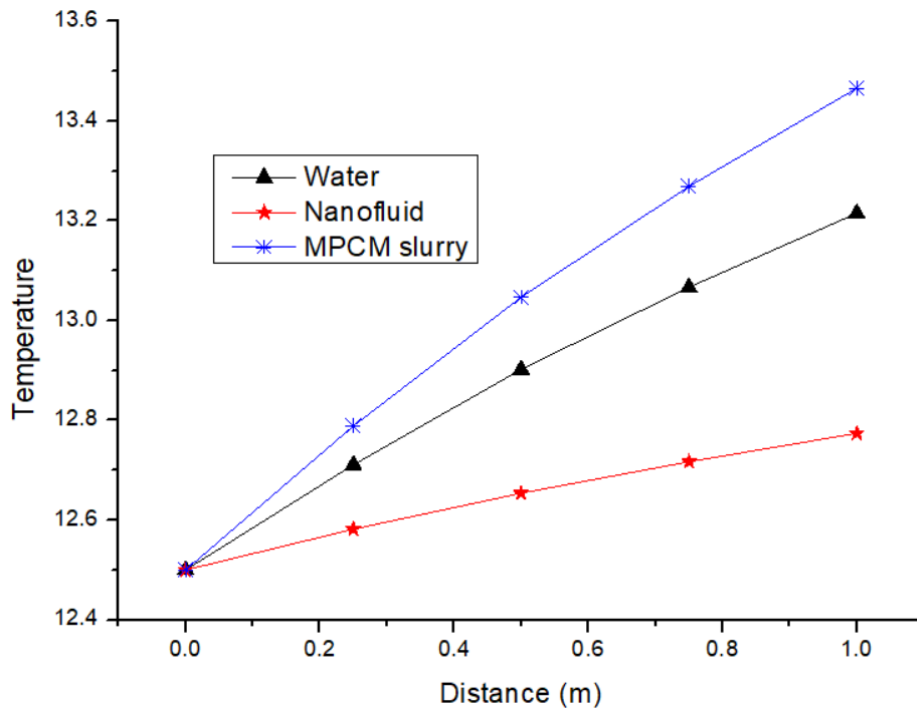
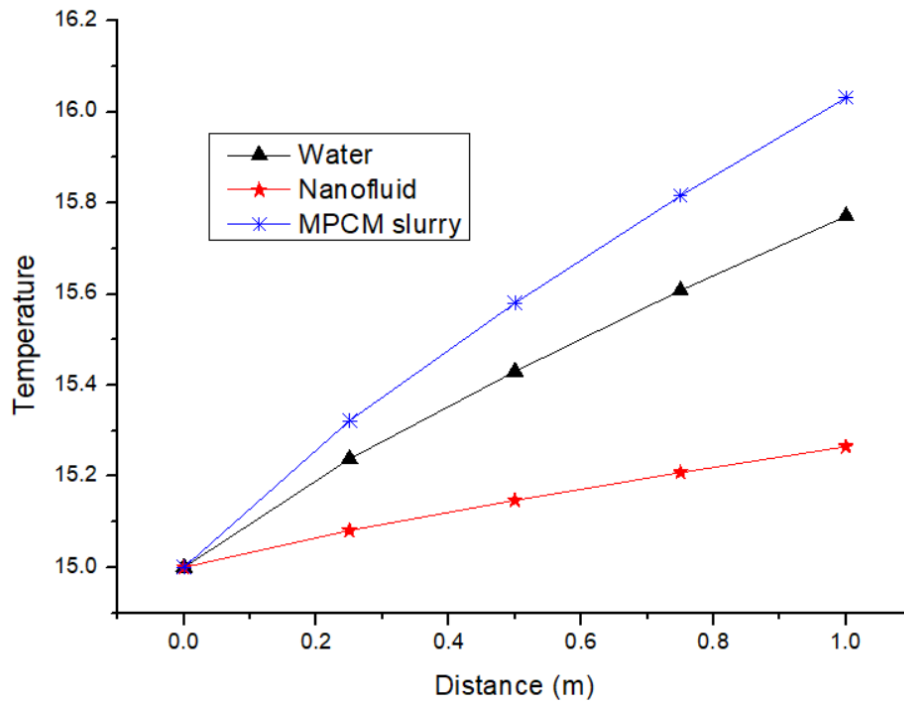**Figure 55: Temperature rise for spirally corrugated pipe (inlet temperture = 12.5^{0}C).**
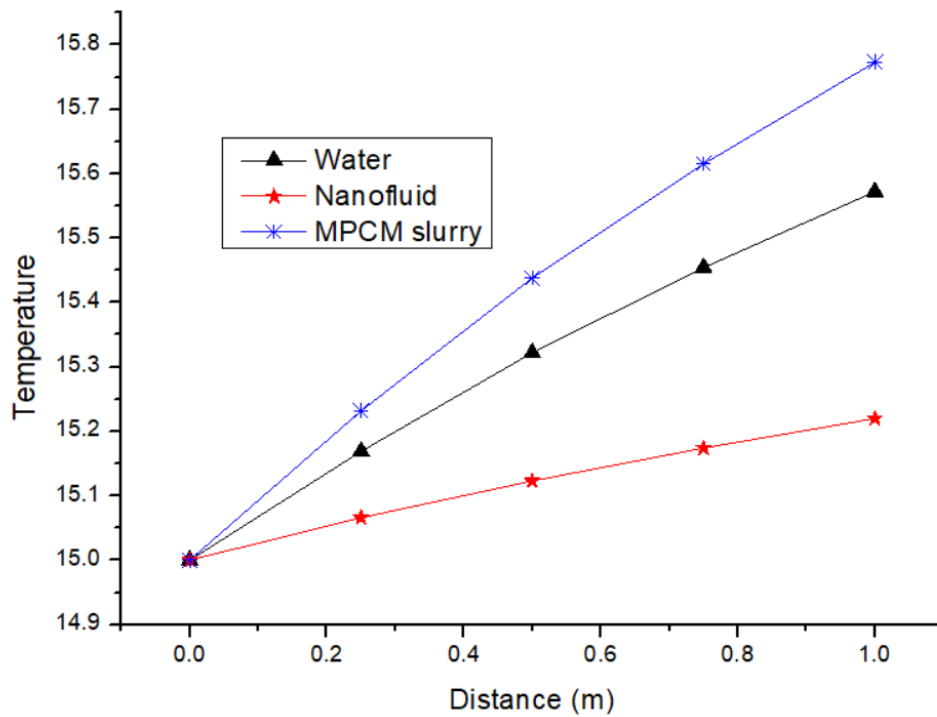
Figure 56: Temperature rise for spirally corrugated pipe (inlet temperature = 15^{0}C).

5.2.4 For Re = 7500, (Plain pipe)

The difference in outlet temperature of all the three fluids can be seen in Fig. 57. When the inlet temperature is T_{w1}, the maximum temperature rise is for MPCM slurry, i.e., 0.472^0C. Similarly, for inlet temperatures of T_{w2} and T_{w3}, MPCM slurry got the maximum temperature rise of 0.393^0C and 0.315^0C, respectively. The results are shown in Fig. 58 and 59.
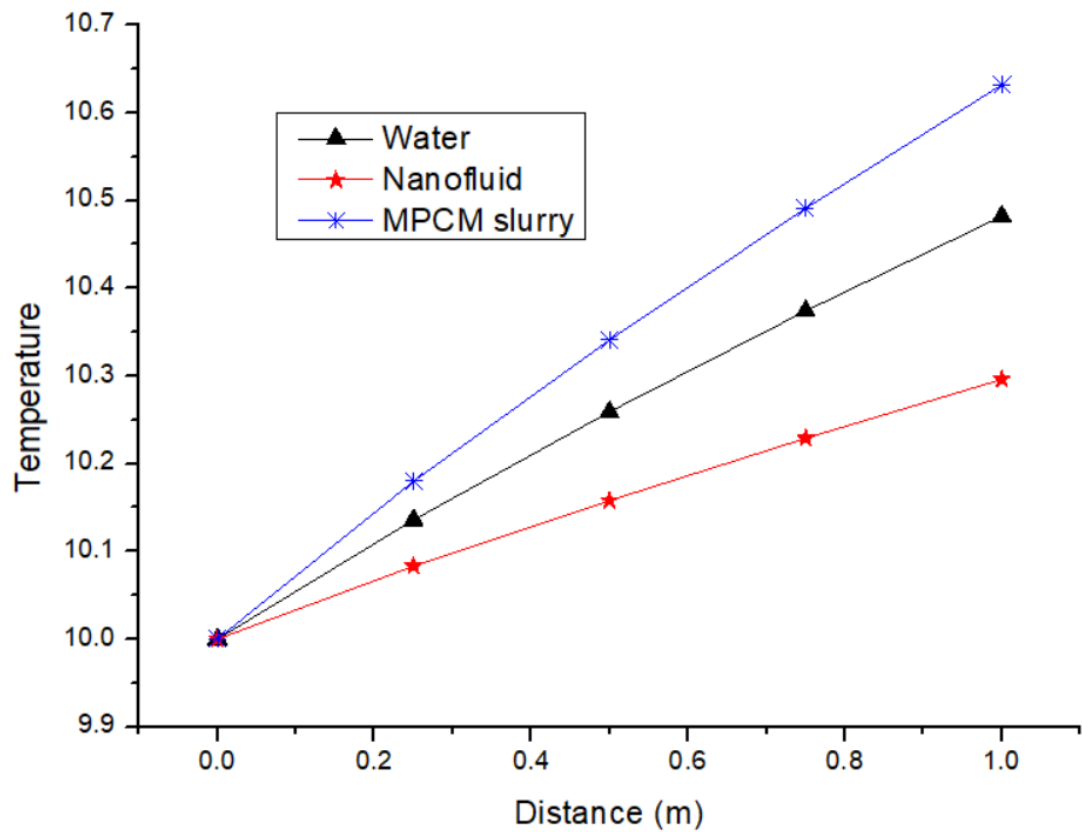

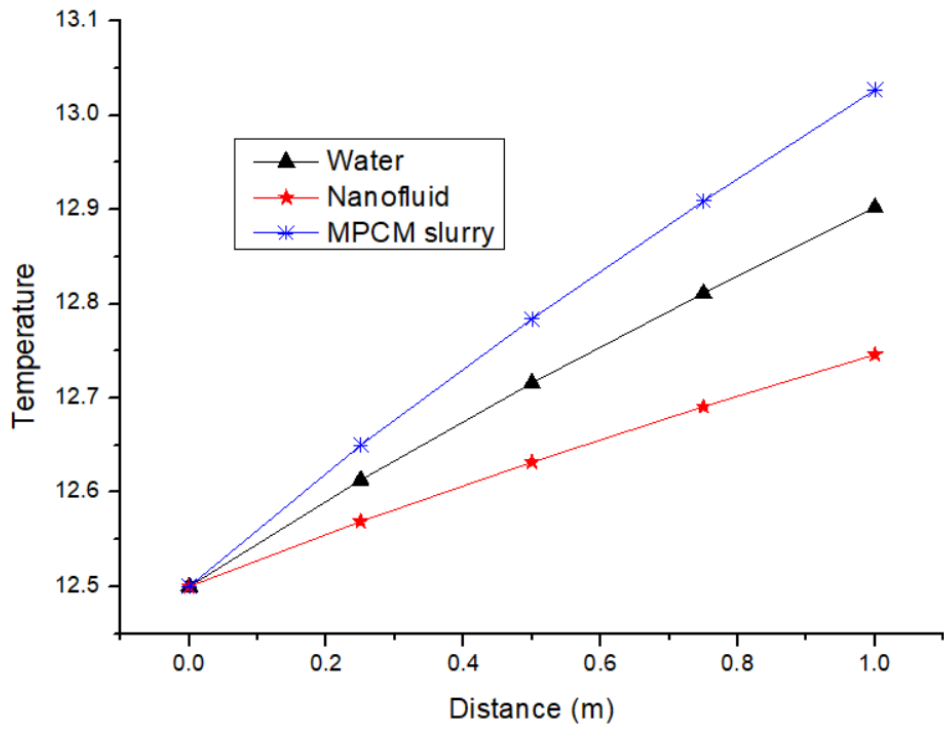**Figure 57: Temperature rise for plain pipe (inlet temperature = 10^0C).**

Figure 58: Temperature rise for plain pipe (inlet temperature = 12.5⁰C).

Figure 59: Temperature rise for plain pipe (inlet temperature = 15⁰C).

117

5.2.5 For Re = 10000, (Spirally Corrugated pipe).

The difference in outlet temperature of all the three fluids can be seen in Fig. 60. When the inlet temperature is T_{w1}, then the maximum temperature rise is for MPCM slurry, i.e., at a capacity of 0.94^0C. The difference in temperatures of water and MPCM slurry is 0.247^0C. Similar results were found to be other inlet temperatures of 12.5^0C and 15^0C (Fig. 61 and 62). In these cases, MPCM slurry showed a maximum temperature rise of 0.7830C and 0.6270C for inlet temperatures of T_{w2} and T_{w3}.
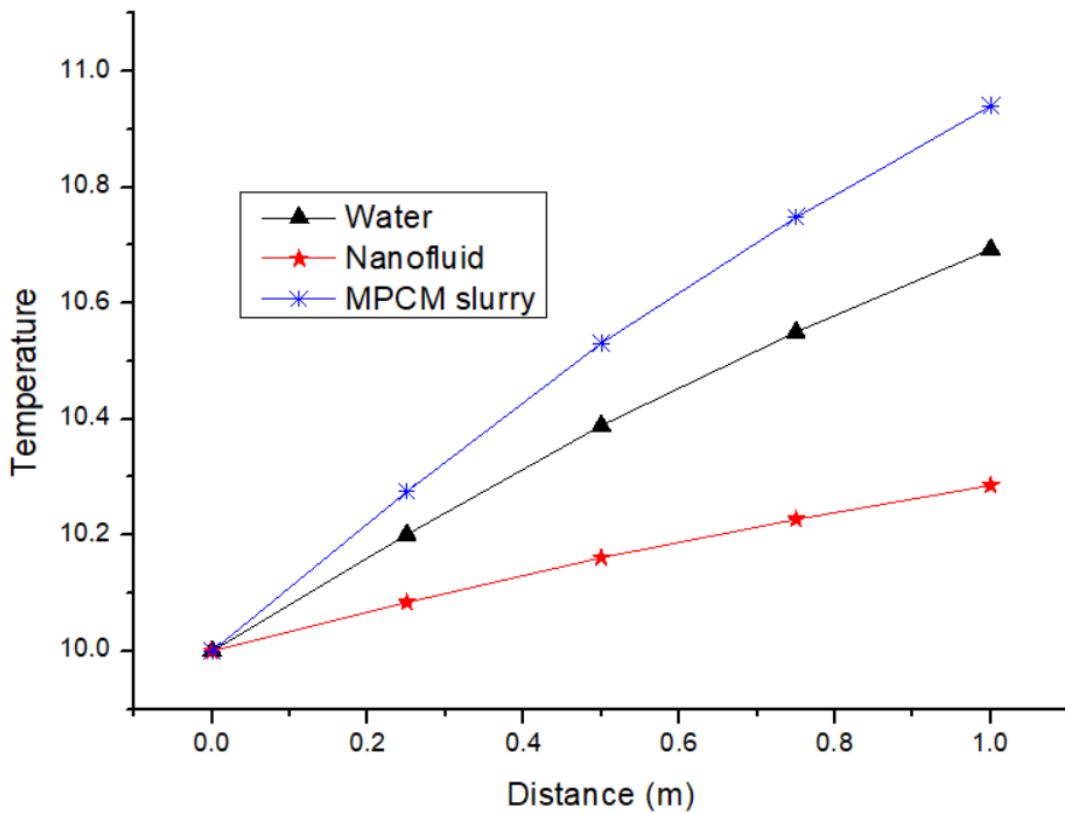
Figure 60: Temperature rise for spirally corrugated pipe (inlet temperature = 10^0C).
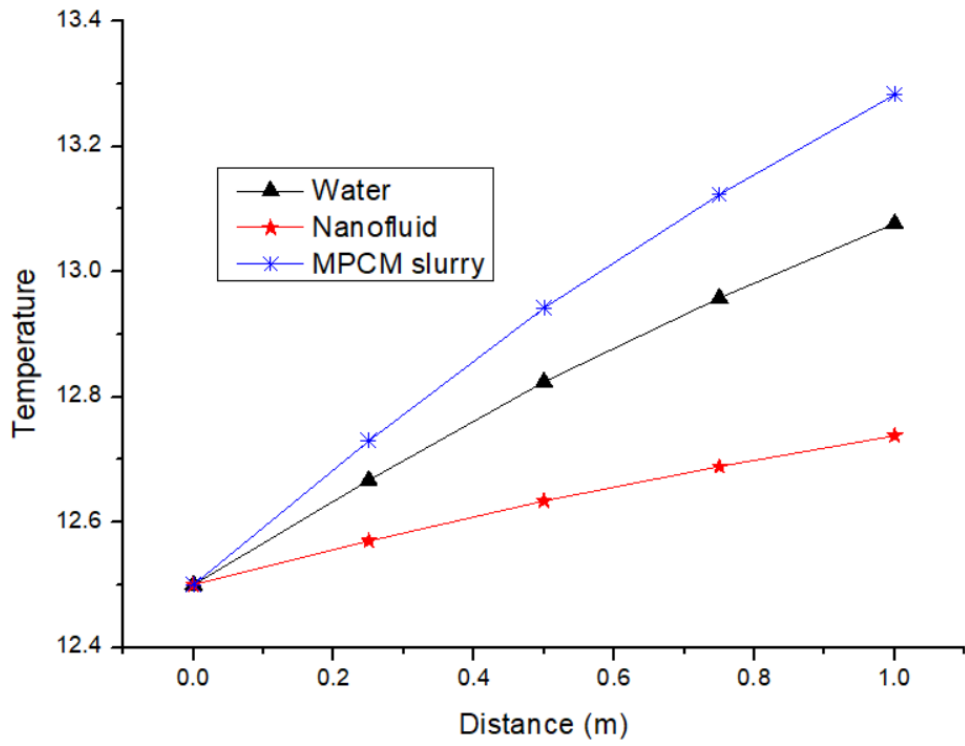
Figure 61: Temperature rise for spirally corrugated pipe (inlet temperature = 12.5⁰C).
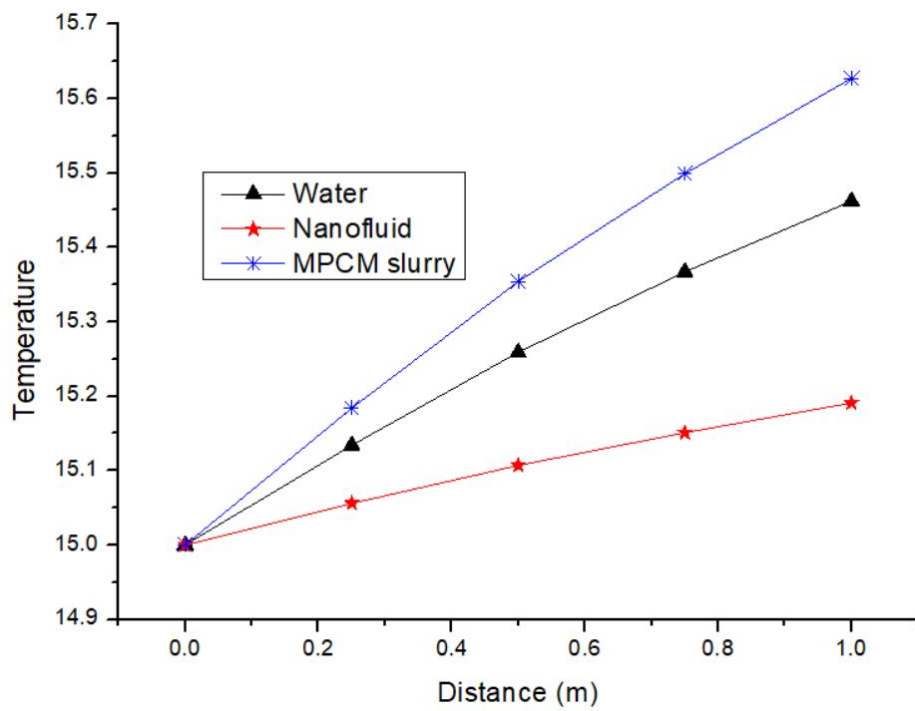
Figure 62: Temperature rise for spirally corrugated pipe (inlet temperature = 15⁰C).

5.2.6 For Re = 10000, (Plain pipe)

The difference in outlet temperature of all the three fluids can be seen in Fig. 62. When the inlet temperature is T_{w1}, the maximum temperature rise is for MPCM slurry, i.e., $0.378{}^{0}C$. Similarly, for inlet temperatures of T_{w2} and T_{w3}, MPCM slurry got the maximum temperature rise of $0.315{}^{0}C$ and $0.252{}^{0}C$, respectively. The results are shown in Fig. 63 and 64.
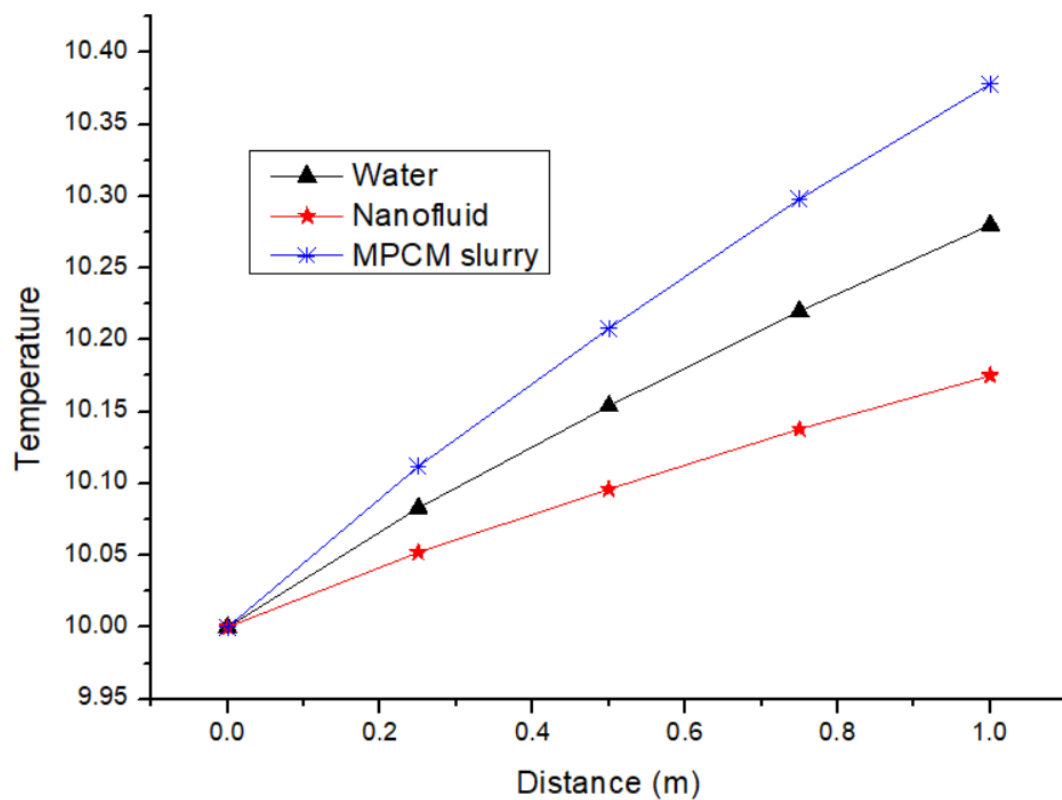
Figure 63: Temperature rise for plain pipe (inlet temperature = $10{}^{0}C$).
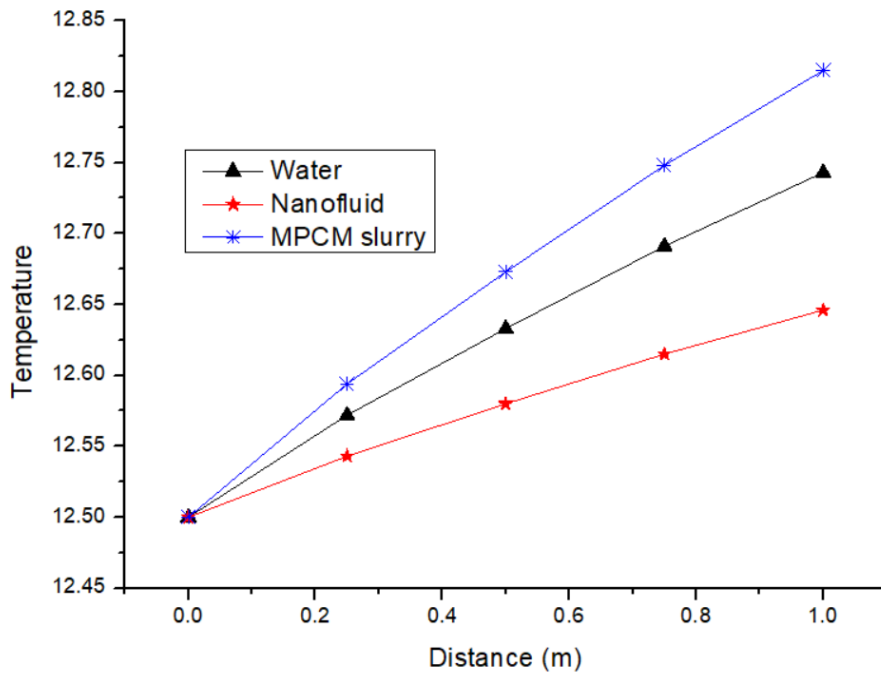
Figure 64: Temperature rise for plain pipe (inlet temperature = 12.5⁰C).

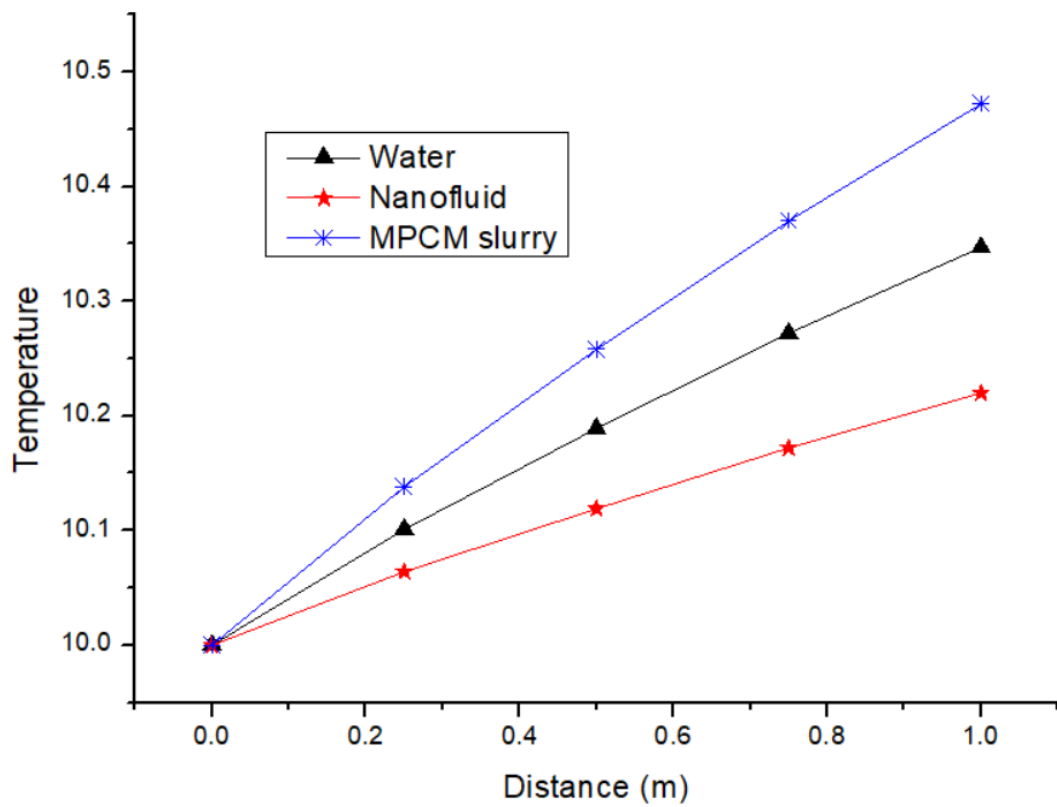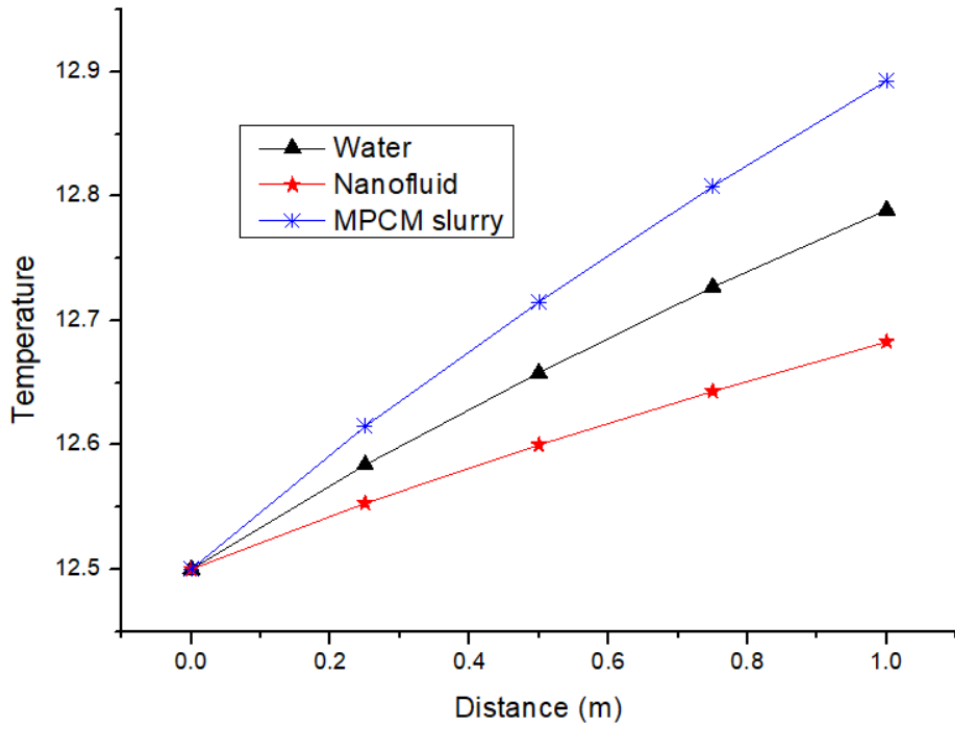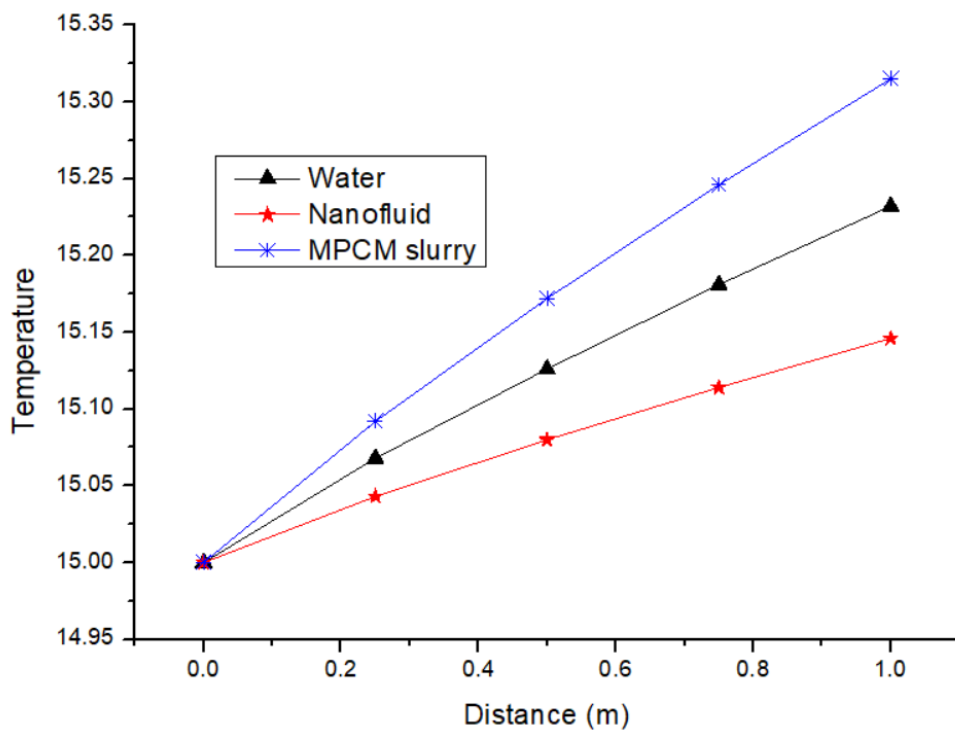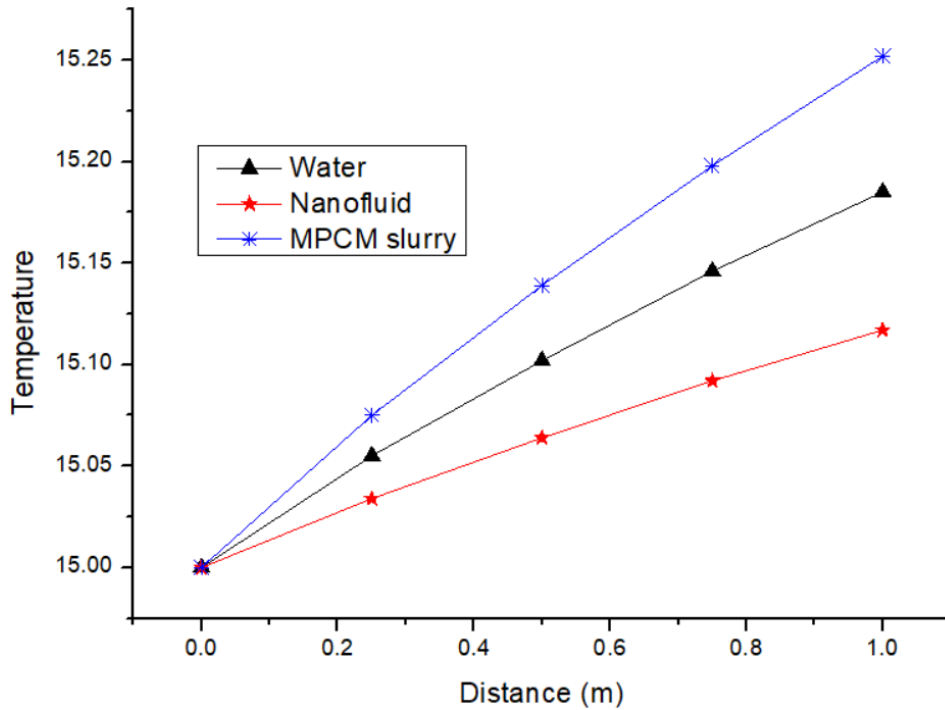**Figure 65: Temperature rise for plain pipe (inlet temperature = 15⁰C).**

121

The simulations were carried out for two seasons (summer and winter). The result reveals that there is apparent temperature variation while comparing the two geometries. But, based on the output of the CFD simulations, it can be established that the pipe geometries can have a significant impact on the performance of the GHE system. Although pressure drop was more in the spiral pipe, it can be decided and worked upon in future studies. This study confirms the objective that the spirally corrugated pipe geometry is the appropriate pipe geometry for higher heat transfer.

Also, when we compare the working fluids, MPCM slurry wins over other fluids. Although it is a bit costly for long-term usage, it can be considered a viable alternative for conventional fluids.

If we compare the COP of water for plain pipe and spirally corrugated pipe, we can see a percentage increase of 18.18%. If we compare the COP of all three fluids for plain pipe, then we can see that COP of MPCM slurry is the highest again. The difference between COP of water and MPCM slurry is almost four times. The difference between COP of water and Nanofluid is 1.7 times more or slightly higher than double.

Also, when we compare the Spirally corrugated pipe, we find that COP of MPCM slurry is 4.07 times higher when compared to the water. Also, the COP of nanofluid is found to be 1.63 times higher than that of water. We can see that the difference in COP of nanofluid for the plain pipe and spirally corrugated pipe is 9.5%, and the difference in COP of MPCM slurry for the plain and spirally corrugated pipe is 18.3% high.

Table 14: COP of fluid for the Winter season.

Summer	Plain pipe	Spirally Corrugated pipe
Water	1.1	1.2
Al_2O_3 - water nanofluid	1.87	1.959
MPCM slurry	4.48	4.89

6 CONCLUSION

For a buildings' energy requirement, numerous energy-saving passive heating and cooling purposes have been introduced. GSHP is one such technology that uses shallow geothermal energy. This thesis aims to study the cooling and healing potential of the GHE system with modified geometry. The CFD simulations were carried out using Ansys FLUENT. In this study, two different pipe geometries such as circular and spirally corrugated pipe geometry, are used. Also, three working fluids, i.e., Water, Al_2O_3- water, and MPCM slurry, were analyzed at three different inlet temperatures and three Re values. The simulations were carried out for two seasons (summer and winter). The results reveal that there was appreciable temperature variation while comparing the two geometries.

From this study following conclusions have been drawn:

- The maximum temperature drop was observed at the lowest Re of 5000. Spirally corrugated pipe is the best performing geometry. When compared to plain pipe, it showed better results for all inlet temperature values of both seasons.
- MPCM slurry comes out as the better-working fluid in terms of thermal performance. Although due to high-pressure drop, water can be used if the length of the pipe is not a concern.
- With an increase in Reynolds number, the flow velocity increases resulting in less temperature drop or rise, as the fluid does not get much time to carry heat.
- As we know, in heat exchangers, corrugations and surface modifications are commonly used because they are very effective in heat transfer enhancement. Spiral corrugation also promotes secondary recirculation flow by inducing non-axial velocity components. When comparing both geometries, the Spirally corrugated pipe had maximum temperature difference at all Re and T_{in} values.
- Spiral corrugation increases heat transfer enhancement due to secondary flow swirls and surface curvatures pass by fluid layers, which also causes pressure losses; also, with an increase in Re, the pressure drop increases. The result

reveals that there was apparent temperature variation while comparing the two geometries. But, based on the result of the CFD simulations, it can be established that the pipe geometries can have a significant impact on the performance of the GHE system.

- In terms of COP, it is seen that COP of the system having MPCM slurry as working fluid is the top-performing fluid. It gives a cooling COP of 5.02 when used in spirally corrugated pipe GHE compared to 4.42 for the plain pipe. Similarly, in the winter season, the heating COP of this system for the spirally corrugated pipe is 4.89, and for plain pipe, it is 4.48. Similarly, we can see a significant increase in COP of nanofluids too. For the summer season, the difference in COP of nanofluid for spirally corrugated pipe and the plain pipe is 0.47.

- Numerous studies show that the thickness of the pipe has a minimal impact on the performance, thus can be ignored. In general, the thickness of the pipe varies between 0.002 to 0.006 m.

- Several studies show that the pipe material is not vital for the thermal performance of the GHE in the case of EAHE but is very important for GSHP. Therefore, cost, durability, and corrosion resistance must be the criterion for selecting the material. Materials most studied so far are steel, PVC, HDPE (High-Density Polyethylene), copper, zinc, aluminium, and concrete.

6.1 Contribution to the existing knowledge

The simulations carried out in the research are mainly focused on seeing the effect of novel pipe geometry on GHE. It would be of great help in designing the novel systems with spirally corrugated pipe layout as it will not increase the rate of heat transfer for the same area and help reduce overall space requirement for long pipe length. Also, it was found that the pumping power required for MPCM slurry is higher when compared to other fluids, but simultaneously we can see that it provides the highest heat transfer. If we design pipe so that central flow is not much disturbed and fluid near the surface swirls, we can significantly decrease pressure drop. Thus, the designers can choose

between these two factors for a trade-out to achieve maximum effectiveness at a low cost.

6.2 Future Work

- Further analysis can be done considering the whole GSHP system and including its complete cost analysis.
- Because soil properties also affect thermal performance, a study with various backfill materials can understand its effect along with our novel pipe design.
- PCM can also be integrated into this system to provide constant energy.
- Solar or Wind energy can be integrated to run it as a stand-alone system.

BIBLIOGRAPHY

[1]   H. Nautiyal, S. K. Singal, and A. Sharma, 'Small hydropower for sustainable energy development in India', *Renew. Sustain. Energy Rev.*, vol. 15, no. 4, pp. 2021–2027, 2011.

[2]   N. L. Panwar, S. C. Kaushik, and S. Kothari, 'Role of renewable energy sources in environmental protection : A review', *Renew. Sustain. Energy Rev.*, vol. 15, no. 3, pp. 1513–1524, 2011.

[3]   UNDP, *World Energy Assessment. Energy and the challenge of Sustainability.* 2000.

[4]   R. K. Gera, Y. Parvej, and H. Soni, 'Renewable Energy Scenario in India : Opportunities and Challenges', no. 1, pp. 10–16, 2013.

[5]   E. Union, 'Impact Assessment', *Comm. Staff Work. Pap.*, vol. 72, pp. 1–49, 2012.

[6]   D. Industries, 'In the summer in Tokyo , people take part in Cool Biz but do not feel cool !? 80 % of the foreign workers take part in Cool Biz but complain about not being able to implement it completely . How do the foreign workers battle the summer in Tokyo ?', pp. 1–10, 2015.

[7]   F. O. F. Petroleum, 'Functioning of petroleum conservation research association', vol. 1937, 2016.

[8]   C. Peretti, A. Zarrella, M. De Carli, and R. Zecchin, 'The design and environmental evaluation of earth-to-air heat exchangers (EAHE). A literature review', *Renewable and Sustainable Energy Reviews*, vol. 28. Elsevier, pp. 107–116, 2013.

[9]   L. Ozgener, 'A review on the experimental and analytical analysis of earth to air

heat exchanger (EAHE) systems in Turkey', *Renew. Sustain. Energy Rev.*, vol. 15, no. 9, pp. 4483–4490, 2011.

[10] S. K. Soni, M. Pandey, and V. N. Bartaria, 'Ground coupled heat exchangers: A review and applications', *Renew. Sustain. Energy Rev.*, vol. 47, pp. 83–92, 2015.

[11] M. K. Ghosal, G. N. Tiwari, and N. S. L. Srivastava, 'Thermal modeling of a greenhouse with an integrated earth to air heat exchanger : an experimental validation', vol. 36, pp. 219–227, 2004.

[12] T. S. Bisoniya, A. Kumar, and P. Baredar, 'Energy metrics of earth-air heat exchanger system for hot and dry climatic conditions of India', *Energy Build.*, vol. 86, no. March, pp. 214–221, 2015.

[13] J. Sobti and S. K. Singh, 'Earth-air heat exchanger as a green retrofit for Chandigarh — a critical review', *Geotherm. Energy*, pp. 1–9, 2015.

[14] G. Florides and S. Kalogirou, 'Ground heat exchangers-A review of systems, models and applications', *Renew. Energy*, vol. 32, no. 15, pp. 2461–2478, 2007.

[15] V. Bansal, R. Misra, G. Das Agrawal, and J. Mathur, 'Performance analysis of earth-pipe-air heat exchanger for summer cooling', *Energy Build.*, vol. 42, no. 5, pp. 645–648, 2010.

[16] Viorel Badescu, 'Simple and accurate model for the ground heat exchanger of a passive house', *Renew. Energy*, vol. 32, pp. 845–855, 2007.

[17] H. N. S. M.Jamil Ahmad, G.N Tiwari, Anil Kumar Singh, Manisha Sharma, 'Heating / cooling potential and carbon credit', *Int. J. ENERGY Environ.*, vol. 1, no. September 2016, pp. 133–148, 2010.

[18] V. Bansal, R. Misra, G. Das, and J. Mathur, 'Transient effect of soil thermal conductivity and duration of operation on performance of Earth Air Tunnel Heat Exchanger', *Appl. Energy*, vol. 103, pp. 1–11, 2013.

[19] T. S. Bisoniya, A. Kumar, and P. Baredar, 'Cooling Potential Evaluation of Earth-Air Heat Exchanger System for Summer Season', *Int. J. Eng. Tech. Reseach(IJETR)*, vol. 2, no. 4, pp. 309–316, 2014.

[20] M. S. Sodha, D. Buddhi, and K. R. Campus, 'OPTIMIZATION OF PIPE PARAMETERS OF A N', vol. 34, no. 6, pp. 465–470, 1993.

[21] G. Mihalakakou, M. Santamouris, and D. Asimakopoulos, 'Modelling the thermal performance of earth-to-air heat exchangers', *Sol. Energy*, vol. 53, no. 3, pp. 301–305, 1994.

[22] F. Ascione, L. Bellia, and F. Minichiello, 'Earth-to-air heat exchangers for Italian climates', *Renew. Energy*, vol. 36, no. 8, pp. 2177–2188, 2011.

[23] K. H. Lee and R. K. Strand, 'The cooling and heating potential of an earth tube system in buildings', vol. 40, pp. 486–494, 2008.

[24] B. Peuportier, 'Thermal and environmental assessment of a passive building equipped with an earth-to-air heat exchanger in France', vol. 82, pp. 820–831, 2008.

[25] P. Tittelein, G. Achard, and E. Wurtz, 'Modelling earth-to-air heat exchanger behaviour with the convolutive response factors method', *Appl. Energy*, vol. 86, no. 9, pp. 1683–1691, 2009.

[26] R. Ralegaonkar, M. V. Kamath, and V. A. Dakwale, 'Design and Development of Geothermal Cooling System for Composite Climatic Zone in India', *J. Inst. Eng. Ser. A*, vol. 95, no. 3, pp. 179–183, 2014.

[27] T. Choudhury and A. K. Misra, 'Minimizing changing climate impact on buildings using easily and economically feasible earth to air heat exchanger technique', pp. 947–954, 2014.

[28] H. K. Dhruw, G. Sahu, P. K. Sen, R. Sharma, and S. Bohidar, 'A Review Paper

on Earth Tube Heat Exchanger', vol. 3, no. Xi, pp. 415–417, 2015.

[29]   A. K. Chaturvedi and V. N. Bartaria, 'Performance of Earth Tube Heat Exchanger of air-a review', *Intrnational J. Mech. Eng. Robot. Reseach*, vol. 4, no. 1, 2015.

[30]   W. Thomas, Y. Coulibaly, and E. S. Traoré, 'Earth-Air Heat Exchangers for Passive Air Conditioning : Case Study Burkina Faso', vol. 17, no. 1, pp. 21–32, 2012.

[31]   S. Jakhar, R. Misra, V. Bansal, and M. S. Soni, 'Thermal performance investigation of earth air tunnel heat exchanger coupled with a solar air heating duct for northwestern India', *Energy Build.*, vol. 87, pp. 360–369, 2015.

[32]   P. S. Sikarwar, 'A Review on Performance of Air Conditioner with Ground', vol. 5, no. 2, pp. 79–82, 2014.

[33]   F. Chlela, A. Husaunndee, P. Riederer, and C. Inard, 'Numerical Evaluation of Earth to Air Heat Exchangers and Heat Recovery Ventilation Systems', *Int. J. Vent.*, vol. 3315, no. August, pp. 30–42, 2016.

[34]   A. D. Singh, 'Earth air Tunnels'.

[35]   S. Mongkon, S. Thepa, P. Namprakai, and N. Pratinthong, 'Cooling performance and condensation evaluation of horizontal earth tube system for the tropical greenhouse', *Energy Build.*, vol. 66, pp. 104–111, 2013.

[36]   M. De Paepe and A. Janssens, 'Thermo-hydraulic design of earth-air heat exchangers', vol. 35, pp. 389–397, 2003.

[37]   M. Bojic, 'NUMERICAL SIMULATION, TECHNICAL AND ECONOMIC EVALUATION OF AIR-TO-EARTH HEAT EXCHANGER COUPLED', *Energy*, vol. 22, no. 12, pp. 1151–1158, 1997.

[38]   P. N. Razdan, R. K. Agarwal, and Singh R., 'Geothermal Energy Resources and its Potential in India', *Earth Sci. India,* vol. 7, no. I, pp. 14–18, 2013.

[39]   A. Sehli, A. Hasni, and M. Tamali, 'The potential of earth-air heat exchangers for low energy cooling of buildings in South Algeria', *Energy Procedia*, vol. 18, pp. 496–506, 2012.

[40]   M. Hossein Abbaspour-Fard, A. Gholami, and M. Khojastehpour, 'Evaluation of an Earth-to-Air Heat Exchanger for the North-East of Iran with Semi-Arid Climate', *Int. J. Green Energy*, vol. 8, no. April 2016, pp. 499–510, 2011.

[41]   K. M. B. D.Y.Goswami, 'Use Of Underground Air Tunnels For Heating And Cooling Agricultural And Residential Buildings', *Fact Sheet EES*, vol. 78, pp. 1–4, 1993.

[42]   J. Vaz, M. A. Sattler, D. Elizaldo, and L. A. Isoldi, 'Experimental and numerical analysis of an earth – air heat exchanger', *Energy Build.*, vol. 43, no. 9, pp. 2476–2482, 2011.

[43]   S. Brum, J. Vaz, L. Alberto, O. Rocha, E. Domingues, and L. André, 'A new computational modeling to predict the behavior of Earth-Air Heat Exchangers', *Energy Build.*, vol. 64, pp. 395–402, 2013.

[44]   H. Su, X. Liu, L. Ji, and J. Mu, 'A numerical model of a deeply buried air – earth – tunnel heat exchanger', *Energy Build.*, vol. 48, pp. 233–239, 2012.

[45]   M. Benhammou and B. Draoui, 'Parametric study on thermal performance of earth-to-air heat exchanger used for cooling of buildings', *Renew. Sustain. Energy Rev.*, vol. 44, pp. 348–355, 2015.

[46]   D. Yang, Y. Guo, and J. Zhang, 'Evaluation of the thermal performance of an earth-to-air heat exchanger (EAHE) in a harmonic thermal environment', *Energy Convers. Manag.*, vol. 109, pp. 184–194, 2016.

[47] D. A. and M. V. M. Santamouris, G.Mihalakakou, C.A.Balaras, A.Argiriou, 'Use of Buried pipes for energy conservation in cooling of agricultural greenhouses', *Sol. Energy*, vol. 55, no. 2, pp. 111–124, 1995.

[48] B. Yassine, K. Ghali, N. Ghaddar, G. Chehab, and I. Srour, 'Effectiveness of the earth tube heat exchanger system coupled to a space model in achieving thermal comfort in rural areas', *Int. J. Sustain. Energy*, vol. 33, no. 3, pp. 567–586, 2013.

[49] A. A. Serageldin, A. K. Abdelrahman, and S. Ookawara, 'Earth-Air Heat Exchanger thermal performance in Egyptian conditions : Experimental results , mathematical model , and Computational Fluid Dynamics simulation', *Energy Convers. Manag.*, vol. 122, pp. 25–38, 2016.

[50] S. Barakat, A. Ramzy, A. M. Hamed, and S. H. El Emam, 'Enhancement of gas turbine power output using earth to air heat exchanger (EAHE) cooling system', *ENERGY Convers. Manag.*, vol. 111, pp. 137–146, 2016.

[51] S. Uddin, R. Ahmed, and M. Rahman, 'Performance evaluation and life cycle analysis of earth to air heat exchanger in a developing country', *Energy Build.*, vol. 128, pp. 254–261, 2016.

[52] G. Gan, 'Simulation of dynamic interactions of the earth – air heat exchanger with soil and atmosphere for preheating of ventilation air', *Appl. Energy*, vol. 158, pp. 118–132, 2015.

[53] M. Kepes *et al.*, 'Numerical investigation about the improvement of the thermal potential of an Earth-Air Heat Exchanger (EAHE) employing the Constructal Design method', vol. 80, pp. 538–551, 2015.

[54] S. F. Ahmed, M. M. K. Khan, M. T. O. Amanullah, M. G. Rasul, and N. M. S. Hassan, 'Performance assessment of earth pipe cooling system for low energy buildings in a subtropical climate', *ENERGY Convers. Manag.*, vol. 106, pp. 815–825, 2015.

[55] A. Nur, Z. Sanusi, A. Azlan, and A. Zamri, 'Achieving Cooler Soil as an Effective Heat Sink for Earth-to-Air Heat Exchanger (EAHE) Cooling Technology in Malaysia Tropical Climate', pp. 804–809, 2014.

[56] N. Aziah, M. Ariffin, A. Nur, Z. Sanusi, and A. M. Noor, 'MATERIALS FOR THE EARTH AIR PIPE HEAT EXCHANGER (EAPHE) SYSTEM AS A PASSIVE GROUND COOLING TECHNOLOGY FOR HOT-HUMID CLIMATE', no. November, 2014.

[57] M. Benhammou, B. Draoui, M. Zerrouki, and Y. Marif, 'Performance analysis of an earth-to-air heat exchanger assisted by a wind tower for passive cooling of buildings in arid and hot climate', *ENERGY Convers. Manag.*, vol. 91, pp. 1–11, 2015.

[58] J. Xamán, I. Hernández-pérez, J. Arce, G. Álvarez, L. Ramírez-dávila, and F. Noh-pat, 'Numerical study of earth-to-air heat exchanger : The effect of thermal insulation', *Energy Build.*, vol. 85, pp. 356–361, 2014.

[59] S. Carlucci, G. Cattarin, L. Pagliano, and M. Pietrobon, 'Optimization of the installation of an Earth-to-Air Heat Exchanger and detailed design of a dedicated experimental set-up', vol. 504, pp. 2158–2161, 2014.

[60] J. A. H.-C. S.E. Diaz-Mendez ⇑, C. Patiño-Carachure, 'Reducing the energy consumption of an earth – air heat exchanger with a PID control system', *ENERGY Convers. Manag.*, vol. 77, pp. 1–6, 2014.

[61] A. Nur, Z. Sanusi, A. Azlan, and A. Zamri, 'Seeking Underground for Potential Heat Sink in Malaysia for Earth Air Heat Exchanger (EAHE) Application', pp. 542–546, 2014.

[62] F. Niu, Y. Yu, D. Yu, and H. Li, 'Investigation on soil thermal saturation and recovery of an earth to air heat exchanger under different operation strategies', *Appl. Therm. Eng.*, 2015.

[63]   F. Niu, Y. Yu, D. Yu, and H. Li, 'Heat and mass transfer performance analysis and cooling capacity prediction of earth to air heat exchanger', *Appl. Energy*, vol. 137, pp. 211–221, 2015.

[64]   F. Ascione, D. D. Agostino, C. Marino, and F. Minichiello, 'Earth-to-air heat exchanger for NZEB in Mediterranean climate', *Renew. Energy*, vol. 99, pp. 553–563, 2016.

[65]   M. K. Ghosal, G. N. Tiwari, and N. S. L. Srivastava, 'Thermal modeling of a greenhouse with an integrated earth to air heat exchanger: an experimental validation', *Energy Build.*, vol. 36, no. 3, pp. 219–227, Mar. 2004.

[66]   V. Bansal, R. Misra, G. Das Agrawal, and J. Mathur, 'Performance analysis of earth-pipe-air heat exchanger for winter heating', *Energy Build.*, vol. 41, no. 11, pp. 1151–1154, 2009.

[67]   A. Chel and G. N. Tiwari, 'Performance evaluation and life cycle cost analysis of earth to air heat exchanger integrated with adobe building for New Delhi composite climate', *Energy Build.*, vol. 41, no. 1, pp. 56–66, 2009.

[68]   Y. Yu, H. Li, F. Niu, and D. Yu, 'Investigation of a coupled geothermal cooling system with earth tube and solar chimney', *Appl. Energy*, vol. 114, pp. 209–217, 2014.

[69]   R. Kumar, S. Ramesh, and S. C. Kaushik, 'Performance evaluation and energy conservation potential of earth – air – tunnel system coupled with non-air-conditioned building', vol. 38, pp. 807–813, 2003.

[70]   A. Mathur, A. Srivastava, J. Mathur, and S. Mathur, 'Transient effect of soil thermal diffusivity on performance of EATHE system', *Energy Reports*, vol. 1, pp. 17–21, 2015.

[71]   A. K. Chaturvedi and V. N. Bartaria, 'PERFORMANCE OF EARTH TUBE

HEAT EXCHANGER COOLING OF AIR — A REVIEW', vol. 4, no. 1, 2015.

[72] A. Thakur and A. Sharma, 'CFD Analysis of Earth-Air Heat Exchanger to Evaluate the Effect of Parameters on Its Performance', pp. 14–19, 2015.

[73] A. Singh, 'Performance Analysis of Earth-Air Tunnel System used for Air-Conditioning of the College Classroom', *J. Energy Technol. Policy*, vol. 5, no. 8, pp. 71–79, 2015.

[74] G. D. A. Sunil Kumar Khandelwal1*, Anuj Mathur2, 'The Design of Earth Air Tunnel Heat Exchanger System for an Institute Library', *Int. J. Sci. Eng. Technol. Vol.*, vol. 4, no. 3, pp. 141–145, 2015.

[75] A. Mathur, A. Kumar, P. Verma, S. Mathur, and G. D. Agrawal, 'Investigation of soil thermal saturation and recovery under intermittent and continuous operation of EATHE', *Energy Build.*, vol. 109, pp. 291–303, 2015.

[76] M. Kaushal, P. Dhiman, S. Singh, and H. Patel, 'Finite Volume and Response Surface Methodology based performance prediction and optimization of a hybrid earth to air tunnel heat exchanger', *Energy Build.*, 2015.

[77] S. Jakhar, M. S. Soni, and N. Gakkhar, 'Performance analysis of earth water heat exchanger for concentrating photovoltaic cooling', *Energy Procedia*, vol. 90, no. December 2015, pp. 145–153, 2016.

[78] D. A. ManojkumarDubey, Dr. J.L.Bhagoria, 'Earth Air Heat Exchanger in Parallel Connection', *Int. J. Engineeering Trends Technol.*, vol. 4, no. June, pp. 2463–2467, 2013.

[79] A. K. Misra, M. Gupta, M. Lather, and H. Garg, 'Design and Performance Evaluation of Low Cost Earth to Air Heat Exchanger Model Suitable for Small Buildings in Arid and Semi Arid Regions', vol. 00, no. 0000, pp. 1–4, 2014.

[80] S. K. Soni, M. Pandey, and V. N. Bartaria, 'Energy metrics of a hybrid earth air

heat exchanger system for summer cooling requirements', *Energy Build.*, 2016.

[81]   S. Jakhar, R. Misra, M. S. Soni, and N. Gakkhar, 'Parametric simulation and experimental analysis of earth air heat exchanger with solar air heating duct', pp. 1–8, 2016.

[82]   N. Hatraf, F. Chabane, A. Brima, N. Moummi, and A. Moummi, 'Parametric Study of to Design an Earth to Air Heat Exchanger with Experimental Validation', *Eng. J.*, vol. 18, no. 2, pp. 41–54, Apr. 2014.

[83]   D. Y. Goswami and A. S. Dhaliwal, 'Heat Transfer Analysis in Environmental Control Using an Underground Air Tunnel', vol. 107, no. May 1985, 2015.

[84]   H. Li, Y. Yu, F. Niu, M. Sha, and B. Chen, 'Performance of a coupled cooling system with earth-to-air heat exchanger and solar chimney', vol. 62, pp. 468–477, 2014.

[85]   J. Abed and A. Wahid, 'Sustainable Design of Wind-catcher of an Earth-to-Air Heat Exchanger in Hot Dry Areas', vol. 6, no. 4, pp. 582–589, 2015.

[86]   Z. Li, W. Zhu, T. Bai, and M. Zheng, 'Experimental study of a ground sink direct cooling system in cold areas', vol. 41, pp. 1233–1237, 2009.

[87]   L. Incopera, DeWitt, Bergman, *Fundamentals of Heat and Mass Transfer.* .

[88]   R. Misra, V. Bansal, G. Das, J. Mathur, and T. K. Aseri, 'CFD analysis based parametric study of derating factor for Earth Air Tunnel Heat Exchanger', *Appl. Energy*, vol. 103, pp. 266–277, 2013.

[89]   T. S. Bisoniya, A. Kumar, and P. Baredar, 'Study on Calculation Models of Earth-Air Heat Exchanger Systems', vol. 2014, 2014.

[90]   P. M. Congedo, G. Colangelo, and G. Starace, 'CFD simulations of horizontal ground heat exchangers: A comparison among different configurations', *Appl.*

Therm. Eng., vol. 33–34, no. 1, pp. 24–32, 2012.

[91]   H. Benli, 'A performance comparison between a horizontal source and a vertical source heat pump systems for a greenhouse heating in the mild climate Elaziğ, Turkey', in *Applied Thermal Engineering*, 2013, vol. 50, no. 1, pp. 197–206.

[92]   K. Bakirci, 'Evaluation of the performance of a ground-source heat-pump system with series GHE (ground heat exchanger) in the cold climate region', *Energy*, vol. 35, no. 7, pp. 3088–3096, Jul. 2010.

[93]   N. Kayaci and H. Demir, 'Comparative performance analysis of building foundation Ground heat exchanger', *Geothermics*, vol. 83, p. 101710, Jan. 2020.

[94]   J. Luo, J. Rohn, M. Bayer, A. Priess, L. Wilkmann, and W. Xiang, 'Heating and cooling performance analysis of a ground source heat pump system in Southern Germany', *Geothermics*, vol. 53, pp. 57–66, Jan. 2015.

[95]   T. Sivasakthivel, K. Murugesan, and P. K. Sahoo, 'Optimization of ground heat exchanger parameters of ground source heat pump system for space heating applications', *Energy*, vol. 78, pp. 573–586, Dec. 2014.

[96]   G. Emmi, A. Zarrella, M. De Carli, and A. Galgaro, 'An analysis of solar assisted ground source heat pumps in cold climates', *Energy Convers. Manag.*, vol. 106, pp. 660–675, Dec. 2015.

[97]   A. Girard, E. J. Gago, T. Muneer, and G. Caceres, 'Higher ground source heat pump COP in a residential building through the use of solar thermal collectors', *Renew. Energy*, vol. 80, pp. 26–39, Aug. 2015.

[98]   N. Zhu, J. Wang, and L. Liu, 'Performance evaluation before and after solar seasonal storage coupled with ground source heat pump', *Energy Convers. Manag.*, vol. 103, pp. 924–933, Jul. 2015.

[99]   S. Yoon, S. R. Lee, and G. H. Go, 'Evaluation of thermal efficiency in different

types of horizontal ground heat exchangers', *Energy Build.*, vol. 105, pp. 100–105, Aug. 2015.

[100] V. R. Tarnawski, W. H. Leong, T. Momose, and Y. Hamada, 'Analysis of ground source heat pumps with horizontal ground heat exchangers for northern Japan', *Renew. Energy*, vol. 34, no. 1, pp. 127–134, Jan. 2009.

[101] H. Kim, Y. Nam, S. Bae, J. S. Choi, and S. B. Kim, 'A Study on the Effect of Performance Factor on GSHP System through Real-Scale Experiments in Korea', *Energies*, vol. 13, no. 3, p. 554, 2020.

[102] H. Javadi, S. S. M. Ajarostaghi, S. S. Mousavi, and M. Pourfallah, 'Thermal analysis of a triple helix ground heat exchanger using numerical simulation and multiple linear regression', *Geothermics*, vol. 81, pp. 53–73, Sep. 2019.

[103] H. Fujii, K. Nishi, Y. Komaniwa, and N. Chou, 'Numerical modeling of slinky-coil horizontal ground heat exchangers', *Geothermics*, vol. 41, pp. 55–62, Jan. 2012.

[104] H. Esen, M. Inalli, M. Esen, and K. Pihtili, 'Energy and exergy analysis of a ground-coupled heat pump system with two horizontal ground heat exchangers', *Build. Environ.*, vol. 42, no. 10, pp. 3606–3615, Oct. 2007.

[105] R. R. Dasare and S. K. Saha, 'Numerical study of horizontal ground heat exchanger for high energy demand applications', *Appl. Therm. Eng.*, vol. 85, pp. 252–263, Jun. 2015.

[106] B. Asgari, M. Habibi, and A. Hakkaki-Fard, 'Assessment and comparison of different arrangements of horizontal ground heat exchangers for high energy required applications', *Appl. Therm. Eng.*, vol. 167, p. 114770, Feb. 2020.

[107] P. C. Mukesh Kumar, J. Kumar, and S. Suresh, 'Experimental investigation on convective heat transfer and friction factor in a helically coiled tube with

Al2O3/water nanofluid', *J. Mech. Sci. Technol.*, vol. 27, no. 1, pp. 239–245, Jan. 2013.

[108] G. Diglio, C. Roselli, M. Sasso, and U. Jawali Channabasappa, 'Borehole heat exchanger with nanofluids as heat carrier', *Geothermics*, vol. 72, pp. 112–123, Mar. 2018.

[109] N. Naili, M. Hazami, I. Attar, and A. Farhat, 'Assessment of surface geothermal energy for air conditioning in northern Tunisia: Direct test and deployment of ground source heat pump system', *Energy Build.*, vol. 111, pp. 207–217, Jan. 2016.

[110] Y. Wu, G. Gan, A. Verhoef, P. L. Vidale, and R. G. Gonzalez, 'Experimental measurement and numerical simulation of horizontal-coupled slinky ground source heat exchangers', *Appl. Therm. Eng.*, vol. 30, no. 16, pp. 2574–2583, Nov. 2010.

[111] Y. Wu, G. Gan, R. G. Gonzalez, A. Verhoef, and P. L. Vidale, 'Prediction of the thermal performance of horizontal-coupled ground-source heat exchangers', *Int. J. Low-Carbon Technol.*, vol. 6, no. 4, pp. 261–269, Dec. 2011.

[112] N. Naili, M. Hazami, I. Attar, and A. Farhat, 'In-field performance analysis of ground source cooling system with horizontal ground heat exchanger in Tunisia', *Energy*, vol. 61, pp. 319–331, Nov. 2013.

[113] N. Kayaci and H. Demir, 'Numerical modelling of transient soil temperature distribution for horizontal ground heat exchanger of ground source heat pump', *Geothermics*, vol. 73, pp. 33–47, May 2018.

[114] N. Naili, I. Attar, M. Hazami, and A. Farhat, 'Experimental Analysis of Horizontal Ground Heat Exchanger for Northern Tunisia', *J. Electron. Cool. Therm. Control*, vol. 02, no. 03, pp. 44–51, 2012.

[115] S. Selamat, A. Miyara, and K. Kariya, 'Numerical study of horizontal ground heat exchangers for design optimization', *Renew. Energy*, vol. 95, pp. 561–573, Sep. 2016.

[116] A. Flaga-Maryanczyk, J. Schnotale, J. Radon, and K. Was, 'Experimental measurements and CFD simulation of a ground source heat exchanger operating at a cold climate for a passive house ventilation system', *Energy Build.*, vol. 68, no. PARTA, pp. 562–570, Jan. 2014.

[117] M. J. Kim, S. R. Lee, S. Yoon, and G. H. Go, 'Thermal performance evaluation and parametric study of a horizontal ground heat exchanger', *Geothermics*, vol. 60, pp. 134–143, Mar. 2016.

[118] '(PDF) Horizontal Ground Heat Exchanger Design for Ground-Coupled Heat Pumps'. [Online]. Available: https://www.researchgate.net/publication/233530173_Horizontal_Ground_Heat _Exchanger_Design_for_Ground-Coupled_Heat_Pumps. [Accessed: 19-Mar-2021].

[119] K. S. Lee, E. C. Kang, Y. J. Kim, and E. J. Lee, 'Model verification and justification study of spirally corrugated pipes in a ground-air heat exchanger application', *Energies*, vol. 12, no. 21, 2019.

[120] S. Rainieri and G. Pagliarini, 'Convective heat transfer to temperature dependent property fluids in the entry region of corrugated tubes', *Int. J. Heat Mass Transf.*, vol. 45, no. 22, pp. 4525–4536, Oct. 2002.

[121] A. Z. Dellil, 'Numerical simulation of a spiral wall', *Mechanika*, vol. 20, no. 1, pp. 42–48, 2014.

[122] K. Mimura and A. Isozaki, 'Heat transfer and pressure drop of corrugated tubes', *Desalination*, vol. 22, no. 1–3, pp. 131–139, Dec. 1977.

[123] J. G. Withers, 'Tube-side heat transfer and pressure drop for tubes having helical internal ridging with turbulent/transitional flow of single-phase fluid. Part 1. Single-helix ridging', *Heat Transf. Eng.*, vol. 2, no. 1, pp. 48–58, 1980.

[124] A. Yutaka, N. Hiroshi, and M. Faghri, 'Heat transfer and pressure drop characteristics in a corrugated duct with rounded corners', *Int. J. Heat Mass Transf.*, vol. 31, no. 6, pp. 1237–1245, Jun. 1988.

[125] 'Investigation of heat transfer and pressure drop augmentation for turbulent flow in spirally enhanced tubes - Search results - Pascal and Francis Bibliographic Databases'. [Online]. Available: https://pascal-francis.inist.fr/vibad/index.php?action=getRecordDetail&idt=6867687.

[126] S. Rainieri, F. Bozzoli, and G. Pagliarini, 'Experimental investigation on the convective heat transfer in straight and coiled corrugated tubes for highly viscous fluids: Preliminary results', *Int. J. Heat Mass Transf.*, vol. 55, no. 1–3, pp. 498–504, Jan. 2012.

[127] S. Pethkool, S. Eiamsa-ard, S. Kwankaomeng, and P. Promvonge, 'Turbulent heat transfer enhancement in a heat exchanger using helically corrugated tube', *Int. Commun. Heat Mass Transf.*, vol. 38, no. 3, pp. 340–347, Mar. 2011.

[128] Z. S. Kareem, M. N. Mohd Jaafar, T. M. Lazim, S. Abdullah, and A. F. Abdulwahid, 'Heat transfer enhancement in two-start spirally corrugated tube', *Alexandria Eng. J.*, vol. 54, no. 3, pp. 415–422, 2015.

[129] Z. jiang Jin, F. qiang Chen, Z. xin Gao, X. fei Gao, and J. yuan Qian, 'Effects of pitch and corrugation depth on heat transfer characteristics in six-start spirally corrugated tube', *Int. J. Heat Mass Transf.*, vol. 108, no. October, pp. 1011–1025, 2017.

[130] Z. jiang Jin, B. zhan Liu, F. qiang Chen, Z. xin Gao, X. fei Gao, and J. yuan Qian, 'CFD analysis on flow resistance characteristics of six-start spirally

corrugated tube', *Int. J. Heat Mass Transf.*, vol. 103, no. October 2017, pp. 1198–1207, 2016.

[131] J. Y. Qian, M. R. Chen, Z. Wu, X. L. Liu, Z. J. Jin, and B. Sundén, 'A geometric study on shell side heat transfer and flow resistance of a six-start spirally corrugated tube', *Numer. Heat Transf. Part A Appl.*, vol. 73, no. 8, pp. 565–582, 2018.

[132] K. S. Lee, E. C. Kang, Y. J. Kim, and E. J. Lee, 'Model verification and justification study of spirally corrugated pipes in a ground-air heat exchanger application', *Energies*, vol. 12, no. 21, Oct. 2019.

[133] A. Bejan and A. Kraus, *Heat transfer handbook*. 2003.

[134] M. Kong, J. L. Alvarado, C. Thies, S. Morefield, and C. P. Marsh, 'Field evaluation of microencapsulated phase change material slurry in ground source heat pump systems', *Energy*, vol. 122, pp. 691–700, 2017.

[135] N. A. Usri, W. H. Azmi, R. Mamat, K. A. Hamid, and G. Najafi, *Heat Transfer Augmentation of Al2O3 Nanofluid in 60:40 Water to Ethylene Glycol Mixture*, vol. 79. Elsevier B.V., 2015.

[136] C. Y. Zhao and G. H. Zhang, 'Review on microencapsulated phase change materials (MEPCMs): Fabrication, characterization and applications', *Renew. Sustain. Energy Rev.*, vol. 15, no. 8, pp. 3813–3832, 2011.

[137] M. Corcione, M. Cianfrini, and A. Quintino, 'Pumping Energy Saving Using Nanoparticle Suspensions as Heat Transfer Fluids', *J. Heat Transfer*, vol. 134, no. 12, p. 121701, 2012.

[138] C. Yang, M. R. Chen, J. Y. Qian, Z. Wu, Z. J. Jin, and B. Sunden, 'Heat Transfer Study of a Hybrid Smooth and Spirally Corrugated Tube', *Heat Transf. Eng.*, vol. 42, no. 3–4, pp. 242–250, 2021.

List of Publication

1. Aashish Sharma and Ravindra D. Jilte; "Thermohydraulic performance of modified Ground Heat Exchanger for Different Working Fluids - Numerical Approach", International Journal of Aquatic Science, 12 (3) 2280-2291. http://www.journal-aquaticscience.com/article_136908.html (WoS)

2. Aashish Sharma, Ravindra D. Jilte and Sudhanshu Dogra; "Performance Evaluation of Ground Heat Exchanger Using Novel Spirally Corrugated Pipe Geometry- A CFD Approach", AIP Conference Proceedings, 2281 (2020). https://doi.org/10.1063/5.0026240 (Scopus)

3. Aashish Sharma and Ravindra D. Jilte; "Effect of pipe parameters on the ground heat exchanger performance: a review", International Conference of Advance Research and Innovation (ICARI-21), 30 January 2021.

4. Aashish Sharma and Ravindra D. Jilte; "Heat transfer enhancement in the ground heat exchanger for summer season using nanofluid: A CFD approach", International Conference of Advance Research and Innovation (ICARI-21), 30 January 2021.

5. Namrata Bordoloi, Aashish Sharma, Himanshu, and Varun; "An intense review on advancements of Earth Air Heat Exchanger", Renewable and Sustainable Energy Reviews, 89 (2018) 261-280. https://doi.org/10.1016/j.rser.2018.03.056 (SCI)

Appendix

A1. Temperature Readings from experimental setup

TEMPERATURE READING FROM SETUP

	10:00 AM	11:00 AM	12:00 AM	Avg	Final Temp
INLET	20.4	20.5	20.7	20.6	20.6
T1	23.3	23.5	23.7	23.5	23.5
T2	23.6	23.9	24.2	23.9	23.9
T3	24.1	24.3	24.6	24.4	24.4
T4	24.4	24.5	24.8	24.6	24.6
T5	24.6	24.9	25.3	25	25
T6	24.8	25.1	25.5	25.2	25.2
OUTLET	24.9	25.3	25.7	25.3	25.3

A2. Temperature values calculated from numerical simulation of Plain pipe

Summer

		T1			T2			T3		
Length	**Re**	**Water**	**Nanofluid**	**MPCM**	**Water**	**Nanofluid**	**MPCM**	**Water**	**Nanofluid**	**MPCM**
0	5000	35	35	35	37.5	37.5	37.5	40	40	40
0.25	5000	34.762	34.851	34.678	37.203	37.313	37.097	39.644	39.776	39.517
0.5	5000	34.57	34.728	34.42	36.962	37.16	36.774	39.354	39.592	39.13
0.75	5000	34.392	34.614	34.184	36.74	37.018	36.48	39.088	39.421	38.777
1	5000	34.229	34.509	33.969	36.536	36.886	36.211	38.844	39.263	38.454
0	7500	35	35	35	37.5	37.5	37.5	40	40	40
0.25	7500	34.831	34.893	34.768	37.289	37.367	37.211	39.746	39.84	39.653
0.5	7500	34.678	34.796	34.562	37.098	37.245	36.953	39.517	39.694	39.343
0.75	7500	34.546	34.711	34.385	36.933	37.139	36.731	39.32	39.567	39.078
1	7500	34.428	34.635	34.227	36.785	37.044	36.534	39.142	39.453	38.84
0	10000	35	35	35	37.5	37.5	37.5	40	40	40
0.25	10000	34.866	34.916	34.816	37.333	37.394	37.27	39.799	39.873	39.725
0.5	10000	34.741	34.836	34.646	37.206	37.295	37.058	39.611	39.754	39.469
0.75	10000	34.633	34.767	34.501	37.042	37.209	36.877	39.45	39.651	39.252
1	10000	34.538	34.706	34.373	36.923	37.132	36.717	39.307	39.559	39.06

Winter

Length	Re	T1			T2			T3		
		Water	Nanofluid	MPCM	Water	Nanofluid	MPCM	Water	Nanofluid	MPCM
0	5000	10	10	10	12.5	12.5	12.5	15	15	15
0.25	5000	10.356	10.122	10.483	12.797	12.602	12.903	15.238	15.081	15.322
0.5	5000	10.646	10.22	10.871	13.038	12.684	13.226	15.43	15.147	15.58
0.75	5000	10.912	10.312	11.224	13.26	12.76	13.52	15.608	15.208	15.816
1	5000	11.156	10.398	11.547	13.464	12.832	13.789	15.771	15.265	16.031
0	7500	10	10	10	12.5	12.5	12.5	15	15	15
0.25	7500	10.254	10.098	10.347	12.711	12.582	12.789	15.169	15.066	15.232
0.5	7500	10.483	10.185	10.657	12.902	12.654	13.047	15.322	15.123	15.438
0.75	7500	10.68	10.26	10.922	13.067	12.717	13.269	15.454	15.174	15.615
1	7500	10.858	10.329	11.16	13.215	12.774	13.466	15.572	15.22	15.773
0	10000	10	10	10	12.5	12.5	12.5	15	15	15
0.25	10000	10.201	10.084	10.275	12.667	12.57	12.73	15.134	15.056	15.184
0.5	10000	10.389	10.161	10.531	12.824	12.634	12.942	15.259	15.107	15.354
0.75	10000	10.55	10.227	10.748	12.958	12.689	13.123	15.367	15.151	15.499
1	10000	10.693	10.286	10.94	13.077	12.738	13.283	15.462	15.191	15.627

A3. Temperature values calculated from numerical simulation of Spirally corrugated pipe

Summer

Length	Re	T1			T2			T3		
		Water	Nanofluid	MPCM	Water	Nanofluid	MPCM	Water	Nanofluid	MPCM
0	5000	35	35	35	37.5	37.5	37.5	40	40	40
0.25	5000	34.909	34.945	34.88	37.389	37.431	37.35	39.867	39.917	39.82
0.5	5000	34.827	34.894	34.773	37.289	37.368	37.216	39.747	39.842	39.659
0.75	5000	34.751	34.847	34.673	37.196	37.309	37.091	39.636	39.771	39.509
1	5000	34.679	34.803	34.579	37.108	37.254	36.973	39.53	39.704	39.368
0	7500	35	35	35	37.5	37.5	37.5	40	40	40
0.25	7500	34.932	34.958	34.908	37.416	37.447	37.385	39.899	39.936	39.862
0.5	7500	34.874	34.92	34.828	37.342	37.4	37.285	39.811	39.881	39.742
0.75	7500	34.819	34.886	34.754	37.273	37.357	37.192	39.728	39.828	39.63
1	7500	34.768	34.854	34.685	37.211	37.317	37.107	39.653	39.78	39.528
0	10000	35	35	35	37.5	37.5	37.5	40	40	40
0.25	10000	34.945	34.966	34.925	37.427	37.457	37.406	39.918	39.948	39.888
0.5	10000	34.898	34.936	34.861	37.364	37.42	37.327	39.848	39.904	39.792
0.75	10000	34.854	34.908	34.802	37.305	37.385	37.252	39.782	39.862	39.703
1	10000	34.815	34.883	34.748	37.252	37.354	37.185	39.723	39.825	39.622

Winter

Length	Re	T1			T2			T3		
		Water	Nanofluid	MPCM	Water	Nanofluid	MPCM	Water	Nanofluid	MPCM
0	5000	10	10	10	12.5	12.5	12.5	15	15	15
0.25	5000	10.136	10.083	10.18	12.613	12.569	12.65	15.089	15.055	15.12
0.5	5000	10.259	10.158	10.341	12.716	12.632	12.784	15.168	15.106	15.227
0.75	5000	10.374	10.229	10.491	12.811	12.691	12.909	15.243	15.153	15.327
1	5000	10.482	10.296	10.632	12.902	12.746	13.027	15.313	15.197	15.421
0	7500	10	10	10	12.5	12.5	12.5	15	15	15
0.25	7500	10.101	10.064	10.138	12.584	12.553	12.615	15.068	15.043	15.092
0.5	7500	10.189	10.119	10.258	12.658	12.6	12.715	15.126	15.08	15.172
0.75	7500	10.272	10.172	10.37	12.727	12.643	12.808	15.181	15.114	15.246
1	7500	10.347	10.22	10.472	12.789	12.683	12.893	15.232	15.146	15.315
0	10000	10	10	10	12.5	12.5	12.5	15	15	15
0.25	10000	10.083	10.052	10.112	12.572	12.543	12.594	15.055	15.034	15.075
0.5	10000	10.154	10.096	10.208	12.633	12.58	12.673	15.102	15.064	15.139
0.75	10000	10.22	10.138	10.298	12.691	12.615	12.748	15.146	15.092	15.198
1	10000	10.28	10.175	10.378	12.743	12.646	12.815	15.185	15.117	15.252